CHAPTER 3

RESULTS AND DISCUSSION

3.1 Syntheses of racemic spirocyclopentanone–anthracene adducts ((±)-76-*i* and (±)-76-*ii*) and cyclopentanones ((±)-134-*i* and (±)-134-*ii*) from piperine (75)[63]

3.1.1 Syntheses of 3′-methoxycarbonyl-4′-(2-(3,4-methylenedioxy)phenyl) vinyl-5′-piperidinecarbonyl-1′-cyclopentanone-2′-spiro-11-9,10-dihydro-9,10-ethanoanthracenes ((±)-76-*i* and (±)-76-*ii*) from piperine (75)

Black pepper (*P. nigrum L.*) (10.00 g) was extracted with EtOH (150 ml) for 1 h. The crude extract was evaporated to dryness and then purified by flash column chromatography on silica gel to afford piperine (**75**) in 1% yield. The physical properties, ^{1}H NMR data and ^{1}H NMR spectrum were shown in Table 3.1 and Figure 3.1.

Table 3.1 ^{1}H-NMR data of piperine (**75**)

Compound	Physical property	m.p. (°C)	Chemical shift (δ, ppm)
75	yellow crystals	205.9–207.6	1.54–1.71 (m, 6H, CH_2-3″, 4″, 5″), 3.53 (brs, 2H, CH_2-2″ or 6″), 3.64 (brs, 2H, CH_2-2″ or 6″), 5.98 (s, 2H, CH_2-7′), 6.44 (d (J = 14.6 Hz), 1H, CH-2), 6.70–6.83 (m, 3H, CH-4, 5, 5′), 6.89 (dd (J = 8.0, 1.1 Hz), 1H, CH-6′), 6.98 (d (J = 1.0 Hz), 1H, CH-2′), 7.40 (ddd (J = 14.7, 8.2, 1.6 Hz), 1H, CH-3) (Figure 3.1)

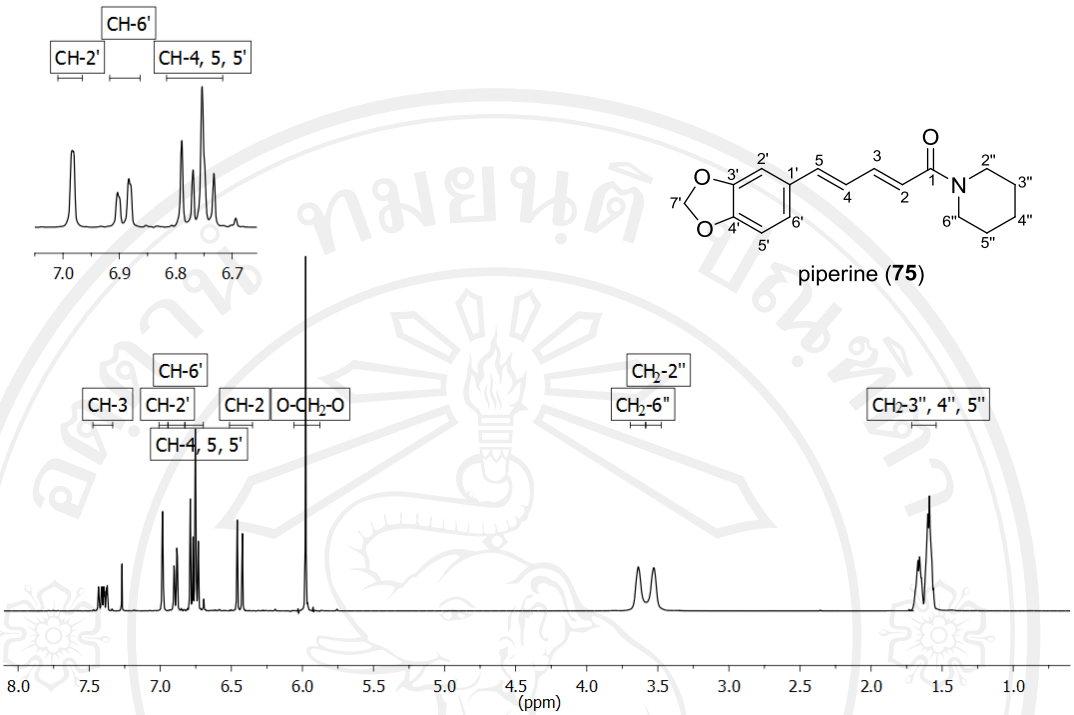

Figure 3.1 ^{1}H-NMR spectrum of piperine (**75**)

Then, dimethyl itaconate–anthracene adduct ((±)-**74**) was reacted with piperine (**75**) *via* tandem Michael addition–Dieckmann condensation reactions. An enolate anion (**118** or **119**) of dimethyl itaconate–anthracene adduct, generated from (±)-**74** by treatment with lithium diisopropylamide (LDA, 1.2 equiv.) in THF at 0 °C, readily reacted with piperine (**75**) at 0 °C to provide, after leaving the reaction mixture to stir at room temperature for 3 days followed by 10% hydrochloride acid work-up, the spirocyclopentanone–anthracene adduct as mixture of diastereoisomers. The crude spirocyclopentanone adduct was purified by flash column chromatography on silica gel to afford two diastereomeric spirocyclopentanone–anthracene adducts, (±)-**76**-*i* (23% yield) and (±)-**76**-*ii* (15% yield) (Scheme 3.1).

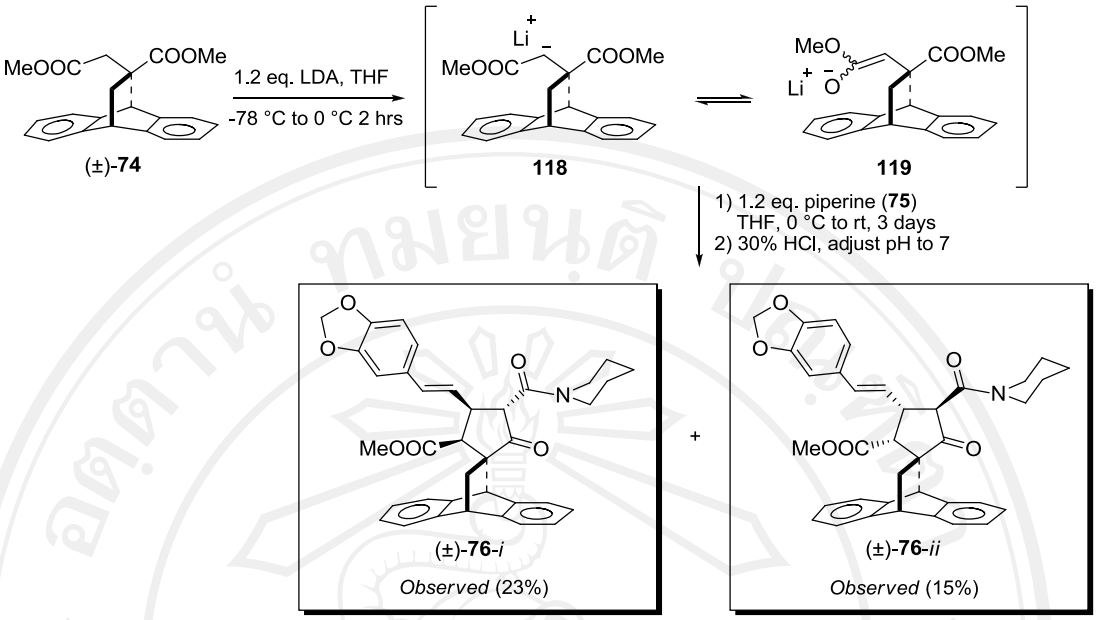

Scheme 3.1 Tandem Michael addition–Dieckmann condensation reactions

The relative stereochemistry of spirocyclopentanone–anthracene adduct (±)-**76**-*i* and (±)-**76**-*ii* were characterized by ^{1}H-NMR technique as shown in Table 3.2, Figures 3.2 and 3.3, respectively. The spirocyclopentanone–anthracene adduct (±)-**76**-*i* shows proton H_c was observed at δ 2.80 ppm as doublet (J = 7.1 Hz) which is *cis*-configuration with proton H_d. The proton H_e was observed at δ 3.85 ppm as doublet (J = 9.9 Hz) which is *trans*-configuration with proton H_d. The spirocyclopentanone–anthracene adduct (±)-**76**-*ii* shows proton H_c was observed at δ 2.30 ppm as doublet (J = 6.5 Hz) which is *cis*-configuration with proton H_d. The proton H_e was observed at δ 3.98 ppm as doublet (J = 11.3 Hz) which is *trans*-configuration with proton H_d. The methyl ester groups of spirocyclopentanone–anthracene adduct (±)-**76**-*i* and (±)-**76**-*ii* was observed at δ 3.53 and 3.76 ppm respectively, it should be noticed that the chemical shifts at δ 3.53 ppm was much higher than for normal methyl ester absorption, this may be due to deshielding effect of the aromatic nuclei.

Table 3.2 ^{1}H-NMR data of spirocyclopentanone–anthracene adducts (±)-**76**-*i* and (±)-**76**-*ii*

Compound	Physical property	m.p. (°C)	Chemical shift (δ, ppm)
(±)-**76**-*i*	white crystals	205.9–207.6	1.41–1.72 (m, 6H, CH_2-3′′′′′, 4′′′′′, 5′′′′′), 1.29, 2.22, 4.30 (ABX system, J = 12.7, 2.7, 2.5 Hz, 3H, H_a, H_b, H_x), 2.80 (d, J = 7.1 Hz, 1H, H_c), 3.31–3.49 (m, 2H, CH_2-2′′′′′ or 6′′′′′), 3.53 (s, 3H, COOMe-2′′), 3.74–3.82, 3.88–3.94 (m, 2H, CH_2-2′′′′′ or 6′′′′′), 3.85 (d, J = 9.9 Hz, 1H, H_e), 4.39–4.54 (m, 1H, H_d), 4.84 (s, 1H, H_y), 5.78 (dd, J = 15.7, 8.0 Hz, 1H, H_f), 5.94 (s, 2H, CH_2-7′′′′), 6.52 (d, J = 15.6 Hz, 1H, H_g), 6.73–6.82 (m, 3H, ArH-piperine) 6.98–7.45 (m, 8H, ArH–anthracene) (Figure 3.2)
(±)-**76**-*ii*	white crystals	223.4–225.9	1.33–1.74 (m, 6H, CH_2-3′′′′′, 4′′′′′, 5′′′′′), 1.88, 2.05, 4.35 (ABX system, J = 12.8, 3.0, 2.3 Hz, 3H, H_a, H_b, H_x), 2.30 (d, J = 6.5 Hz, 1H, H_c), 3.25–3.34, 3.48–3.56 (m, 2H, CH_2-2′′′′′ or 6′′′′′), 3.58–3.68 (m, 2H, CH_2-2′′′′′ or 6′′′′′), 3.76 (s, 3H, COOMe-2′′), 3.88–3.95 (m, 1H, H_d), 3.98 (d, J = 11.3 Hz, 1H, H_e) 4.40 (s, 1H, H_y), 5.70 (dd, J = 15.7, 7.3 Hz, 1H, H_f), 5.92 (s, 2H, CH_2-7′′′′), 6.31 (d, J = 15.7 Hz, 1H, H_g), 6.65–6.75 (m, 3H, ArH-piperine), 6.98– 7.46 (m, 8H, ArH–anthracene) (Figure 3.3)

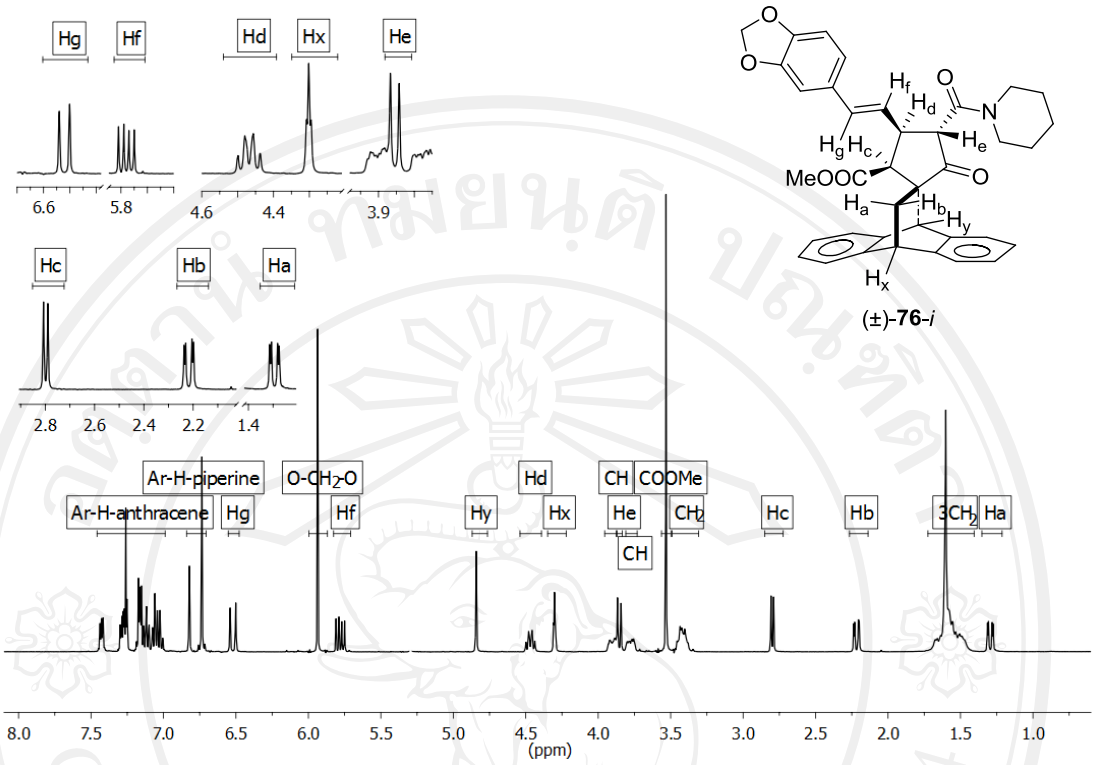

Figure 3.2 ^{1}H-NMR spectrum of spirocyclopentanone–anthracene adduct (±)-**76**-*i*

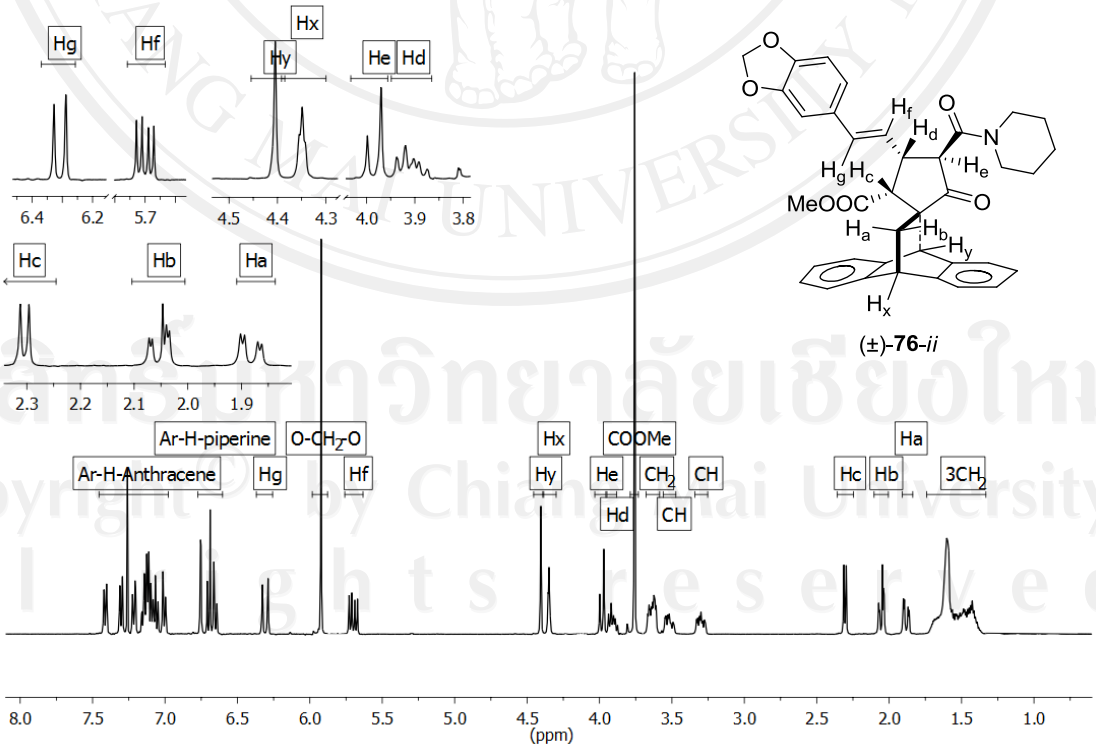

Figure 3.3 ^{1}H-NMR spectrum of spirocyclopentanone–anthracene adduct (±)-**76**-*ii*

The relative stereochemistry configuration of cyclopentanone ring was confirmed by NOE enhancement and X-ray crystallographic techniques. The spiro-cyclopentanone–anthracene adduct (±)-**76**-*i* was deduced by NOE enhancement as shown in Figure 3.4, the proton H_y is enhanced with proton H_c and H_d, which is proton H_c and proton H_d on the lower-face. The spirocyclopentanone–anthracene adduct (±)-**76**-*ii* was deduced by NOE enhancement as shown in Figure 3.5, the proton H_a is enhanced with proton H_c and H_d which is proton H_c and proton H_d on the upper-face.

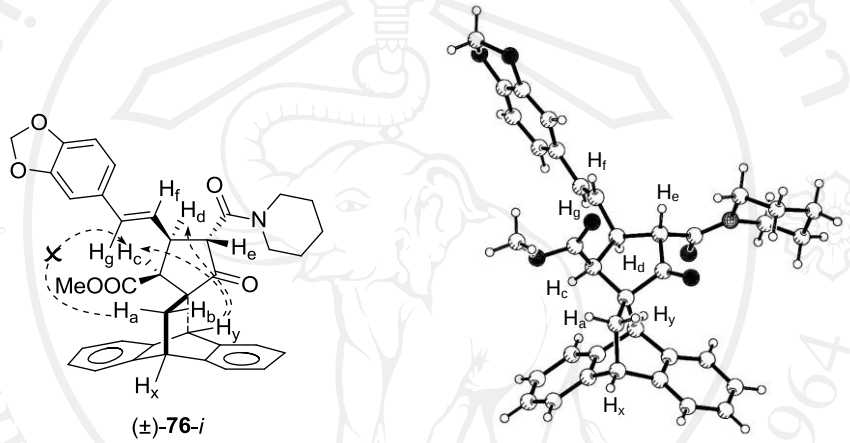

Figure 3.4 NOE correlations observed and X-ray crystallographic picture (PLATON) of spirocyclopentanone–anthracene adduct (±)-**76**-*i*

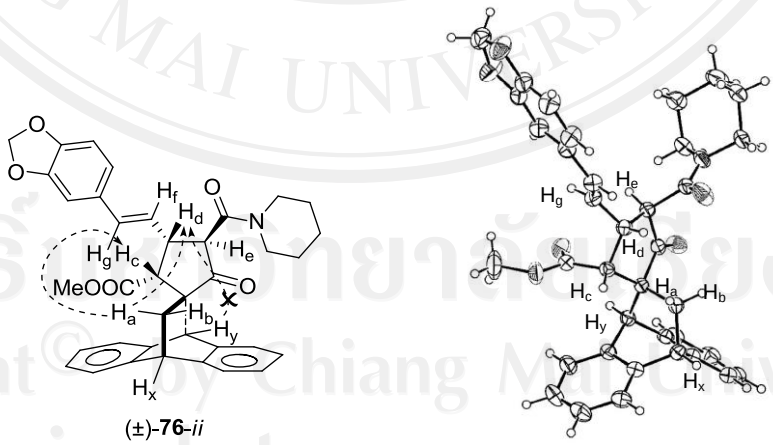

Figure 3.5 NOE correlations observed and X-ray crystallographic picture (ORTEP) of spirocyclopentanone–anthracene adduct (±)-**76**-*ii*

Results shown above indicated that the spirocyclopentanone–anthracene adduct (±)-**76**-*i* was the major product from the tandem Michael addition–Dieckmann condensation reactions between the anions (**118** and **119**) and piperine (**75**). This could be explained in terms of the favorable chair-like transition states (**122** and **123**) where upon all large substituents occupied the less sterically demanding equatorial orientations (Scheme 3.2).

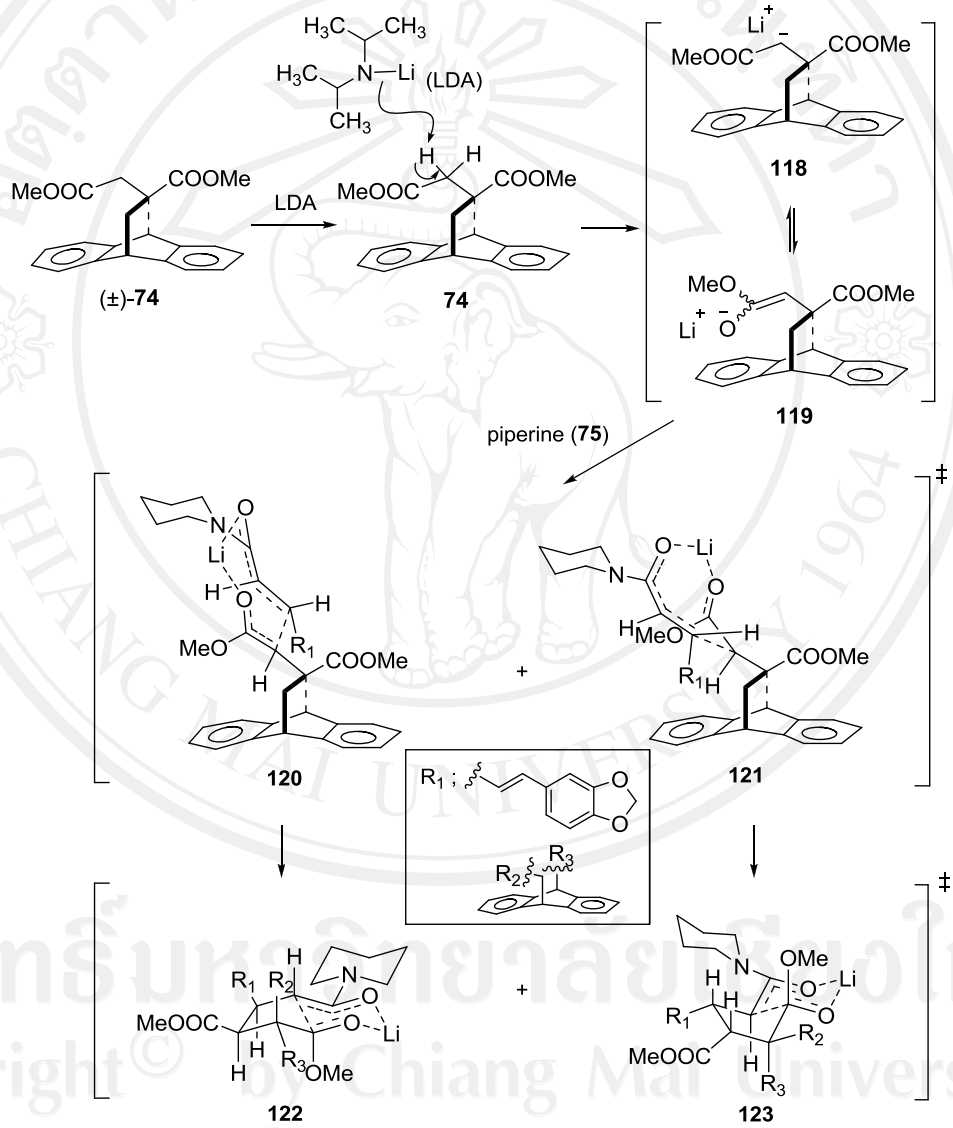

Scheme 3.2 Mechanism of tandem Michael addition–Dieckmann condensation reactions of (±)-**76**-*i* and (±)-**76**-*ii*

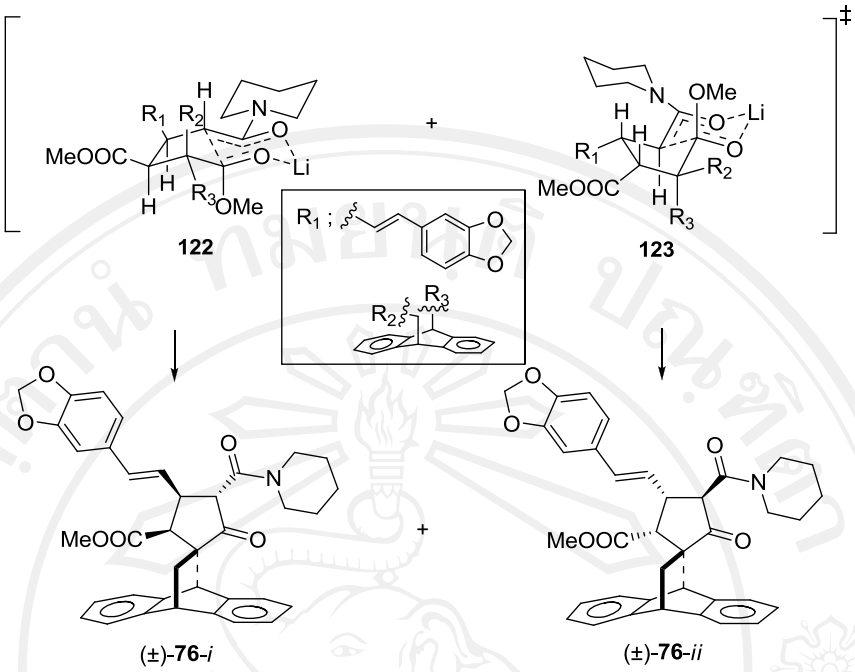

Scheme 3.2 Mechanism of tandem Michael addition–Dieckmann condensation reactions of (±)-**76**-*i* and (±)-**76**-*ii* (continued)

Result shown in Schemes 3.3 and 3.4 indicated that the transition states (**124 – 129**) were less favorable as compared to **122** and **123** because all large substituents occupied the more sterically demanding axial orientations.

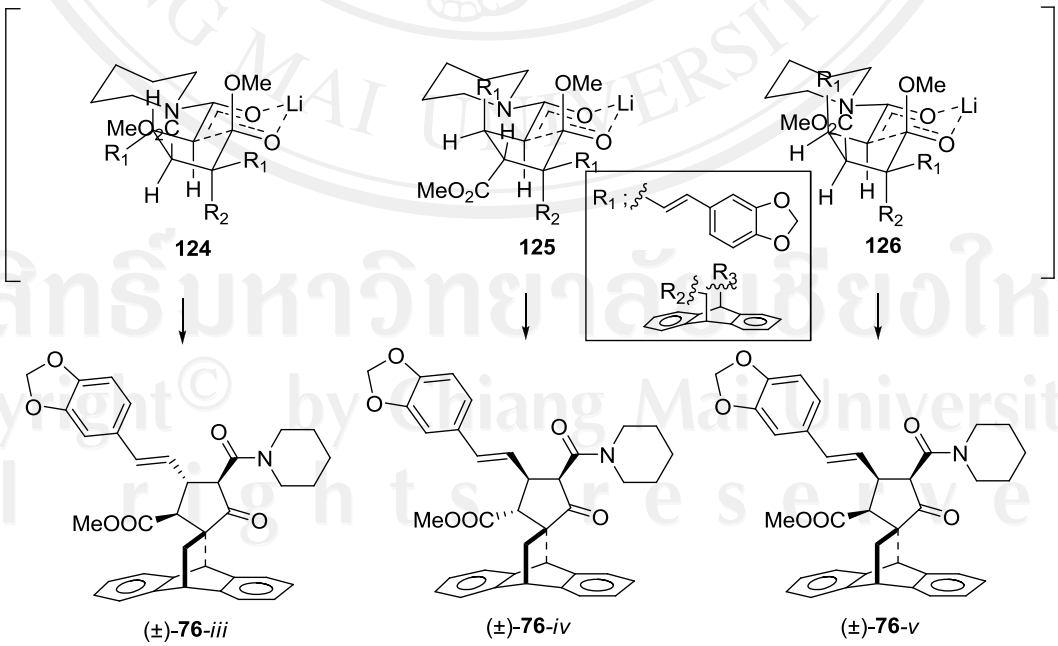

Scheme 3.3 Transition state of adducts (±)-**76**-*iii* – (±)-**76**-*v* *via* tandem Michael addition–Dieckmann condensation reactions

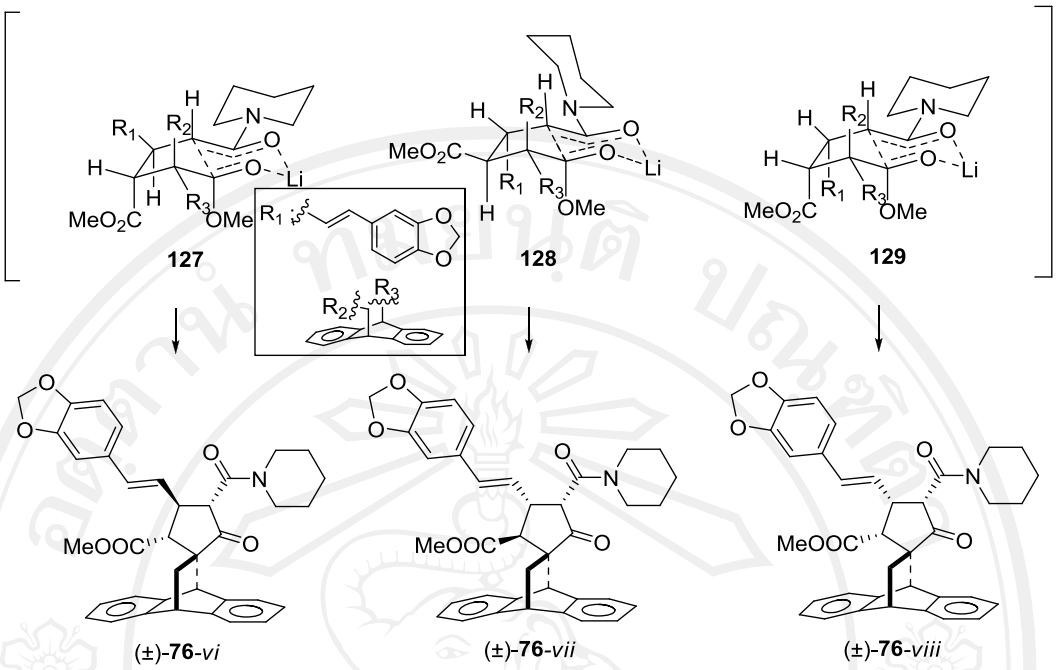

Scheme 3.4 Transition state of adducts (±)-**76**-*vi* – (±)-**76**-*viii* *via* tandem Michael addition–Dieckmann condensation reactions

3.1.2 Syntheses of 2,2-dimethyl-3-methoxycarbonyl-4-(2-(3,4-methylene-dioxy)phenyl)vinyl-5-piperidinecarbonyl-1-cyclopentanones ((±)-134-*i* and (±)-134-*ii*) from piperine (75)

Treatment of dimethyl 2,2-dimthyl succinate ((±)-**131**) with LDA (1.2 equiv.) at 0 °C (2 h) gave the corresponding ester enolate anions (**132** and **133**) which reacted with piperine (**75**), after stirring at room temperature for 3 days, to afford the desired product. The crude product was purified by flash column chromatographic separation (silica gel) to give diastereomeric cyclopentanones (±)-**134**-*i* in 23% yield and (±)-**134**-*ii* in 15% yield, as shown in Scheme 3.5.

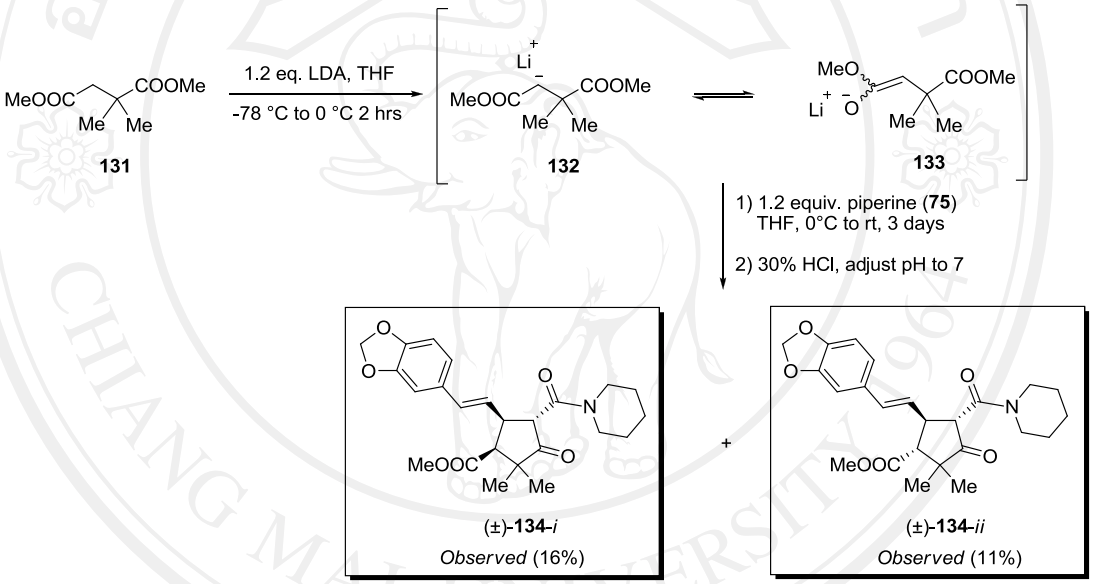

Scheme 3.5 Tandem Michael addition–Dieckmann condensation reactions (±)-**134**-*i* and (±)-**134**-*ii*

The relative stereochemistry of cyclopentanone (±)-**134**-*i* and (±)-**134**-*ii* were assigned by ^{1}H-NMR technique, as shown in Table 3.3, Figures 3.6 and 3.7, respectively.

Table 3.3 ^{1}H-NMR data of cyclopentanones (±)-**134**-*i* and (±)-**134**-*ii*

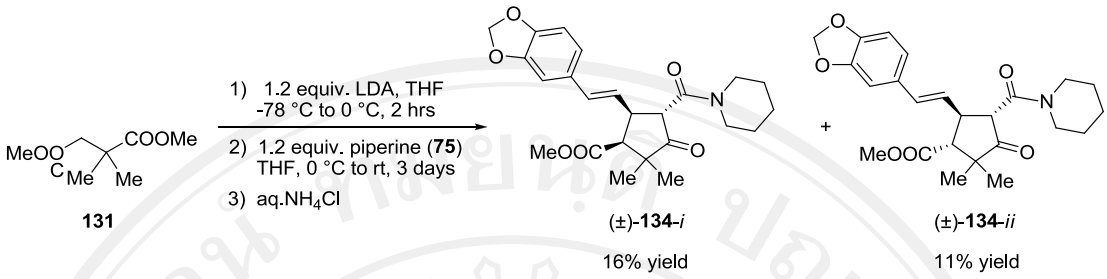

Compound	Physical property	m.p. (°C)	Chemical shift (δ, ppm)
(±)-**134**-*i*	white crystals	122.4–124.5	1.13 (s, 3H, CH_3-6 or 7), 1.25 (s, 3H, CH_3-6 or 7), 1.16–1.95 (m, 6H, CH_2-4′′′′, 5′′′′, 6′′′′), 3.03 (d, J = 6.0 Hz, 1H, H_a), 3.39–3.55, 3.73–3.88 (m, 4H, CH_2-3′′′′, 7′′′′), 3.70 (s, 3H, COOMe-2′), 4.04–4.17 (m, 1H, H_b), 4.11 (m, 1H, H_c), 5.91 (dd, J = 15.7, 7.5 Hz, 1H, H_d), 5.97 (s, 2H, CH_2-7′′′), 6.51 (d, J = 15.7 Hz, 1H, H_e), 6.73-6.80 (m, 2H, ArH-piperine-5′′′, 6′′′), 6.87 (s, 1H, ArH-piperine-2′′′) (Figure 3.6)
(±)-**134**-*ii*	white crystals	151.3–154.8	1.04 (s, 3H, CH_3-6 or 7), 1.27 (s, 3H, CH_3-6 or 7), 1.15–1.85 (m, 6H, CH_2-4′′′′, 5′′′′, 6′′′′), 2.73 (d, J = 11.0 Hz, 1H, H_a), 3.35– 3.56, 3.56–3.69, 3.69–3.82 (m, 4H, H-3′′′′, 7′′′′), 3.75 (s, 3H, COOMe-2′), 3.81 (d, J = 11.1 Hz, 1H, H_c), 4.09 (m, 1H, H_b), 5.90 (dd, J = 15.7, 7.5 Hz, 1H, H_d), 5.96 (s, 2H, CH_2-7′′′), 6.51 (d, J = 15.7 Hz, 1H, H_e), 6.75–6.79 (m, 1H, ArH-piperine-5′′′, 6′′′), 6.90 (d, J = 1.5 Hz,1H, ArH-piperine-2′′′) (Figure 3.7)

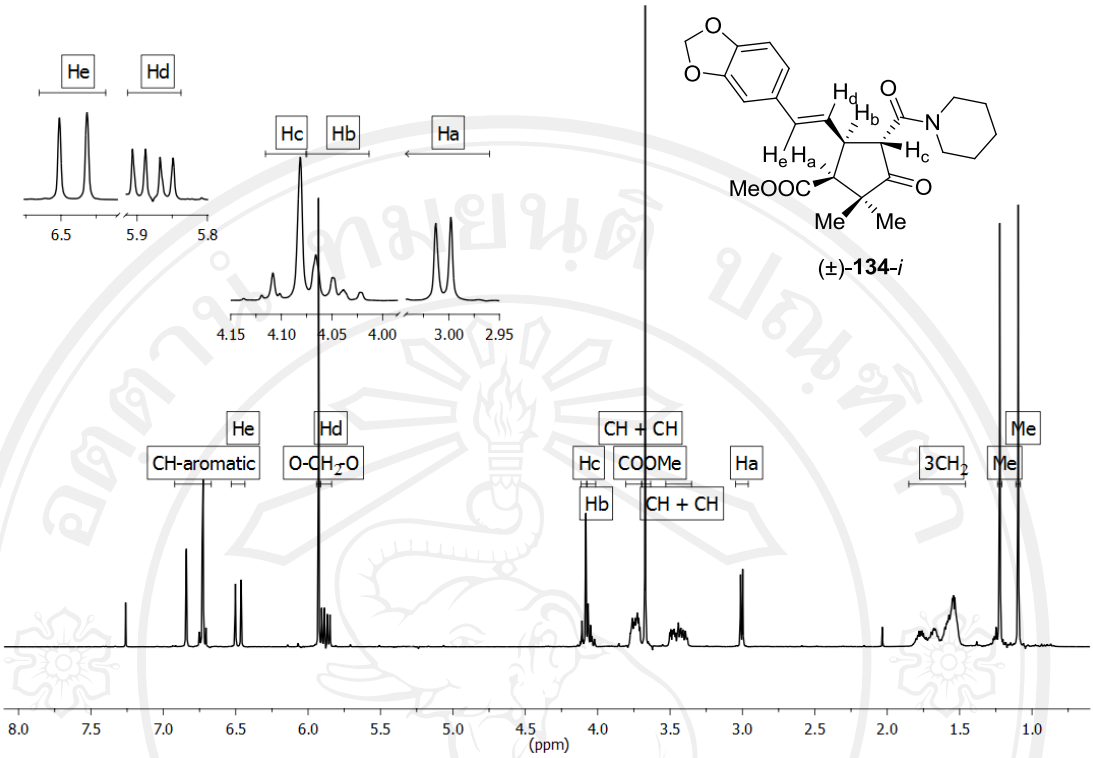

Figure 3.6 ^{1}H-NMR spectrum of cyclopentanone (±)-**134**-*i*

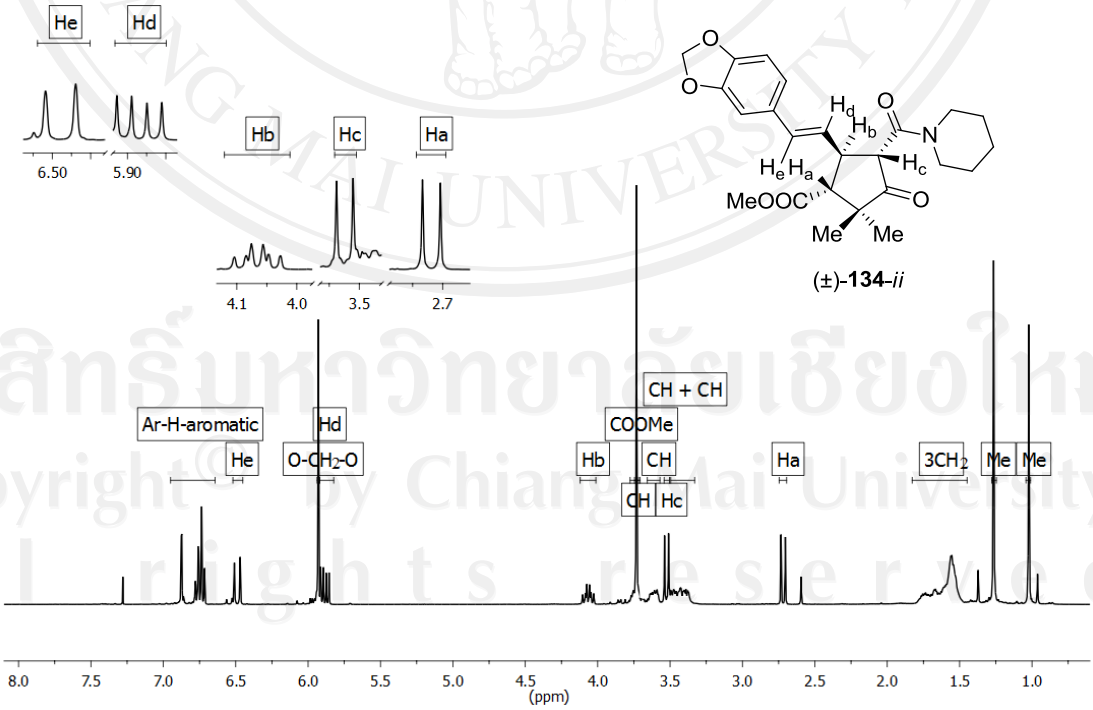

Figure 3.7 ^{1}H-NMR spectrum of cyclopentanone (±)-**134**-*ii*

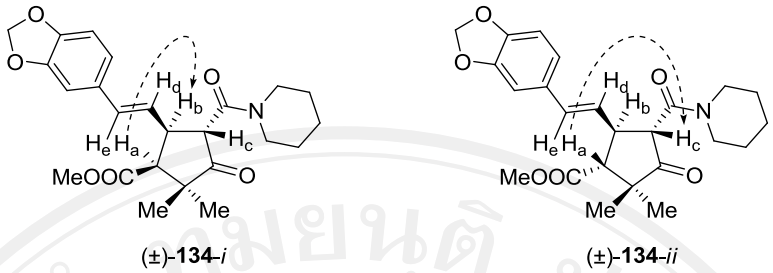

Figure 3.8 NOE correlations observed of cyclopentanones (±)-**134**-*i* and (±)-**134**-*ii*

The racemic cyclopentanone adduct (±)-**134**-*i* was characterized by ^{1}H-NMR techniques, the proton H_a was observed as doublet at δ 3.03 ppm (J = 6.0 Hz) which is *cis*-configuration with H_b, while the proton H_c was observed as multiplets at δ 4.11 ppm. The racemic cyclopentanone adducts (±)-**134**-*ii* displayed proton H_a as doublet at δ 2.73 ppm (J = 11.0 Hz) which is *trans*-configuration with H_b, while the proton H_c was observed as doublet at δ 3.81 ppm (J = 11.1 Hz) which displayed *trans*-configuration with H_b. Therefore, the configuration of cyclopentanone adduct (±)-**134**-*i* is *cis*-(3,4) and *trans*-(4,5) while other isomer is *trans*-(3,4) and *trans*-(4,5). The relative stereochemistry of cyclopentanone ring was determined by NOE enhancement as shown in Figure 3.8.

Results shown above indicated that the cyclopentanone adduct (±)-**134**-*i* was the major product derived from the tandem Michael addition–Dieckmann condensation reactions with the ester enolate anions (**132** and **133**) and piperine (**75**). This could be explained in terms of the favorable chair-like transition state (**132** and **133**) where upon all large substituents occupied the less sterically demanding equatorial orientations (Scheme 3.6). Therefore, transition state **136** was more favorable than transition state **138** and lead to cyclopentanone adduct (±)-**134**-*i* as major product.

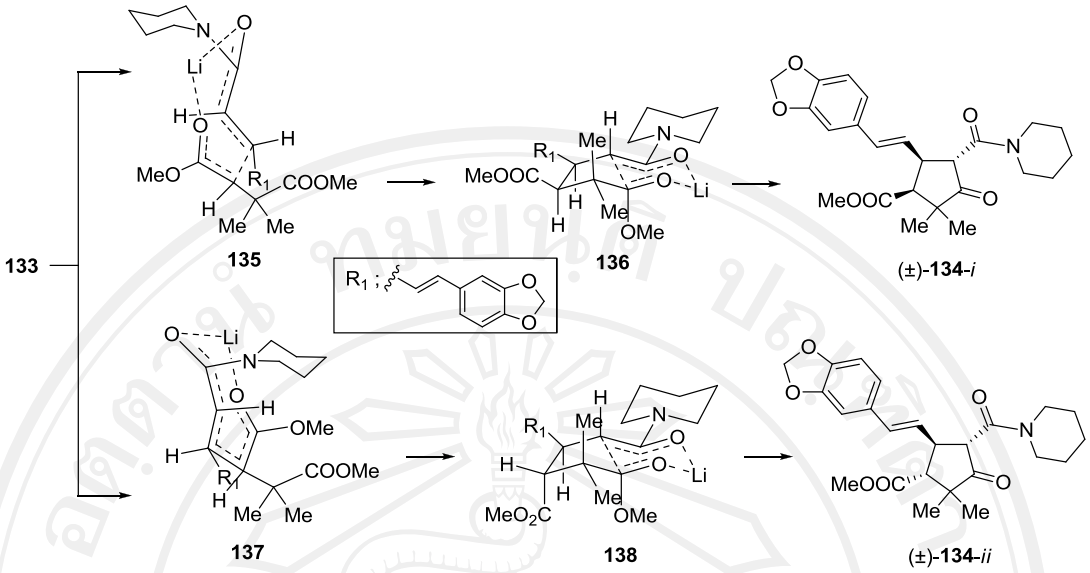

Scheme 3.6 Mechanism of tandem Michael addition–Dieckmann condensations reactions of (±)-**134**-*i* and (±)-**134**-*ii*

3.2 Syntheses of spirocyclopentanone–anthracene adducts (±)-115b-*i*, -*ii* – ((±)-115d-*i*, -*ii* from pentadiene amide derivatives 112b-d

3.2.1 Syntheses of 3′-methoxycarbonyl-4′-(2-(3,4-methylenedioxy)phenyl) vinyl-5′-pyrrolidinecarbonyl-1′-cyclopentanone-2′-spiro-11-9,10-dihydro-9,10-ethanoanthracenes ((±)-115b-*i* and (±)-115b-*ii*) from pentadiene amide 112b

Piperic acid (**105)** was treated with oxalyl chloride ($(COCl)_2$) (1.5 equiv.) at 0 °C allowed to room temperature 2 h. After the period, NEt_3 (2.0 equiv.) was added at 0 °C stirred for 15 minutes. Pyrrolidine (**109**, 2.5 equiv.,) was added at 0 °C allowed to room temperature 2 h. The crude product was purified by column chromatography (silica gel) to afford pentadiene amide **112b** in 70 %yield (Scheme 3.7). The physical properties, ^{1}H NMR data and ^{1}H NMR spectrum were shown in Table 3.4 and Figure 3.9.

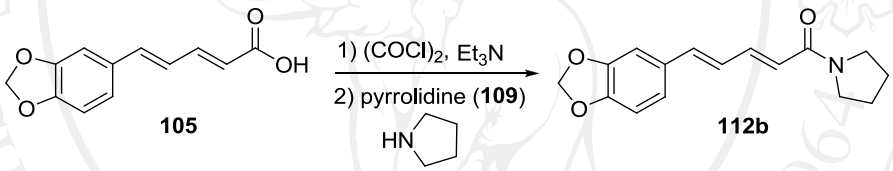

Scheme 3.7 Preparation reaction of pentadiene amide **112b**

Table 3.4 ^{1}H-NMR data of pentadiene amide **112b**

Physical property	m.p. (°C)	Chemical shift (δ, ppm)
yellow crystals	143.8–144.9	1.92 (brs, 4H, CH_2-3″, 4″), 3.56 (t (J = 6.8 Hz), 4H, CH_2-2″, 5″), 5.96 (s, 2H, CH_2-7′), 6.24 (d (J = 14.7 Hz), 1H, CH-2), 6.66–6.84 (m, 3H, CH-4, 5, 5′), 6.89 (dd (J = 8.0, 1.6 Hz), 1H, CH-6′), 6.97 (d (J = 1.6 Hz), 1H, CH-2′), 7.48 (dd (J = 14.8, 10.3 Hz), 1H, CH-3) (Figure 3.9)

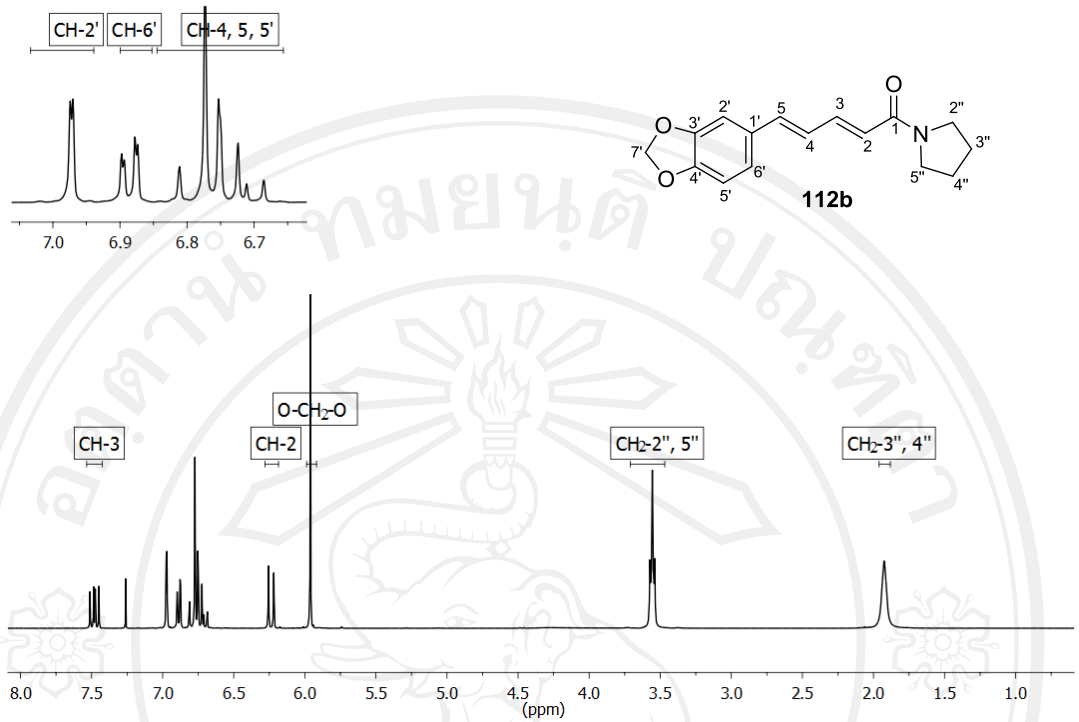

Figure 3.9 ^{1}H-NMR spectrum of pentadiene amide **112b**

Piperic acid (**105**) was treated with oxalyl chloride ($(COCl)_2$) to give acyl chloride (**142**). Then, acyl chloride (**142**) react with pyrrolidine (**113**) provided pentadiene amide **112b** *via* nucleophilic acyl substitution reaction (Scheme 3.8).[97]

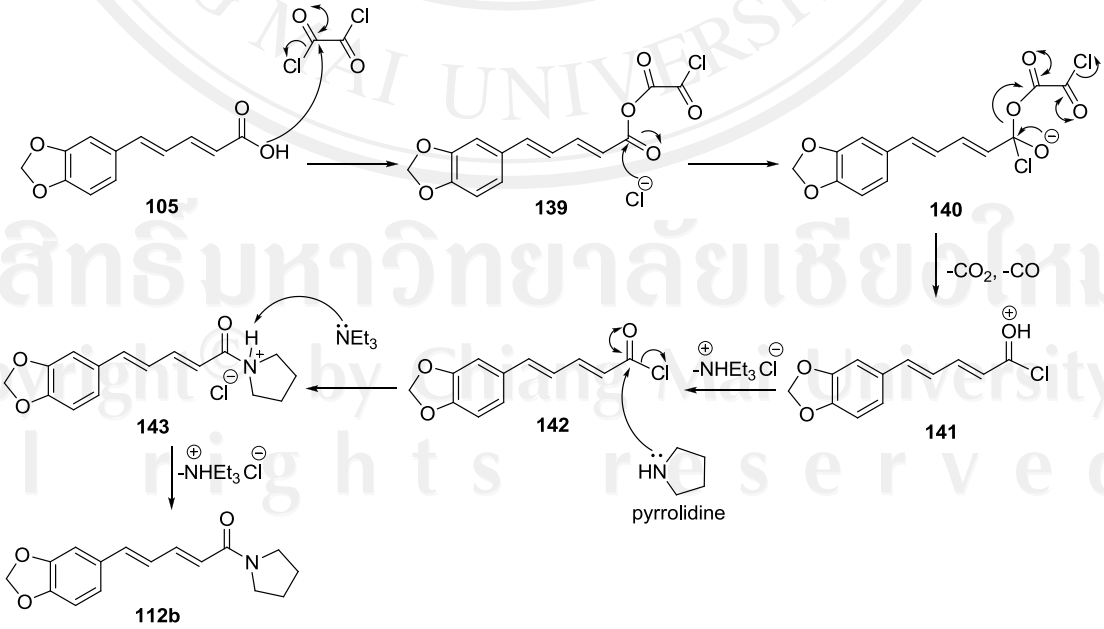

Scheme 3.8 The mechanism of nucleophilic acyl substitution reaction

Then, dimethyl itaconate–anthracene adduct ((±)-**74**) was reacted with pentadiene amide **112b** *via* tandem Michael addition–Dieckmann condensation reactions as shown in Scheme 3.9.

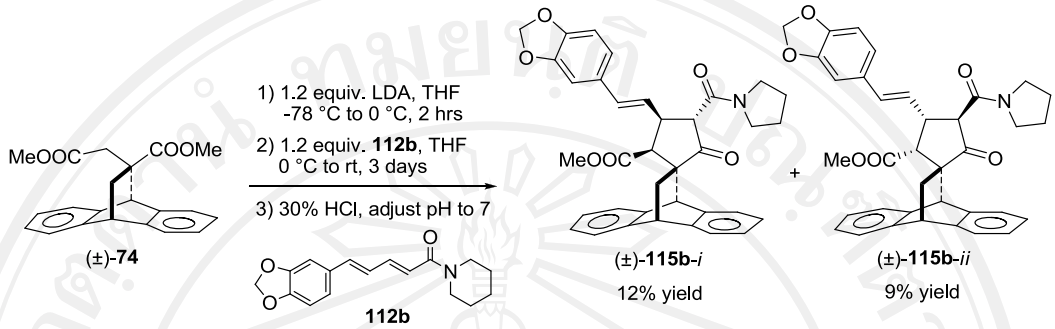

Scheme 3.9 Tandem Michael addition–Dieckmann condensation reactions of (±)-**115b**-*i* and (±)-**115b**-*ii*

An enolate anion (**118** or **119**) of dimethyl itaconate–anthracene adduct, generated from (±)-**74** by treatment with lithium diisopropylamide (LDA, 1.2 equiv.) in THF at 0 °C, readily reacted with pentadiene amide **112b** at 0 °C to provide, after leaving the reaction mixture to stir at room temperature for 3 days followed by 10% hydrochloride acid work-up, the spirocyclopentanone–anthracene adduct as mixture of diastereoisomers. The crude product was purified by flash column chromatography on silica gel to afford diastereomeric spirocyclopentanone–anthracene adducts (±)-**115b**-*i* in 12% yield and (±)-**115b**-*ii* in 9% yield.

Table 3.5 ^{1}H-NMR data of spirocyclopentanone–anthracene adducts (±)-**115b**-*i* and (±)-**115b**-*ii*

Compound	Physical property	m.p. (°C)	Chemical shift (δ, ppm)
(±)-**115b**-*i*	white crystals	121.1–125.4	1.76–1.99 (m, 4H, CH_2-3′′′′′, 4′′′′′), 1.30, 2.21, 4.30 (ABX system (J = 12.7, 2.8, 2.5 Hz), 3H, H_a, H_b, H_x), 2.78 (d (J = 7.0 Hz), 1H, H_c), 3.38–3.47, 3.88–4.00 (m, 2H, CH_2-2′′′′′ or 5′′′′′), 3.48–3.61 (m, 2H, CH_2-2′′′′′ or 5′′′′′), 3.53 (s, 3H, COOMe-2′′), 3.72 (d (J = 10.1 Hz), 1H, H_e), 4.33–4.41 (m, 1H, H_d), 4.92 (s, 1H, H_y), 5.79 (dd (J = 15.7, 8.1 Hz), 1H, H_f), 5.93 (s, 2H, CH_2-7′′′′), 6.53 (d (J = 15.6 Hz), 1H, H_g), 6.74 (d (J = 1.6 Hz), 2H, ArH-5′′′′, 6′′′′), 6.83 (s, 1H, ArH-2′′′′), 6.99–7.42 (m, 8H, ArH–anthracene) (Figure 3.10)
(±)-**115b**-*ii*	white crystals	226.5–230.1	1.68–1.85 (m, 4H, CH_2-3′′′′′, 4′′′′′), 1.90, 2.10, 4.36 (ABX system (J = 12.8, 3.3, 2.4 Hz), 3H, H_a, H_b, H_x), 2.31 (d (J = 6.6 Hz), 1H, H_c), 3.27–3.46 (m, 2H, CH_2-2′′′′′ or 5′′′′′), 3.92–4.00 (m, 2H, CH_2-2′′′′′ or 5′′′′′), 3.77 (s, 3H, COOMe-2′′), 3.80 (d (J = 11.3 Hz), 1H, H_e), 3.86–3.92 (m, 1H, H_d) 4.41 (s, 1H, H_y), 5.69 (dd (J = 15.7, 7.8 Hz), 1H, H_f), 5.91 (s, 2H, CH_2-7′′′′), 6.34 (d (J = 15.7 Hz), 1H, H_g), 6.62–6.74 (m, 2H, ArH-5′′′′, 6′′′′), 6.77 (d (J = 1.4 Hz), 1H, ArH-2′′′′), 6.99–7.45 (m, 8H, ArH–anthracene) (Figure 3.11)

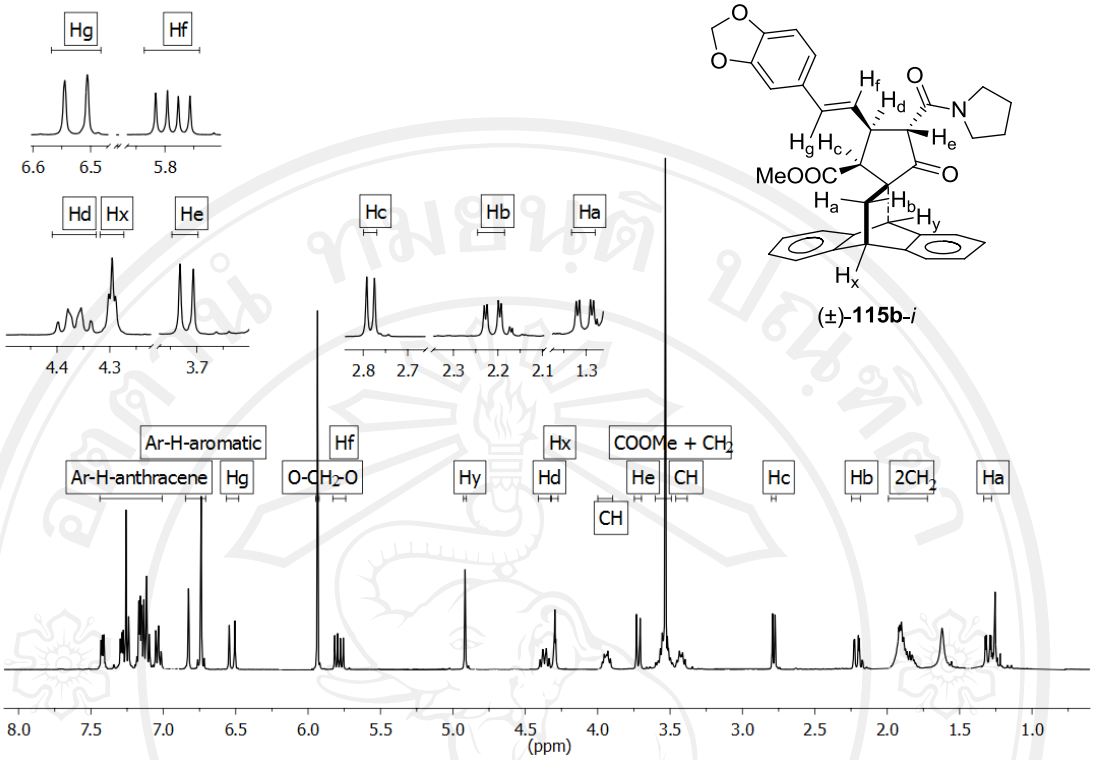

Figure 3.10 ^{1}H-NMR spectrum of spirocyclopentanone–anthracene adduct (±)-**115b**-*i*

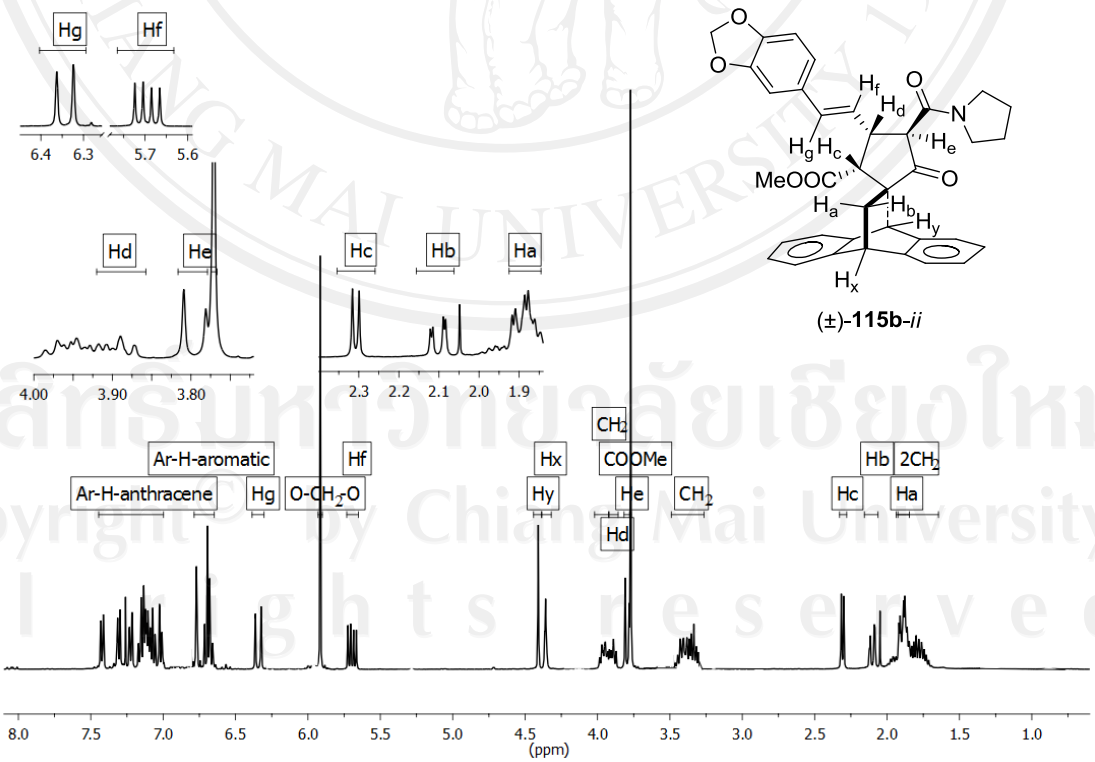

Figure 3.11 ^{1}H-NMR spectrum of spirocyclopentanone–anthracene adduct (±)-**115b**-*ii*

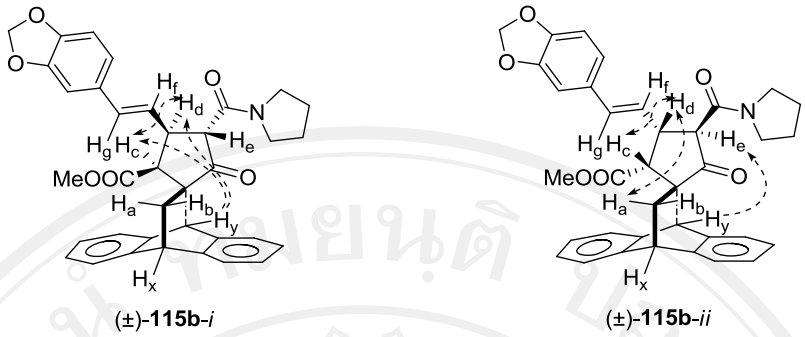

Figure 3.12 NOE correlations observed of spirocyclopentanone–anthracene adducts (±)-**115b**-*i* and (±)-**115b**-*ii*

The mechanism of tandem Michael addition–Dieckmann condensation reactions of spirocyclopentanone–anthracene adducts (±)-**115b**-*i* and (±)-**115b**-*ii* were described in 3.1.1. The relative stereochemistry of the spirocyclopentanone–anthracene adducts (±)-**115b**-*i* and (±)-**115b**-*ii* were assigned by ^{1}H-NMR technique as depicted in Table 3.5, Figures 3.10 and 3.11, respectively.

The spirocyclopentanone–anthracene adduct (±)-**115b**-*i* was characterized by NMR technique, the proton H_c was observed at δ 2.78 ppm as doublet (J = 7.0 Hz) which is *cis*-configuration with proton H_d. The proton H_e was observed at δ 3.72 ppm as doublet (J = 10.1 Hz) which is *trans*-configuration with proton H_d. The proton H_f was observed at δ 5.79 ppm as doublet of doublets (J = 15.7, 8.1 Hz) which is *trans*-configuration with proton H_g and proton H_d. The relative stereochemistry of cyclopentanone ring was determined by NOE enhancement. The proton H_y is enhanced with proton H_c and H_d which is proton H_c and proton H_d on the lower-face, proton H_e on upper-face as shown in Figure 3.12.

The spirocyclopentanone–anthracene adduct (±)-**115b**-*ii* was characterized by NMR techniques, the proton H_c was observed at δ 2.31 ppm as doublet (J = 6.6 Hz) which is *cis*-configuration with proton H_d. The proton H_e was observed at δ 3.80 ppm as doublet (J = 11.3 Hz) which is *trans*-configuration with proton H_d. The proton H_f was observed at δ 5.69 ppm as doublet of doublets (J = 15.7, 7.8 Hz) which is *trans*-configuration with proton H_g and proton H_d. The relative stereochemistry of cyclopentanone ring was determined by NOE enhancement. The proton H_d is enhanced with proton H_c and proton H_a which is proton H_c and proton H_d on the upper-face, proton H_e on lower-face as shown in Figure 3.12.

3.2.2 Syntheses of 5′-(*N*,*N*-diisopropylcarboxamid-1-yl)-3′-methoxycarbonyl-4′-(2-(3,4-methylenedioxy)phenyl)vinyl-1′-cyclopentanone-2′-spiro-11-9,10-dihydro-9,10-ethanoanthracene ((±)-115c-*i* and (±)-115c-*ii*) from pentadiene amide 112c

Piperic acid (**105**) (1.23 g, 5.6 mmol), oxalyl chloride ($(COCl)_2$) (1.5 equiv., 0.7 ml, 8.4 mmol), NEt_3 (2.0 equiv., 1.2 ml, 8.4 mmol), diisopropylamine (**110**) (1.5 equiv., 1.2 ml, 8.4 mmol). Purification of the crude product by column chromato graphy (silica gel) affords pentadiene amide **112c** in 82% yield (Scheme 3.10). The physical properties, ^{1}H NMR data and ^{1}H NMR spectrum were shown in Table 3.6 and Figure 3.13.

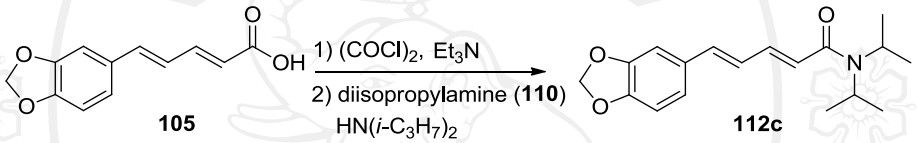

Scheme 3.10 Preparation reaction of pentadiene amide **112c**

Table 3.6 ^{1}H-NMR data of pentadiene amide **112c**

Physical property	m.p. (°C)	Chemical shift (δ, ppm)
yellow crystals	85.9–88.0	1.28 (brs, 6H, CH_3-3″, 4″, 6″ or 7″), 1.34 (brs, 6H, CH_3 -3″, 4″, 6″ or 7″), 3.81 (brs, 1H, CH-2″ or 5″), 4.04 (brs, 1H, CH-2″ or 5″), 5.94 (s, 2H, CH_2-7′), 6.36 (d (J = 14.6 Hz), 1H, CH-2), 6.69–6.73 (m, 2H, CH-4, 5′), 6.75 (d (J = 8.0 Hz), 1H, CH-5), 6.87 (dd (J = 8.1, 1.7 Hz), 1H, CH-6′), 6.97 (d (J = 1.6 Hz), 1H, CH-2′), 7.42 (ddd (J = 14.6, 6.2, 4.1 Hz), 1H, CH-3) (Figure 3.13)

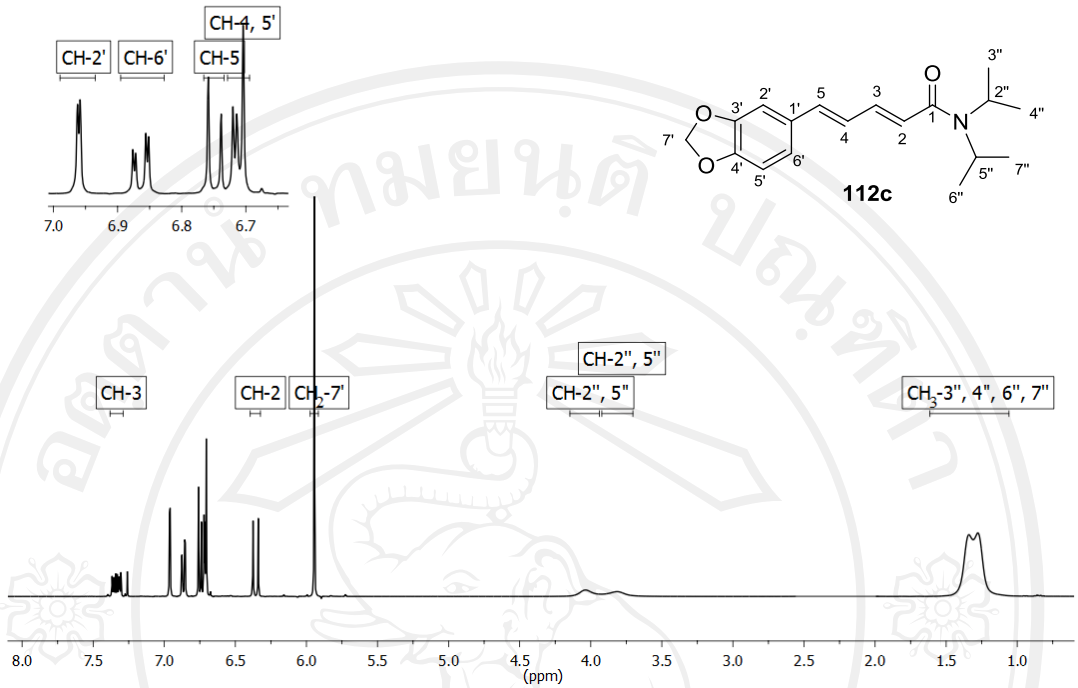

Figure 3.13 ^{1}H-NMR spectrum of pentadiene amide **112c**

Then, dimethyl itaconate–anthracene adduct ((±)-**74**) was reacted with pentadiene amide **112c** *via* tandem Michael addition–Dieckmann condensation reactions (Scheme 3.11).

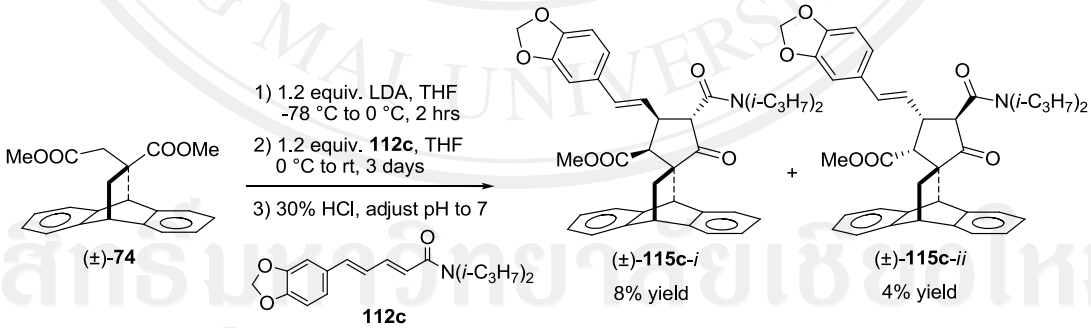

Scheme 3.11 Tandem Michael addition–Dieckmann condensation reactions of (±)-**115c**-*i* and (±)-**115c**-*ii*

An enolate anion (**118** or **119**) of dimethyl itaconate–anthracene adduct, generated from (±)-**74** by treatment with lithium diisopropylamide (LDA, 1.2 equiv.) in THF at 0 °C, readily reacted with pentadiene amide **112c** at 0 °C to provide, after leaving the reaction mixture to stir at room temperature for 3 days followed by 10% hydrochloride acid work-up, the spirocyclopentanone–anthracene adduct as mixture

of diastereoisomers. The crude product was purified by flash column chromatography on silica gel to afford diastereomeric spirocyclopentanone–anthracene adducts (±)-**115c**-*i* in 8% yield and (±)-**115c**-*ii* in 4% yield.

Table 3.7 ^{1}H-NMR data of spirocyclopentanone–anthracene adducts (±)-**115c**-*i* and (±)-**115c**-*ii*

Compound	Physical property	m.p. (°C)	Chemical shift (δ, ppm)
(±)-**115c**-*i*	white crystals	118.5–121.5	1.13 (d (J = 6.7 Hz), 3H, CH_3-3′′′′′, 4′′′′′, 6′′′′′ or 7′′′′′), 1.20 (d (J = 6.5 Hz), 3H, CH_3-3′′′′′, 4′′′′′, 6′′′′′ or 7′′′′′), 1.44 (d (J = 6.7 Hz), 3H, CH_3-3′′′′′, 4′′′′′, 6′′′′′ or 7′′′′′), 1.50 (d (J = 6.7 Hz), 3H, CH_3-3′′′′′, 4′′′′′, 6′′′′′ or 7′′′′′), 1.29, 2.22, 4.30 (ABX system (J = 12.7, 2.8, 2.6 Hz), 3H, H_a, H_b, H_x), 2.81 (d (J = 7.1 Hz), 1H, H_c), 3.37–3.60 (m, 1H, CH-2′′′′′ or 5′′′′′), 4.38–4.47 (m, 1H, CH-2′′′′′ or 5′′′′′), 3.53 (s, 3H, COOMe-2′′), 3.81 (d (J = 9.9 Hz), 1H, H_e), 4.49–4.55 (m, 1H, H_d), 4.87 (s, 1H, H_y), 5.83 (dd (J = 15.7, 7.5 Hz), 1H, H_f), 5.93 (s, 2H, CH_2-7′′′′), 6.48 (d (J = 15.6 Hz), 1H, H_g), 6.72 (d (J = 1.4 Hz), 2H, ArH-5′′′′, 6′′′′), 6.81 (s, 1H, ArH-2′′′′), 6.96–7.45 (m, 8H, ArH–anthracene) (Figure 3.14)

Table 3.7 ^{1}H-NMR data of spirocyclopentanone–anthracene adducts (±)-**115c**-*i* and (±)-**115c**-*ii* (continued)

Compound	Physical property	m.p. (°C)	Chemical shift (δ, ppm)
(±)-**115c**-*ii*	white crystals	145.4–148.5	1.11 (d (J = 6.7 Hz), 3H, CH_3-3′′′′′ or 4′′′′′ or 6′′′′′ or 7′′′′′), 1.20–1.30 (m, 9H, CH_3-3′′′′′ or 4′′′′′ or 6′′′′′ or 7′′′′′), 1.88, 2.12, 4.35 (ABX system (J = 12.8, 3.1, 2.4 Hz), 3H, H_a, H_b, H_x), 2.30 (d (J = 6.2 Hz), 1H, H_c), 3.33–3.48 (m, 1H, CH-2′′′′′ or 5′′′′′), 4.16–4.30 (m, 1H, CH-2′′′′′ or 5′′′′′), 3.74 (s, 3H, COOMe-2′′), 3.91 (d (J = 11.4 Hz), 1H, H_e), 3.80–3.91 (m, 1H, H_d), 4.43 (s, 1H, H_y), 5.72 (dd (J = 15.7, 7.0 Hz), 1H, H_f), 5.91 (s, 2H, CH_2-7′′′′), 6.29 (d (J = 15.7 Hz), 1H, H_g), 6.62 (dd (J = 8.0, 1.5 Hz), 1H, ArH-5′′′′ or 6′′′′), 6.69 (d (J = 8.0 Hz), 1H, ArH-5′′′′ or 6′′′′), 6.71–6.76 (m, 1H, ArH-2′′′′), 6.95–7.45 (m, 8H, ArH–anthracene) (Figure 3.15)

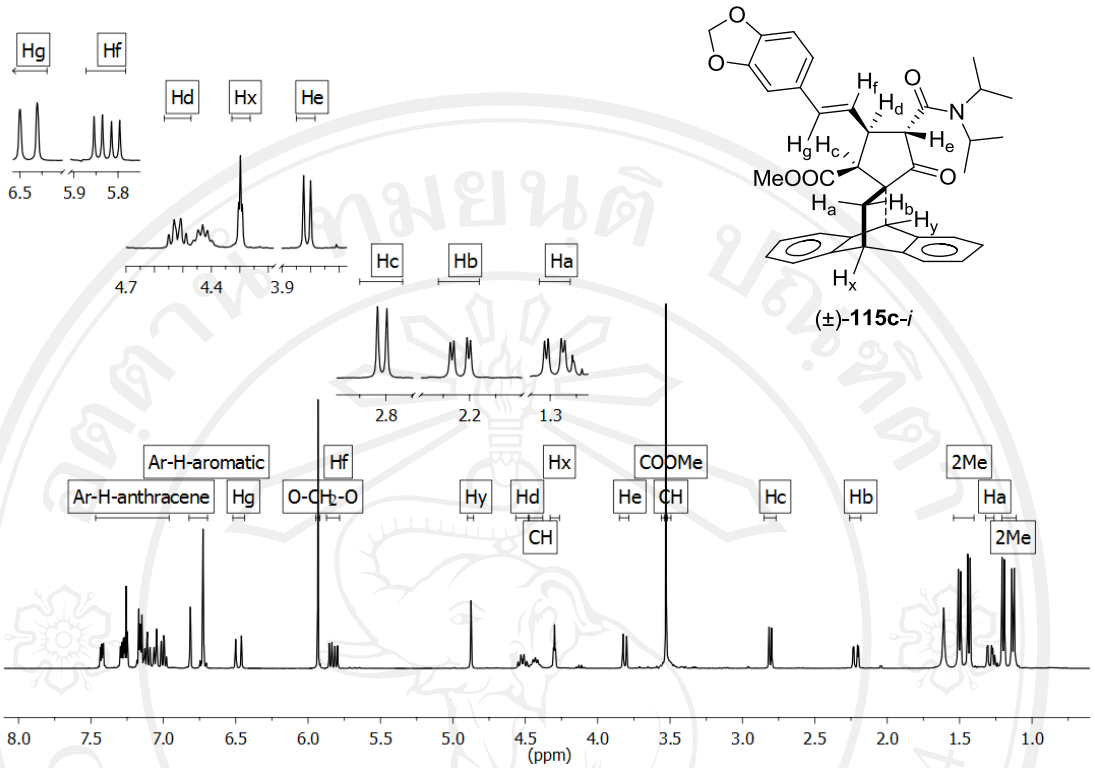

Figure 3.14 ^{1}H-NMR spectrum of spirocyclopentanone–anthracene adduct (±)-**115c**-*i*

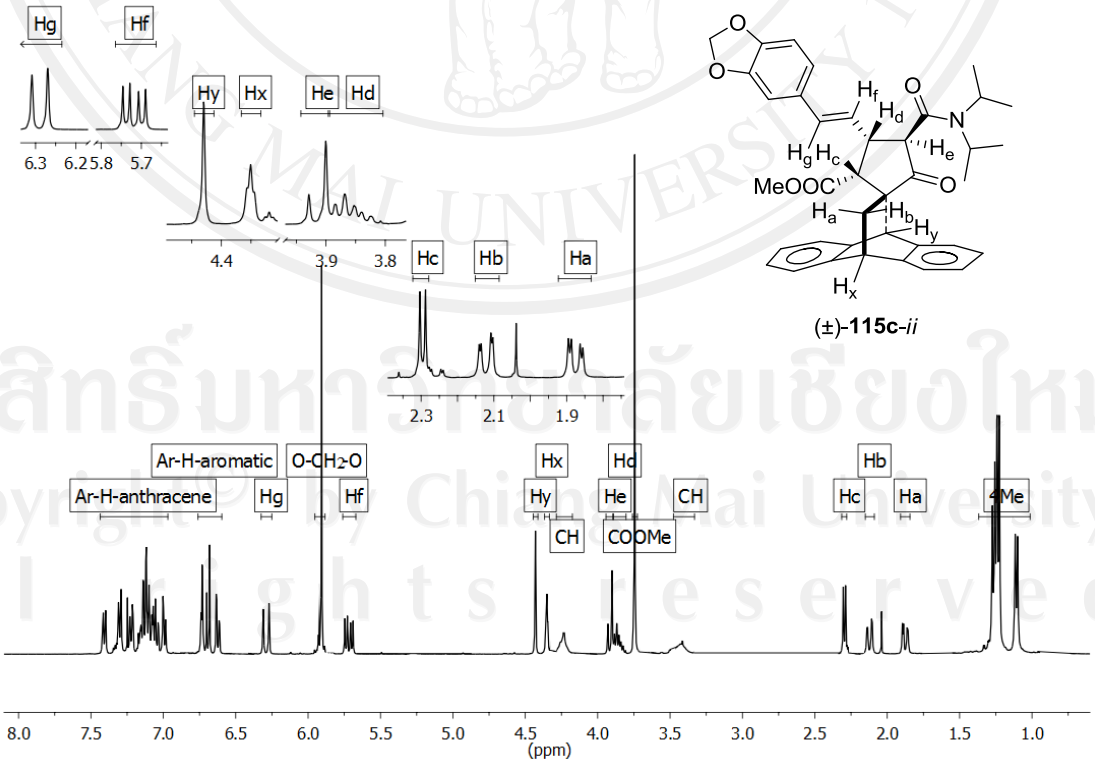

Figure 3.15 ^{1}H-NMR spectrum of spirocyclopentanone–anthracene adduct (±)-**115c**-*ii*

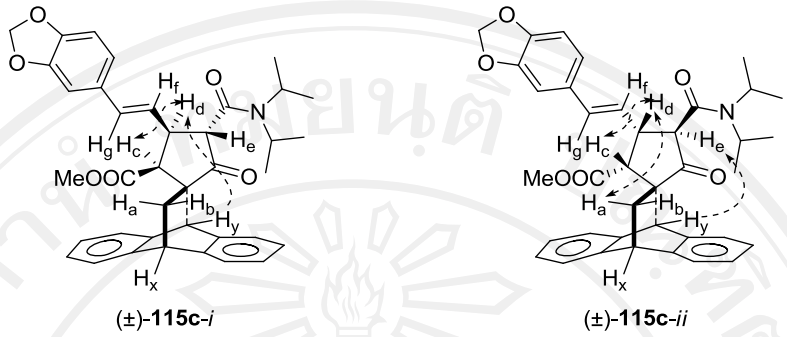

Figure 3.16 NOE correlations observed of spirocyclopentanone–anthracene adduct (±)-**115c**-*i* and (±)-**115c**-*ii*

The mechanism of tandem Michael addition–Dieckmann condensation reactions of spirocyclopentanone–anthracene adducts (±)-**115c**-*i* and (±)-**115c**-*ii* were described in 3.1.1. The relative stereochemistry of the spirocyclopentanone–anthracene adducts (±)-**115c**-*i* and (±)-**115c**-*ii* were assigned by ^{1}H-NMR technique as depicted in Table 3.9, Figures 3.18 and 3.19, respectively.

The spirocyclopentanone–anthracene adducts (±)-**115c**-*i* was characterized by NMR techniques, the proton H_c was observed at δ 2.81 ppm as doublet (J = 7.1 Hz) which is *cis*-configuration with proton H_d. The proton H_e was observed at δ 3.81 ppm as doublet (J = 9.9 Hz) which is *trans*-configuration with proton H_d. The proton H_f was observed at δ 5.83 ppm as doublet of doublets (J = 15.7, 7.5 Hz) which is *trans*-configuration with proton H_g and proton H_d. The relative stereochemistry of cyclopentanone ring was determined by NOE enhancement. The proton H_y is enhanced with proton H_d, proton H_d is enhanced with proton H_c which are proton H_c and proton H_d on the lower-face, proton H_e on upper-face as shown in Figure 3.16.

The spirocyclopentanone–anthracene adducts (±)-**115c**-*ii* was characterized by NMR techniques, the proton H_c was observed at δ 2.30 ppm as doublet (J = 6.2 Hz) which is *cis*-configuration with proton H_d. The proton H_e was observed at δ 3.91 ppm as doublet (J = 11.4 Hz) which is *trans*-configuration with proton H_d. The proton H_f was observed at δ 5.72 ppm as doublet of doublets (J = 15.7, 7.0 Hz) which is *trans*-configuration with proton H_g and proton H_d. The relative stereochemistry of

cyclopentanone ring was determined by NOE enhancement. The proton H_d is enhanced with proton H_c and proton H_a which is proton H_c and proton H_d on the upper-face, proton H_e on lower-face as shown in Figure 3.16.

3.2.3 Syntheses of 5′-(*N*,*N*-dibutylcarboxamid-1-yl)-3′-methoxycarbonyl-4′-(2-(3,4-methylenedioxy)phenyl)vinyl-1′-cyclopentanone-2′-spiro-11-9,10-dihydro-9,10-ethanoanthracene ((±)-115d-*i* and (±)-115d-*ii*) from pentadiene amide 112d

Piperic acid (**105**) (3.10 g, 14.2 mmol), oxalyl chloride ($(COCl)_2$) (1.5 equiv., 1.8 ml, 21.3 mmol), NEt_3 (1.5 equiv., 3.0 ml, 21.3 mmol), dibutylamine (**111**) (1.5 equiv., 3.6 ml, 21.3 mmol). Purification of the crude product by column chromatography (silica gel) affords pentadiene amide **112d** in 86% yield (Scheme 3.12). The physical properties, ^{1}H NMR data and ^{1}H NMR spectrum were shown in Table 3.8 and Figure 3.17.

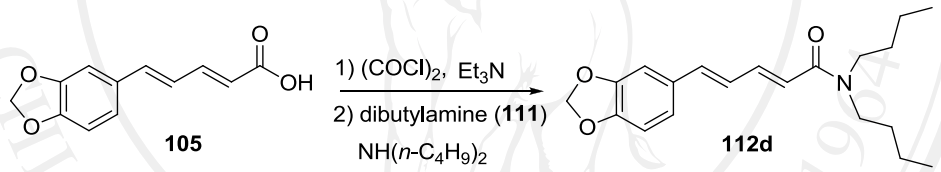

Scheme 3.12 Preparation reaction pentadiene amide **112d**

Table 3.8 ^{1}H-NMR data of pentadiene amide **112d**

Physical property	m.p. (°C)	Chemical shift (δ, ppm)
yellow crystals	95.1–96.2	0.85–1.02 (m, 6H, CH_3-5″, 9″), 1.26–1.41 (m, 4H, CH_2-4″, 8″), 1.43–1.66 (m, 4H, CH_2-3″, 7″), 3.30 (t (J = 7.1 Hz), 2H, CH_2-2″ or 6″), 3.37 (t (J = 7.1 Hz), 2H, CH_2-2″ or 6″), 5.94 (s, 2H, CH_2-7′), 6.33 (d (J = 14.6 Hz), 1H, CH-2), 6.66–6.80 (m, 3H, CH-4, 5, 5′), 6.87 (dd (J = 8.1, 1.7 Hz), 1H, CH-6′), 6.97 (d (J = 1.6 Hz), 1H, CH-2′), 7.42 (ddd (J = 14.6, 6.5, 3.8 Hz), 1H, CH-3) (Figure 3.17)

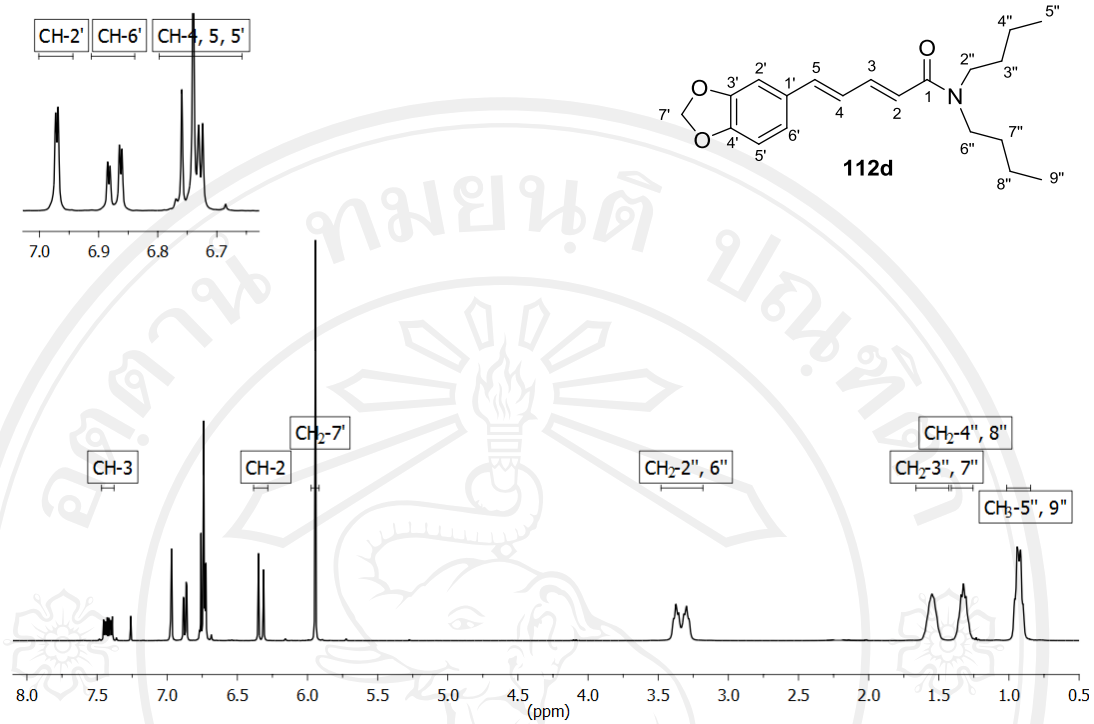

Figure 3.17 ^{1}H-NMR spectrum of pentadiene amide **112d**

Then, dimethyl itaconate–anthracene adduct ((±)-**74**) was reacted with pentadiene amide **112d** *via* tandem Michael addition–Dieckmann condensation reactions (Scheme 3.13).

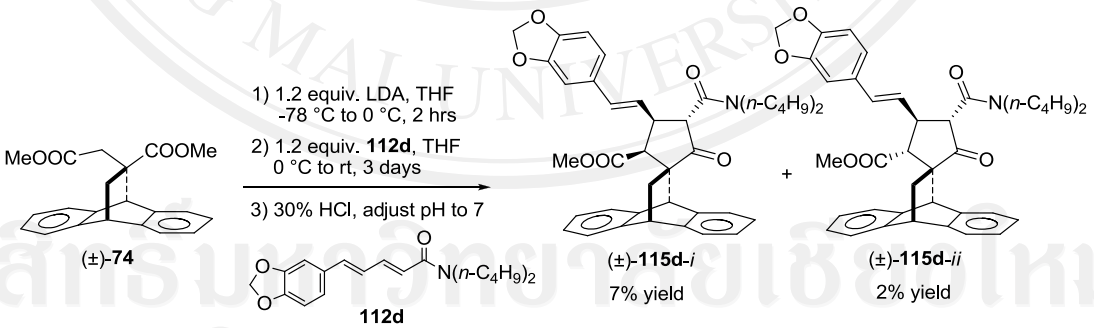

Scheme 3.13 Tandem Michael addition–Dieckmann condensation reactions of (±)-**115d**-*i* and (±)-**115d**-*ii*

An enolate anion (**118** or **119**) of dimethyl itaconate–anthracene adduct, generated from (±)-**74** by treatment with lithium diisopropylamide (LDA, 1.2 equiv.) in THF at 0 °C, readily reacted with pentadiene amide **112d** at 0 °C to provide, after leaving the reaction mixture to stir at room temperature for 3 days followed by 10%

hydrochloride acid work-up, the spirocyclopentanone–anthracene adduct as mixture of diastereoisomers.

The crude product was purified by flash column chromatography on silica gel to afford diastereomeric spirocyclopentanone–anthracene adducts (±)-**115d**-*i* in 7% yield and (±)-**115d**-*ii* in 2% yield.

Table 3.9 ^{1}H-NMR data of spirocyclopentanone–anthracene adducts (±)-**115d**-*i* and (±)-**115d**-*ii*

Compound	Physical property	m.p. (°C)	Chemical shift (δ, ppm)
(±)-**115d**-*i*	white crystals	79.5–81.4	0.86 (t (J = 7.3 Hz), 3H, CH_3-5′′′′′ or 9′′′′′), 0.96 (t (J = 7.3 Hz), 3H, CH_3-5′′′′′ or 9′′′′′), 1.20–1.59 (m, 8H, CH_2-3′′′′′, 4′′′′′, 7′′′′′, 8′′′′′), 1.30, 2.20, 4.30 (ABX system (J = 12.7, 2.6, 2.5 Hz), 3H, H_a, H_b, H_x), 2.80 (d (J = 6.9 Hz), 1H, H_c), 3.03–3.16 (m, 2H, CH_2-2′′′′′ or 6′′′′′), 3.65–3.79 (m, 2H, CH_2-2′′′′′ or 6′′′′′), 3.54 (s, 3H, COOMe-2′′), 3.82 (d (J = 10.1 Hz), 1H, H_e), 4.35–4.44 (m, 1H, H_d), 4.90 (s, 1H, H_y), 5.76 (dd (J = 15.7, 8.2 Hz), 1H, H_f), 5.94 (s, 2H, CH_2-7′′′′), 6.54 (d (J = 15.6 Hz), 1H, H_g), 6.73 (d (J = 0.9 Hz), 2H, ArH-5′′′′, 6′′′′), 6.81 (s, 1H, ArH-2′′′′), 6.97–7.45 (m, 8H, ArH–anthracene) (Figure 3.18)

Table 3.9 ^{1}H-NMR data of spirocyclopentanone–anthracene adducts (±)-**115d**-*i* and (±)-**115d**-*ii* (continued)

Compound	Physical property	m.p. (°C)	Chemical shift (δ, ppm)
(±)-**115d**-*ii*	white crystals	69.8–72.1	0.82 (t (J = 7.3 Hz), 3H, CH_3-5′′′′′ or 9′′′′′), 0.97 (t (J = 7.3 Hz), 3H, CH_3-5′′′′′ or 9′′′′′), 1.17–1.58 (m, 8H, CH_2-3′′′′′, 4′′′′′, 7′′′′′, 8′′′′′), 2.12, 2.29, 4.30 (ABX system (J = 12.2, 3.0, 2.4 Hz), 3H, H_a, H_b, H_x), 2.65 (d (J = 12.2 Hz), 1H, H_c), 2.94 (s, 3H, COOMe-2′′), 2.99–3.13 (m, 2H, CH_2-2′′′′′ or 6′′′′′), 3.50–3.77 (m, 2H, CH_2-2′′′′′ or 6′′′′′), 3.36 (d (J = 9.6 Hz), 1H, H_e), 4.51–4.59 (m, 1H, H_d), 5.03 (s, 1H, H_y), 5.77 (dd (J = 15.6, 8.2 Hz), 1H, H_f), 5.92 (d (J = 0.8 Hz), 2H, CH_2-7′′′′), 6.57 (d (J = 15.6 Hz), 1H, H_g), 6.69–6.78 (m, 2H, ArH-5′′′′, 6′′′′), 6.83 (d (J = 0.9 Hz), 1H, ArH-2′′′′), 6.90–7.33 (m, 8H, ArH–anthracene) (Figure 3.19)

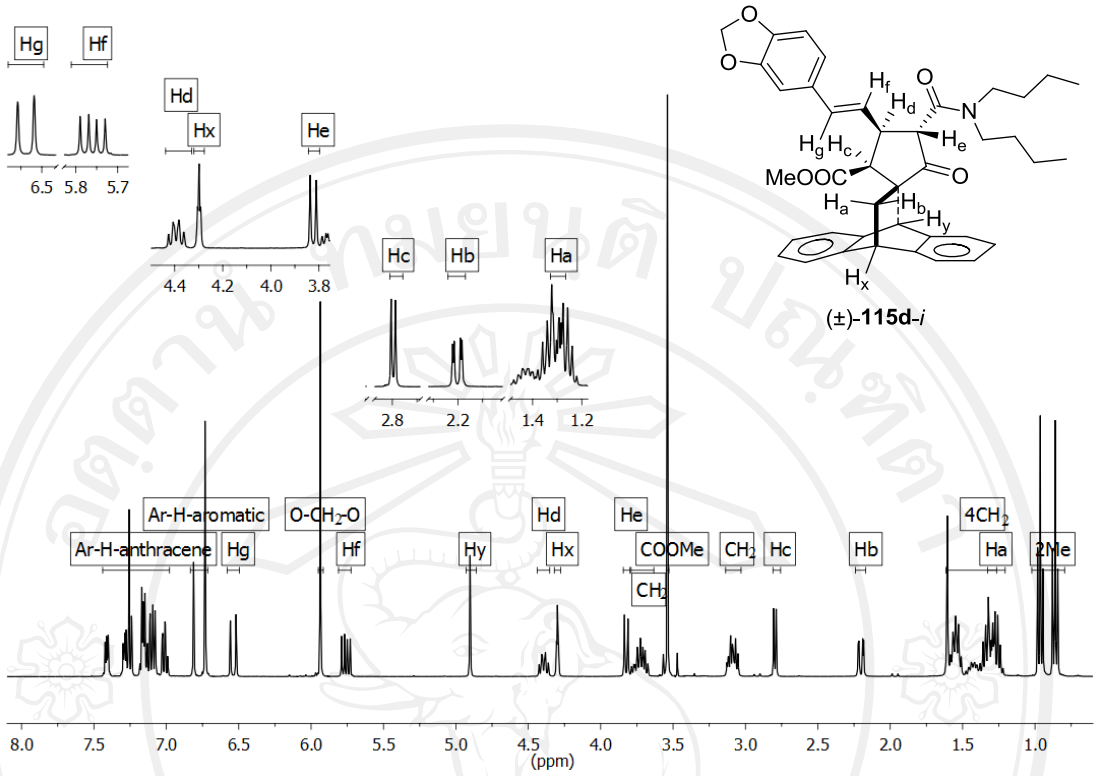

Figure 3.18 ^{1}H-NMR spectrum of spirocyclopentanone–anthracene adduct (±)-**115d**-*i*

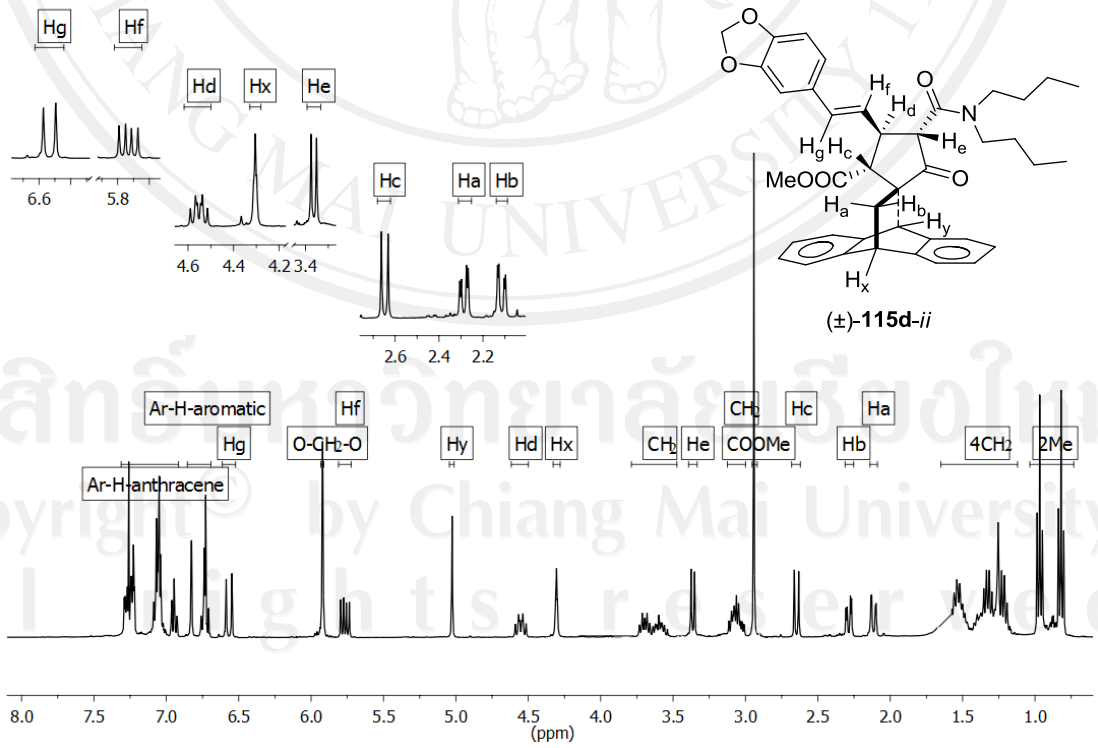

Figure 3.19 ^{1}H-NMR spectrum of spirocyclopentanone–anthracene adduct (±)-**115d**-*ii*

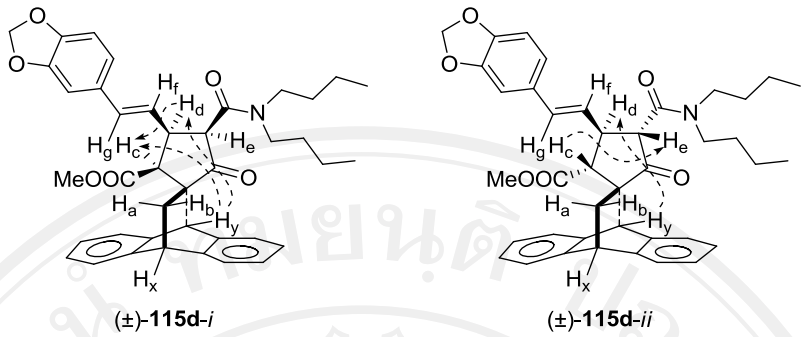

Figure 3.20 NOE correlations observed of spirocyclopentanone–anthracene adducts (±)-**115d**-*i* and (±)-**115d**-*ii*

The mechanism of tandem Michael addition–Dieckmann condensation reactions of spirocyclopentanone–anthracene adducts (±)-**115d**-*i* and (±)-**115d**-*ii* were described in 3.1.2. The relative stereochemistry of the spirocyclopentanone–anthracene adducts (±)-**115d**-*i* and (±)-**115d**-*ii* were assigned by ^{1}H-NMR technique as depicted in Table 3.9, Figures 3.18 and 3.19, respectively.

The spirocyclopentanone–anthracene adducts (±)-**115d**-*i* was characterized by NMR techniques, the proton H_c was observed at δ 2.80 ppm as doublet (J = 6.9 Hz) which is *cis*-configuration with proton H_d. The proton H_e was observed at δ 3.82 ppm as doublet (J = 10.1 Hz) which is *trans*-configuration with proton H_d. The proton H_f was observed at δ 5.76 ppm as doublet of doublets (J = 15.7, 8.2 Hz) which is *trans*-configuration with proton H_g and proton H_d. The relative stereochemistry of cyclopentanone ring was determined by NOE enhancement. The proton H_y is enhanced with proton H_d and proton H_c which is proton H_c and proton H_d on the lower-face, proton H_e on upper-face as shown in Figure 3.20.

The spirocyclopentanone–anthracene adducts (±)-**115d**-*ii* was characterized by NMR techniques, the proton H_c was observed at δ 2.65 ppm as doublet (J = 12.2 Hz) which is *cis*-configuration with proton H_d. The proton H_e was observed at δ 3.36 ppm as doublet (J = 9.6 Hz) which is *trans*-configuration with proton H_d. The proton H_f was observed at δ 5.77 ppm as doublet of doublets (J = 15.6, 8.2 Hz) which is *trans*-configuration with proton H_g and proton H_d. The relative stereochemistry of cyclopentanone ring was determined by NOE enhancement. The proton H_y is enhanced with proton H_d which is proton H_d on the lower-face. The proton H_c is

enhanced with proton H_e which is proton H_c and H_e on the upper-face as shown in Figure 3.20.

3.3 Syntheses of racemic spirocyclopentanone–anthracene adduct (±)-116a-*i*, -*ii* – (±)-116d-*i*, -*ii* from *α,β*-unsaturated amide derivatives 113a-d

3.3.1 Syntheses of 3′-methoxycarbonyl-4′-(3,4-methylenedioxy)phenyl-5′-piperidinecarbonyl-1′-cyclopentanone-2′-spiro-11-9,10-dihydro-9,10-ethano-anthracenes ((±)-116a-*i* and (±)-116a-*ii*) from *α,β*-unsaturated amide 113a

3,4-Methylenedioxy cinnamic acid (**106**) was treated with oxalyl chloride ($(COCl)_2$) (1.5 equiv.) at 0 °C allowed to room temperature 2 h. After the period, NEt_3 (2.0 equiv.) was added at 0 °C stirred for 15 minutes. Piperidine (**108**) (2.5 equiv.) was added at 0 °C allowed to room temperature 2 h. Purification of the crude product by column chromatography (silica gel) affords *α,β*-unsaturated amide **113a** in 96% yield (Scheme 3.14). The physical properties, ^{1}H NMR data and ^{1}H NMR spectrum were shown in Table 3.10 and Figure 3.21.

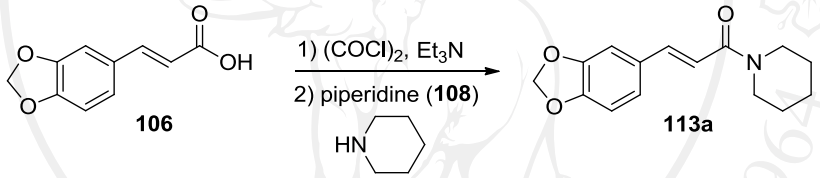

Scheme 3.14 Preparation reaction of *α,β*-unsaturated amide **113a**

Table 3.10 ^{1}H-NMR data of *α,β*-unsaturated amide **113a**

Physical property	m.p. (°C)	Chemical shift (*δ*, ppm)
white crystals	89.0–89.9	1.54–1.73 (m, 6H, CH_2-3″, 4″, 5″), 3.50–3.70 (m, 4H, CH_2-2″, 6″), 5.98 (s, 2H, CH_2-7′), 6.73 d (*J* = 15.3 Hz), 1H, CH-2), 6.79 (d (*J* = 8.0 Hz), 1H, CH-5′), 6.99 (dd (*J* = 8.1, 1.7 Hz), 1H, CH-6′), 7.03 (d (*J* = 1.7 Hz), 1H, CH-2′), 7.57 (d (*J* = 15.3 Hz), 1H, CH-3) (Figure 3.21)

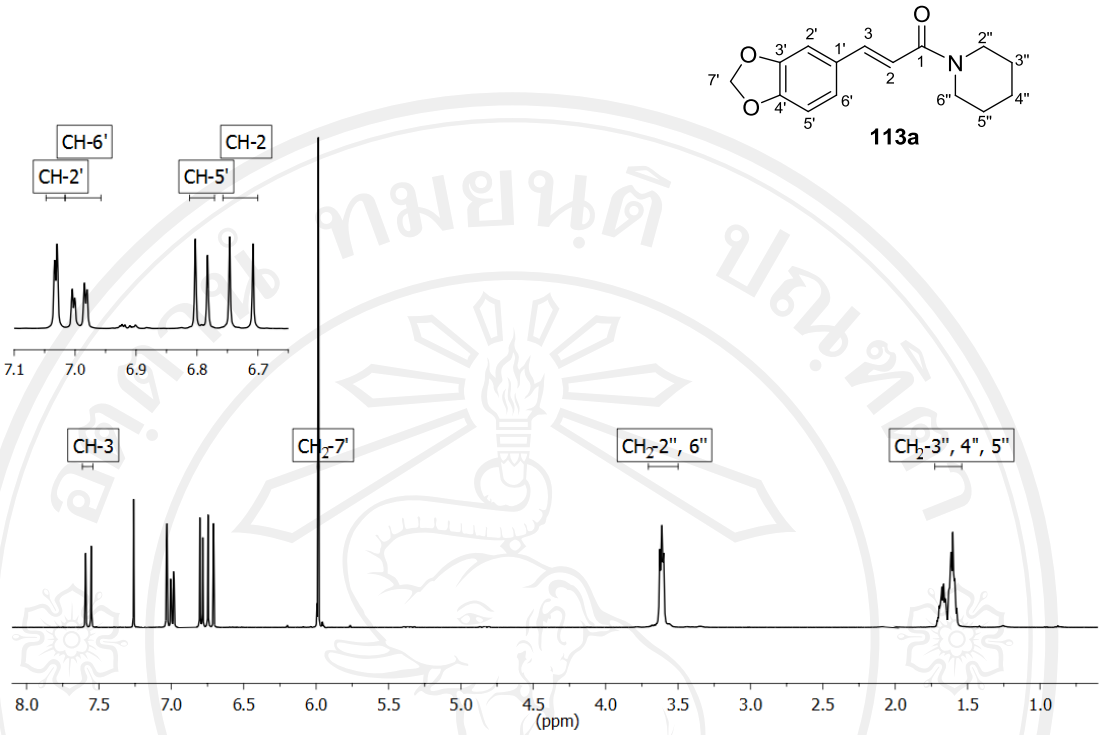

Figure 3.21 ^{1}H-NMR spectrum of *α,β*-unsaturated amide **113a**

Then, dimethyl itaconate–anthracene adduct ((±)-**74**) was reacted with *α,β*-unsaturated amide **113a** *via* tandem Michael addition–Dieckmann condensation reactions (Scheme 3.15).

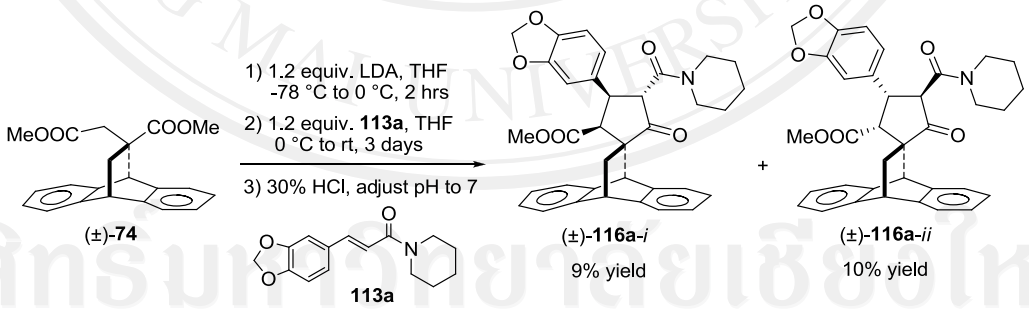

Scheme 3.15 Tandem Michael addition–Dieckmann condensation reactions of (±)-**116a**-*i* and (±)-**116a**-*ii*

An enolate anion (**118** or **119**) of dimethyl itaconate–anthracene adduct, generated from (±)-**74** by treatment with lithium diisopropylamide (LDA, 1.2 equiv.) in THF at 0 °C, readily reacted with *α,β*-unsaturated amide **113a** at 0 °C to provide, after leaving the reaction mixture to stir at room temperature for 3 days followed by 10% hydrochloride acid work-up, the spirocyclopentanone–anthracene adduct as mixture

of diastereoisomers. The crude product was purified by flash column chromatography on silica gel to afford diastereomeric spirocyclopentanone–anthracene adducts (±)-**116a**-*i* in 9% yield and (±)-**116a**-*ii* in 10% yield.

Table 3.11 ^{1}H-NMR data of spirocyclopentanone–anthracene adducts (±)-**116a**-*i* and (±)-**116a**-*ii*

Compound	Physical property	m.p. (°C)	Chemical shift (δ, ppm)
(±)-**116a**-*i*	white crystals	95.2–98.5	1.38–1.72 (m, 6H, CH_2-3′′′′, 4′′′′, 5′′′′), 1.29, 2.25, 4.30 (ABX system (J = 12.7, 2.8, 2.5 Hz), 3H, H_a, H_b, H_x), 2.92 (d (J = 7.0 Hz), 1H, H_c), 3.37–3.51 (m, 2H, CH_2-2′′′′ or 6′′′′), 3.78–3.91 (m, 2H, CH_2-2′′′′ or 6′′′′), 3.30 (s, 3H, COOMe-2′′), 4.24 (d (J = 10.7 Hz), 1H, H_e), 4.93 (dd (J =10.8, 7.1 Hz), 1H, H_d), 4.90 (s, 1H, H_y), 5.92 (s, 2H, CH_2-7′′′), 6.64 (dd (J = 8.1, 1.7 Hz), 1H, ArH-5′′′ or 6′′′), 6.67 (d (J = 1.6 Hz), 1H, ArH-2′′′), 6.72 (d (J = 8.0 Hz), 1H, ArH-5′′′ or 6′′′), 7.00–7.49 (m, 8H, ArH–anthracene) (Figure 3.22)

Table 3.11 ^{1}H-NMR data of spirocyclopentanone–anthracene adducts (±)-**116a**-*i* and (±)-**116a**-*ii* (continued)

Compound	Physical property	m.p. (°C)	Chemical shift (δ, ppm)
(±)-**116a**-*ii*	white crystals	264.5–266.1	1.31–1.74 (m, 6H, CH_2-3′′′′, 4′′′′, 5′′′′), 1.95, 2.10, 4.35 (ABX system (J = 12.8, 3.0, 2.3 Hz), 3H, H_a, H_b, H_x), 2.38 (d (J = 6.2 Hz), 1H, H_c), 3.23–3.33, 3.63–3.71 (m, 2H, CH_2-2′′′′ or 6′′′′), 3.51–3.62 (m, 2H, CH_2-2′′′′ or 6′′′′), 3.47 (s, 3H, COOMe-2′′), 4.28–4.41 (m, 2H, H_d, H_e), 4.44 (s, 1H, H_y), 5.87 (s, 2H, CH_2-7′′′), 6.53 (dd (J = 8.1, 1.6 Hz), 1H, ArH-5′′′ or 6′′′), 6.57 (d (J = 1.6 Hz), 1H, ArH-2′′′), 6.66 (d (J = 8.0 Hz), 1H, ArH-5′′′ or 6′′′), 6.93–7.44 (m, 8H, ArH–anthracene) (Figure 3.23)

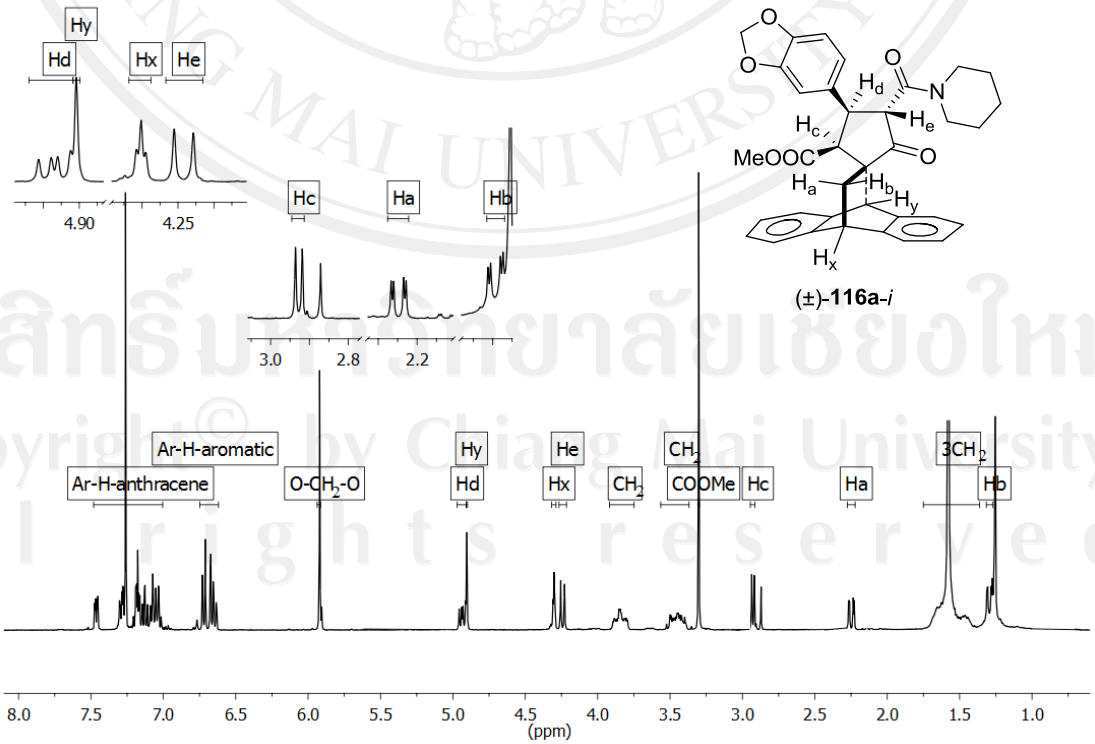

Figure 3.22 ^{1}H-NMR spectrum of spirocyclopentanone–anthracene adduct (±)-**116a**-*i*

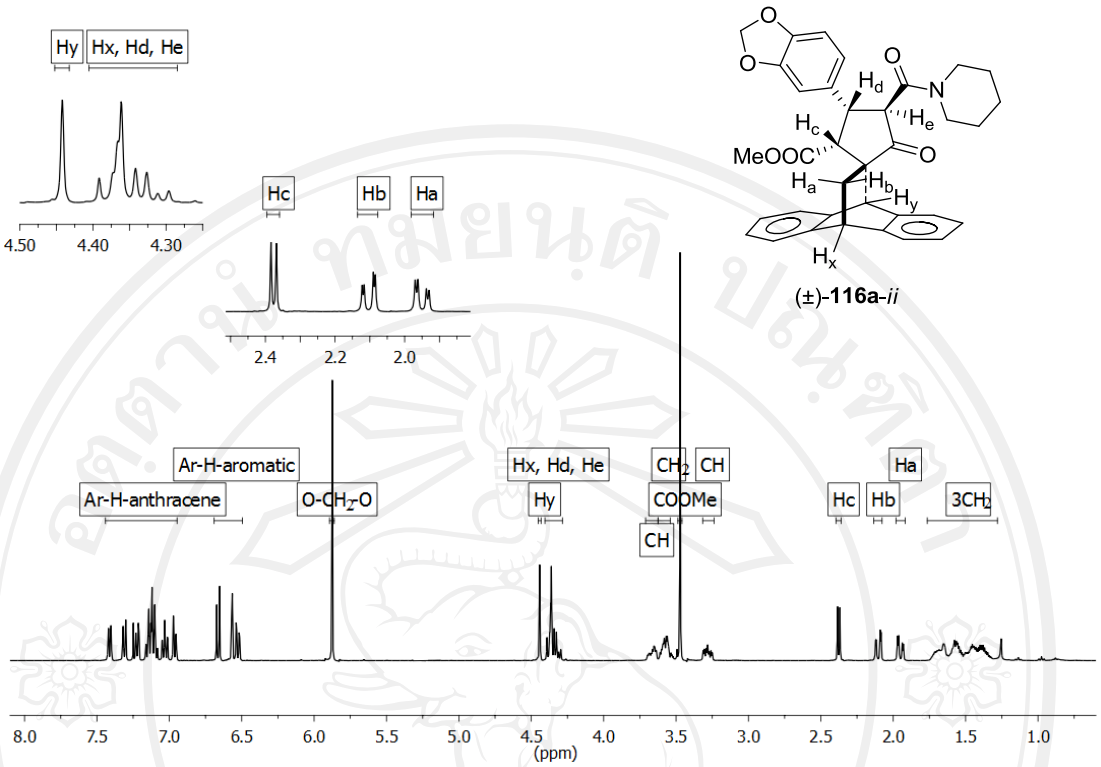

Figure 3.23 ^{1}H-NMR spectrum of spirocyclopentanone–anthracene adduct (±)-**116a**-*ii*

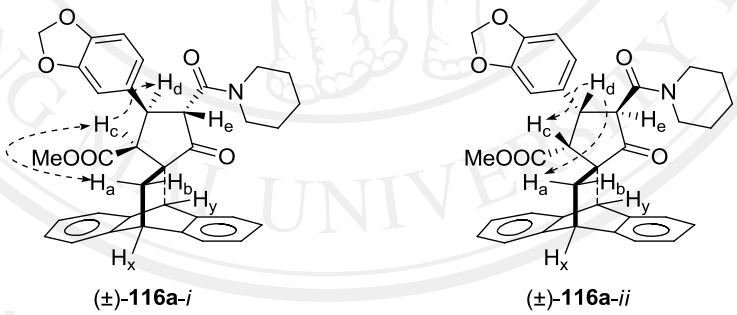

Figure 3.24 NOE correlations observed of spirocyclopentanone–anthracene adduct (±)-**116a**-*i* and (±)-**116a**-*ii*

The mechanism of tandem Michael addition–Dieckmann condensation reactions of spirocyclopentanone–anthracene adducts (±)-**116a**-*i* and (±)-**116a**-*ii* were described in 3.1.1. The relative stereochemistry of the spirocyclopentanone–anthracene adducts (±)-**116a**-*i* and (±)-**116a**-*ii* were assigned by ^{1}H-NMR technique as depicted in Table 3.11, Figures 3.22 and 3.23, respectively.

The spirocyclopentanone–anthracene adducts (±)-**116a**-*i* was characterized by NMR techniques, the proton H_c was observed at δ 2.92 ppm as doublet (J = 7.0

Hz) which is *cis*-configuration with proton H_d. The proton H_e was observed at δ 4.24 ppm as doublet (J = 10.7 Hz) which is *trans*-configuration with proton H_d. The proton H_d was observed at δ 4.93 dd ppm as doublet of doublets (J =10.8, 7.1 Hz). The relative stereochemistry of cyclopentanone ring was determined by NOE enhancement. The proton H_a is enhanced with proton H_c, proton H_c is enhanced with proton H_d which are proton H_c and proton H_d on the lower-face, proton H_e on upper-face as shown in Figure 3.24.

The spirocyclopentanone–anthracene adducts (±)-**116a**-*ii* was characterized by NMR techniques, the proton H_c was observed at δ 2.38 ppm as doublet (J = 6.2 Hz) which is *cis*-configuration with proton H_d. The proton H_d and H_e was observed at δ 4.28–4.41 ppm as multiplet. The relative stereochemistry of cyclopentanone ring was determined by NOE enhancement. The proton H_d is enhanced with proton H_a and proton H_c which is proton H_c and proton H_d on the upper-face, proton H_e on lower-face as shown in Figure 3.24.

3.3.2 Syntheses of 3′-methoxycarbonyl-4′-(3,4-methylenedioxy)phenyl-5′-pyrrolidinecarbonyl-1′-cyclopentanone-2′-spiro-11-9,10-dihydro-9,10-ethano-anthracenes ((±)-116b-*i* and (±)-116b-*ii*) from *α,β*-unsaturated amide 113b

3,4-Methylenedioxy cinnamic acid (**106**) was treated with oxalyl chloride ($(COCl)_2$) (1.5 equiv.) at 0 °C allowed to room temperature 2 h. After the period, NEt_3 (2.0 equiv.) was added at 0 °C stirred for 15 minutes. Pyrrolidine (**109**) (2.5 equiv.) was added at 0 °C allowed to room temperature 2 h. Purification of the crude product by column chromatography (silica gel) affords *α,β*-unsaturated amide **113b** in 83% yield (Scheme 3.16). The physical properties, ^{1}H NMR data and ^{1}H NMR spectrum were shown in Table 3.12 and Figure 3.25.

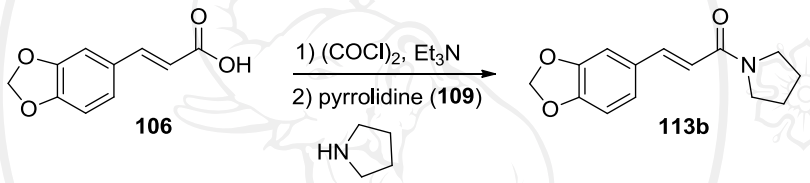

Scheme 3.16 Preparation reaction of *α,β*-unsaturated amide **113b**

Table 3.12 ^{1}H-NMR data of *α,β*-unsaturated amide **113b**

Physical property	m.p. (°C)	Chemical shift (*δ*, ppm)
white crystals	151.9–152.3	1.93 (brs, 4H, CH_2-3″, 4″), 3.58 (t (*J* = 6.7 Hz), 4H, CH_2-2″, 5″), 5.97 (s, 2H, CH_2-7′), 6.54 (d (*J* = 15.4 Hz), 1H, CH-2), 6.78 (d (*J* = 8.0 Hz), 1H, CH-5′), 6.99 (dd (*J* = 8.0, 1.6 Hz), 1H, CH-6′), 7.02 (d (*J* = 1.6 Hz), 1H, CH-2′), 7.61 (d (*J* = 15.4 Hz), 1H, CH-3) (Figure 3.25)

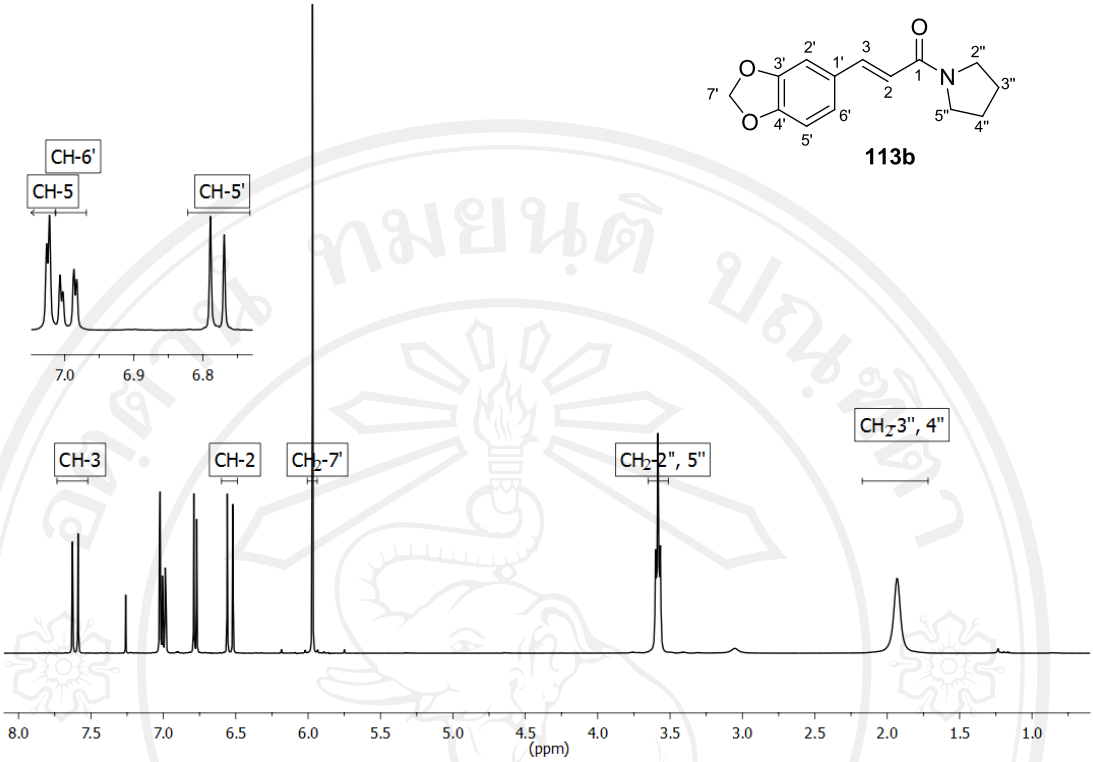

Figure 3.25 ^{1}H-NMR spectrum of *α,β*-unsaturated amide **113b**

Then, dimethyl itaconate–anthracene adduct ((±)-**74**) was reacted with *α,β*-unsaturated amide **113b** *via* tandem Michael addition–Dieckmann condensation reactions, as shown in Scheme 3.17.

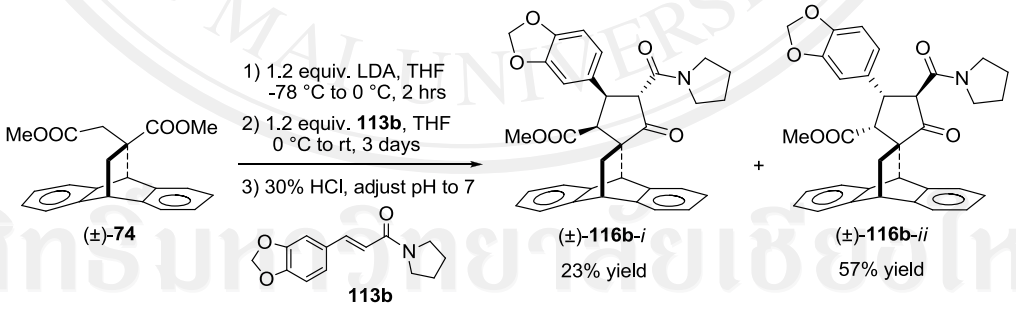

Scheme 3.17 Tandem Michael addition–Dieckmann condensation reactions of (±)-**116b**-*i* and (±)-**116b**-*ii*

An enolate anion (**118** or **119**) of dimethyl itaconate–anthracene adduct, generated from (±)-**74** by treatment with lithium diisopropylamide (LDA, 1.2 equiv.) in THF at 0 °C, readily reacted with *α,β*-unsaturated amide **113b** at 0 °C to provide, after leaving the reaction mixture to stir at room temperature for 3 days followed by 10% hydrochloride acid work-up, the spirocyclopentanone–anthracene adduct as mixture

of diastereoisomers. The crude product was purified by flash column chromatography on silica gel to afford diastereomeric spirocyclopentanone–anthracene adducts (±)-**116b**-*i* in 23% yield and (±)-**116b**-*ii* in 57% yield.

Table 3.13 ^{1}H-NMR data of spirocyclopentanone–anthracene adducts (±)-**116b**-*i* and (±)-**116b**-*ii*

Compound	Physical property	m.p. (°C)	Chemical shift (δ, ppm)
(±)-**116b**-*i*	white crystals	203.8–205.2	1.72–2.00 (m, 4H, CH_2-3′′′′, 4′′′′), 1.30, 2.25, 4.30 (ABX system (J = 12.7, 2.8, 2.6 Hz), 3H, H_a, H_b, H_x), 2.90 (d (J = 7.0 Hz), 1H, H_c), 3.29 (s, 3H, COOMe-2′′), 3.38–3.48, 3.96–4.06 (m, 2H, CH_2 -2′′′′ or 5′′′′), 3.48–3.58 (m, 2H, CH_2-2′′′′ or 5′′′′), 4.10 (d (J = 10.9 Hz), 1H, H_e), 4.84 (dd (J = 10.2, 7.1 Hz), 1H, H_d), 4.99 (s, 1H, H_y), 5.92 (s, 2H, CH_2-7′′′), 6.66 (d (J = 8.1 Hz), 1H, ArH-5′′′ or 6′′′), 6.68 (s, 1H, ArH-2′′′), 6.73 (d (J = 7.9 Hz), 1H, ArH-5′′′ or 6′′′), 7.00–7.50 (m, 8H, ArH–anthracene) (Figure 3.26)

Table 3.13 ^{1}H-NMR data of spirocyclopentanone–anthracene adducts (±)-**116b**-*i* and (±)-**116b**-*ii* (continued)

Compound	Physical property	m.p. (°C)	Chemical shift (δ, ppm)
(±)-**116b**-*ii*	white crystals	254.4–256.3	1.64–1.96 (m, 4H, CH_2-3′′′′, 4′′′′), 1.99, 2.19, 4.40 (ABX system (J = 12.8, 3.0, 2.3 Hz), 3H, H_a, H_b, H_x), 2.41 (d (J = 6.7 Hz), 1H, H_c), 3.25–3.39 (m, 2H, CH_2-2′′′′ or 5′′′′), 3.39–3.49, 3.94–4.09 (m, 2H, CH_2-2′′′′ or 5′′′′), 3.51 (s, 3H, COOMe-2′′), 4.20 (d (J = 12.0 Hz), 1H, H_e), 4.35 (dd (J = 12.0, 6.6 Hz), 1H, H_d), 4.48 (s, 1H, H_y), 5.88 (s, 2H, CH_2-7′′′), 6.58 (dd (J = 8.1, 1.6 Hz), 1H, ArH-5′′′ or 6′′′), 6.62 (d (J = 1.6 Hz), 1H, ArH-2′′′), 6.69 (d (J = 8.0 Hz), 1H, ArH-5′′′ or 6′′′), 6.94–7.51 (m, 8H, ArH–anthracene) (Figure 3.27)

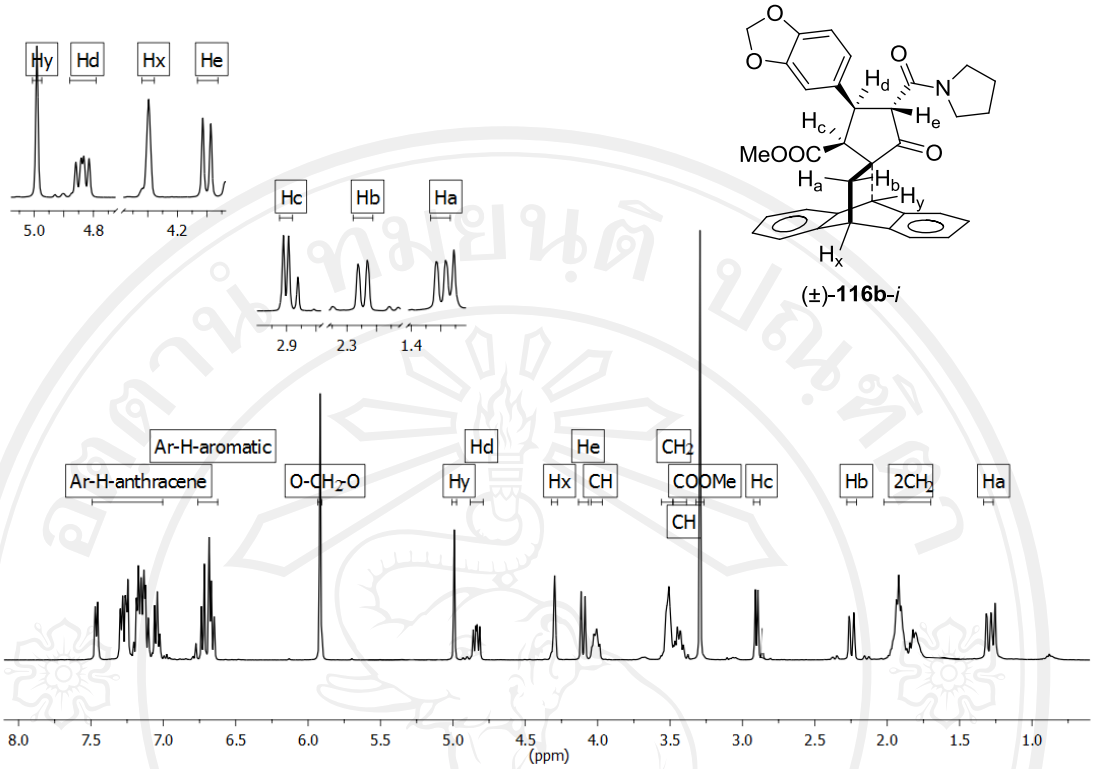

Figure 3.26 ^{1}H-NMR spectrum of spirocyclopentanone–anthracene adduct (±)-**116b**-*i*

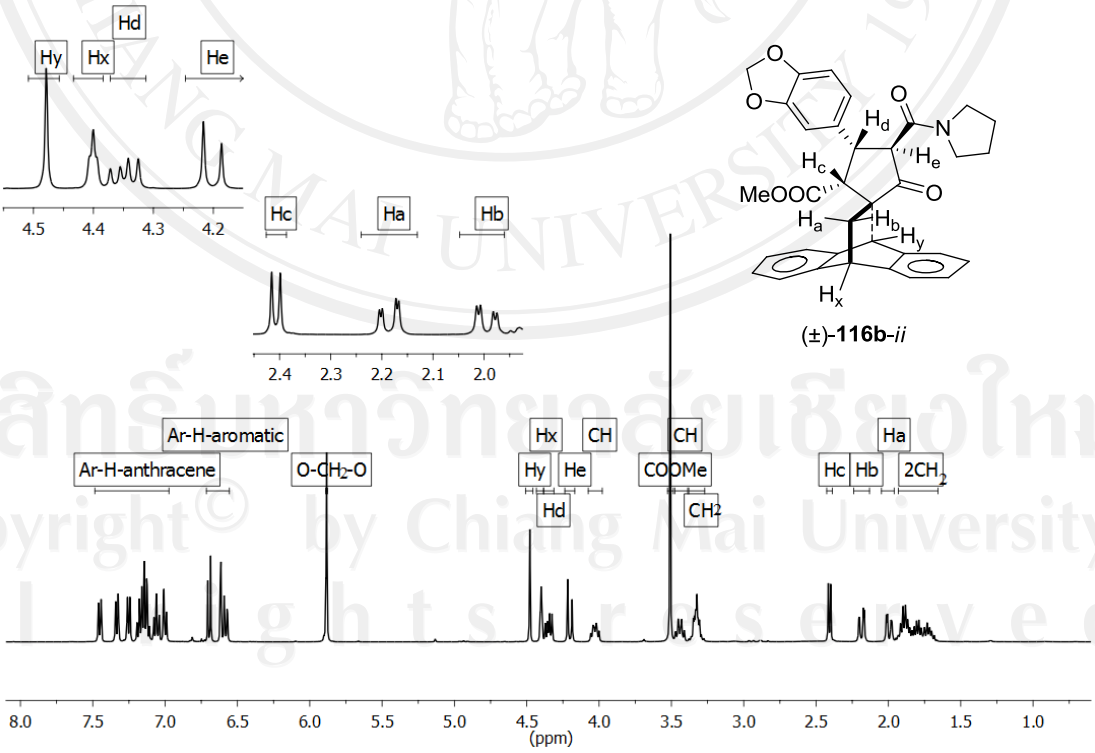

Figure 3.27 ^{1}H-NMR spectrum of spirocyclopentanone–anthracene adduct (±)-**116b**-*ii*

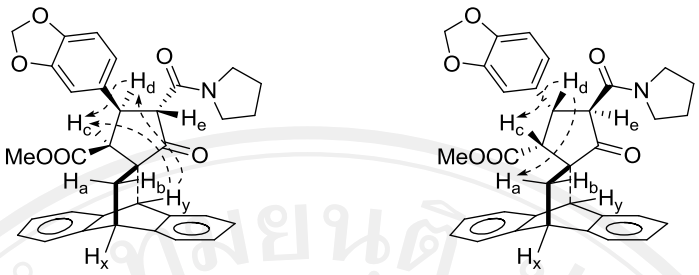

Figure 3.28 NOE correlations observed of spirocyclopentanone–anthracene adduct (±)-**116b**-*i* and (±)-**116b**-*ii*

The mechanism of tandem Michael addition–Dieckmann condensation reactions of spirocyclopentanone–anthracene adducts (±)-**116b**-*i* and (±)-**116b**-*ii* were described in 3.1.1. The relative stereochemistry of the spirocyclopentanone–anthracene adducts (±)-**116b**-*i* and (±)-**116b**-*ii* were assigned by ^{1}H-NMR technique as depicted in Table 3.13, Figures 3.26 and 3.27, respectively.

The spirocyclopentanone–anthracene adducts (±)-**116b**-*i* was characterized by NMR techniques, the proton H_c was observed at δ 2.90 ppm as doublet (J = 7.0 Hz) which is *cis*-configuration with proton H_d. The proton H_e was observed at δ 4.10 ppm as doublet (J = 10.9 Hz) which is *trans*-configuration with proton H_d. The proton H_d was observed at δ 4.84 ppm as doublet of doublets (J = 10.2, 7.1 Hz). The relative stereochemistry of cyclopentanone ring was determined by NOE enhancement. The proton H_y is enhanced with proton H_c and proton H_d, proton H_c is enhanced with proton H_d which are proton H_c and proton H_d on the lower-face, proton H_e on upper-face as shown in Figure 3.28.

The spirocyclopentanone–anthracene adducts (±)-**116b**-*ii* was characterized by NMR techniques, the proton H_c was observed at δ 2.41 ppm as doublet (J = 6.7 Hz) which is *cis*-configuration with proton H_d. The proton H_e was observed at δ 4.20 ppm as doublet (J = 12.0 Hz) which is *trans*-configuration with proton H_d. The proton H_d was observed at δ 4.35 ppm as doublet of doublets (J = 12.0, 6.6 Hz). The relative stereochemistry of cyclopentanone ring was determined by NOE enhancement. The proton H_d is enhanced with proton H_c and proton H_a which is proton H_c and proton H_d on the upper-face, proton H_e on lower-face as shown in Figure 3.28.

3.3.3 Syntheses of 5′-(*N*,*N*-diisopropylcarboxamid-1-yl)-3′-methoxycarbonyl-4′-(3,4-methylenedioxy)phenyl-1′-cyclopentanone-2′-spiro-11-9,10-dihydro-9,10-ethanoanthracenes ((±)-116c-*i* and (±)-116c-*ii*) from *α*,*β*-unsaturated 113c

3,4-Methylenedioxy cinnamic acid (**106**) was treated with oxalyl chloride ($(COCl)_2$) (1.5 equiv.) at 0 °C allowed to room temperature 2 h. After the period, NEt_3 (2.0 equiv.) was added at 0 °C stirred for 15 minutes. Diisopropylamine (**110**) (2.5 equiv.) was added at 0 °C allowed to room temperature 2 h. Purification of the crude product by column chromatography (silica gel) affords *α*,*β*-unsaturated amide **113c** in 76% yield (Scheme 3.18). The physical properties, ^{1}H NMR data and ^{1}H NMR spectrum were shown in Table 3.14 and Figure 3.29.

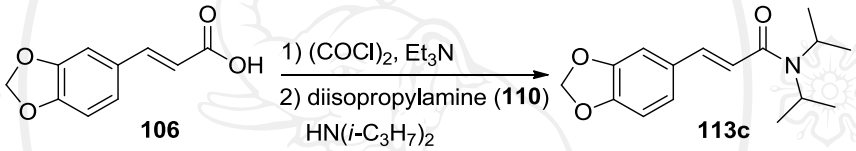

Scheme 3.18 Preparation reaction of *α*,*β*-unsaturated amide **113c**

Table 3.14 ^{1}H-NMR data of *α*,*β*-unsaturated amide **113c**

Physical property	m.p. (°C)	Chemical shift (*δ*, ppm)
yellow liquid	–	1.35 (brs, 12H, CH_3-3″, 4″, 6″, 7″), 3.86 (brs, 1H, CH-2″ or 5″), 4.09 (brs, 1H, CH-2″ or 5‴), 5.99 (s, 2H, CH_2-7′), 6.67 (d (*J* = 15.3 Hz), 1H, CH-2), 6.79 (d (*J* = 8.0 Hz), 1H, CH-5′), 6.98 (dd (*J* = 8.0, 1.6 Hz), 1H, CH-6′), 7.02 (d (*J* = 1.6 Hz), 1H, CH-2′), 7.51 (d (*J* = 15.3 Hz), 1H, CH-3) (Figure 3.29)

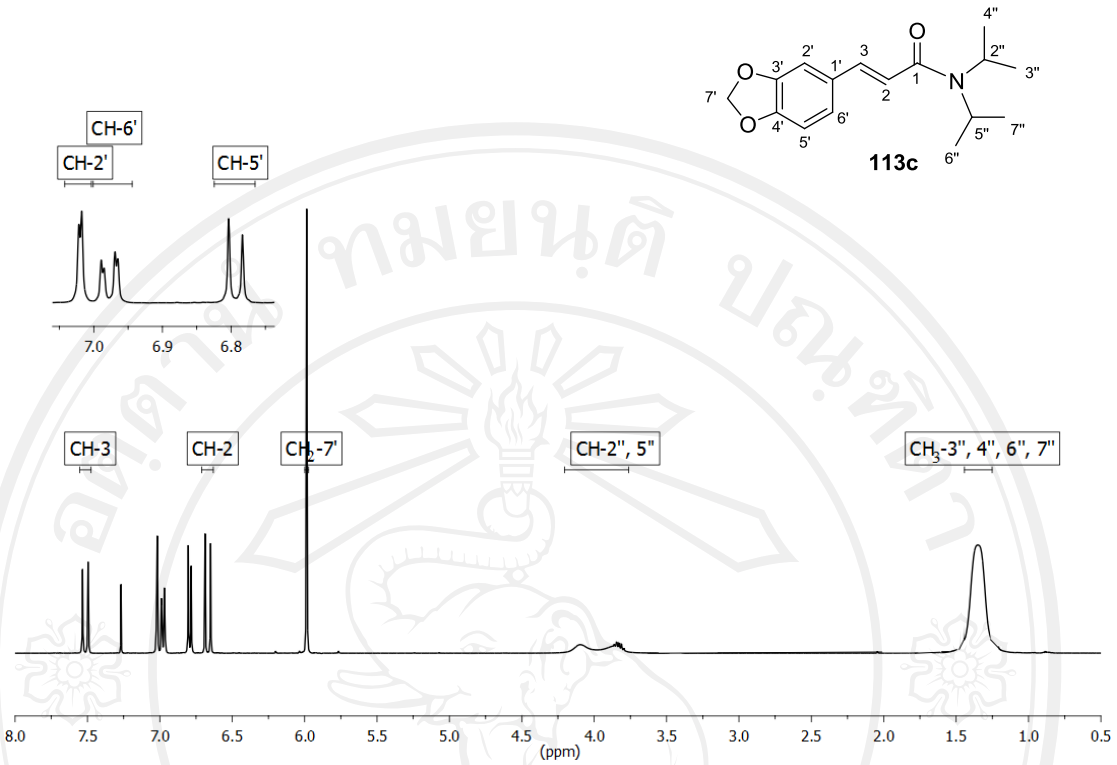

Figure 3.29 ^{1}H-NMR spectrum of *α,β*-unsaturated amide **113c**

Then, dimethyl itaconate–anthracene adduct ((±)-**74**) was reacted with *α,β*-unsaturated amide **113c** *via* tandem Michael addition–Dieckmann condensation reactions (Scheme 3.19).

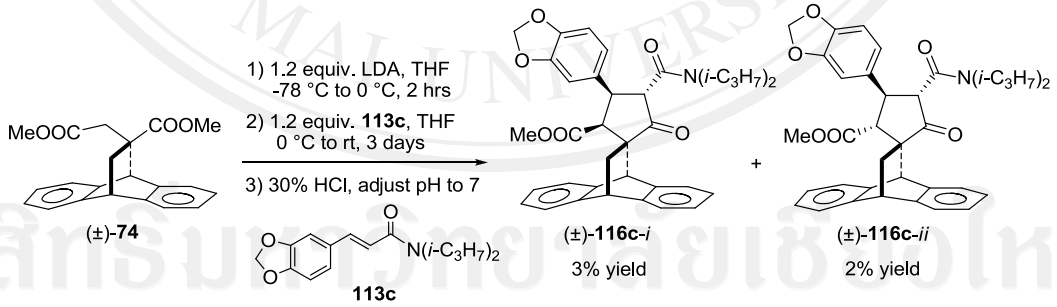

Scheme 3.19 Tandem Michael addition–Dieckmann condensation reactions of (±)-**116c**-*i* and (±)-**116c**-*ii*

An enolate anion (**118** or **119**) of dimethyl itaconate–anthracene adduct, generated from (±)-**74** by treatment with lithium diisopropylamide (LDA, 1.2 equiv.) in THF at 0 °C, readily reacted with *α,β*-unsaturated amide **113c** at 0 °C to provide, after leaving the reaction mixture to stir at room temperature for 3 days followed by 10% hydrochloride acid work-up, the spirocyclopentanone–anthracene adduct as mixture

of diastereoisomers. The crude product was purified by flash column chromatography on silica gel to afford diastereomeric spirocyclopentanone adducts (±)-**116c**-*i* in 3% yield and (±)-**116c**-*ii* in 2% yield.

Table 3.15 ^{1}H-NMR data of spirocyclopentanone–anthracene adducts (±)-**116c**-*i* and (±)-**116c**-*ii*

Compound	Physical property	m.p. (°C)	Chemical shift (δ, ppm)
(±)-**116c**-*i*	white crystals	112.2–115.0	1.14 (d (J = 6.7 Hz), 3H, CH_3-3′′′′ or 4′′′′ or 6′′′′ or 7′′′′), 1.24 (d (J = 6.4 Hz), 3H, CH_3-3′′′′ or 4′′′′ or 6′′′′ or 7′′′′), 1.40 (d (J = 6.7 Hz), 3H, CH_3-3′′′′ or 4′′′′ or 6′′′′ or 7′′′′), 1.50 (d (J = 6.7 Hz), 3H, CH_3-3′′′′ or 4′′′′ or 6′′′′ or 7′′′′), 1.29, 2.23, 4.30 (ABX system (J = 12.8, 2.5, 2.4 Hz), 3H, H_a, H_b, H_x), 2.94 (d (J = 7.0 Hz), 1H, H_c), 3.30 (s, 3H, COOMe-2′′), 3.49 (hept (J = 6.5 Hz), 1H, CH-2′′′′ or 5′′′′), 4.54 (hept (J = 6.5 Hz), 1H, CH-2′′′′ or 5′′′′), 4.20 (d (J = 10.5 Hz), 1H, H_e), 4.94 (s, 1H, H_y), 4.98 (dd (J = 10.5, 7.0 Hz), 1H, H_d), 5.92 (s, 2H, CH_2-7′′′), 6.63 (d (J = 8.1 Hz), 1H, ArH-5′′′ or 6′′′), 6.66 (s, 1H, ArH-2′′′), 6.72 (d (J = 8.0 Hz), 1H, ArH-5′′′ or 6′′′), 6.96–7.50 (m, 8H, ArH–anthracene) (Figure 3.30)

Table 3.15 ^{1}H-NMR data of spirocyclopentanone–anthracene adducts (±)-**116c**-*i* and (±)-**116c**-*ii* (continued)

Compound	Physical property	m.p. (°C)	Chemical shift (δ, ppm)
(±)-**116c**-*ii*	white crystals	170.1–173.9	0.89 (d (J = 6.8Hz), 3H, CH_3-3′′′′ or 4′′′′ or 6′′′′ or 7′′′′), 1.05 (d (J = 6.5 Hz), 3H, CH_3-3′′′′ or 4′′′′ or 6′′′′ or 7′′′′), 1.43 (d (J = 6.7 Hz), 3H, CH_3-3′′′′ or 4′′′′ or 6′′′′ or 7′′′′), 1.50 (d (J = 6.8 Hz), 3H, CH_3-3′′′′ or 4′′′′ or 6′′′′ or 7′′′′), 2.14, 2.35, 4.32 (ABX system (J = 12.3, 3.1, 2.5 Hz), 3H, H_a, H_b, H_x), 2.89 (s, 3H, COOMe-2′′), 2.93 (d (J = 12.7 Hz), 1H, H_c), 3.39–3.52 (m, 1H, CH-2′′′′ or 5′′′′), 4.08–4.21 (m, 1H, CH-2′′′′ or 5′′′′), 3.43 (d (J = 9.7 Hz), 1H, H_e), 5.02–5.10 (m, 1H, H_d), 5.08 (s, 1H, H_y), 5.91 (s, 2H, CH_2-7′′′), 6.71–6.75 (m, 3H, ArH-2′′′, 5′′′, 6′′′), 6.92–7.33 (m, 8H, ArH–anthracene) (Figure 3.31)

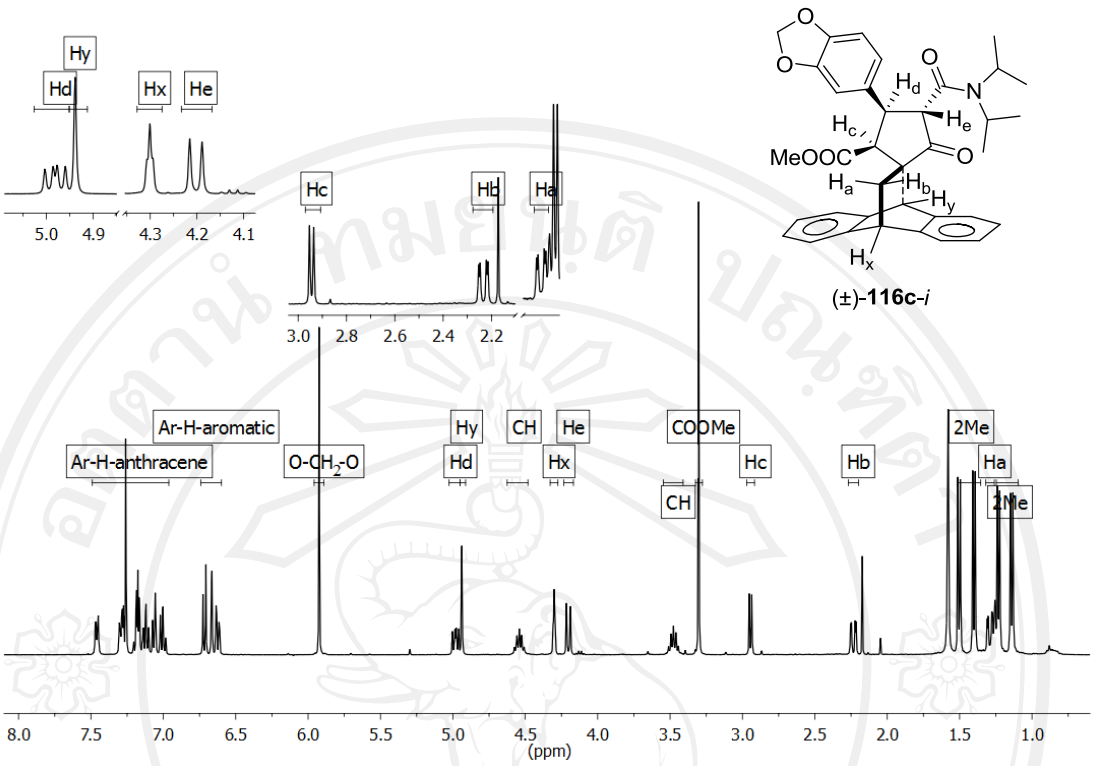

Figure 3.30 ^{1}H-NMR spectrum of spirocyclopentanone–anthracene adduct (±)-**116c**-*i*

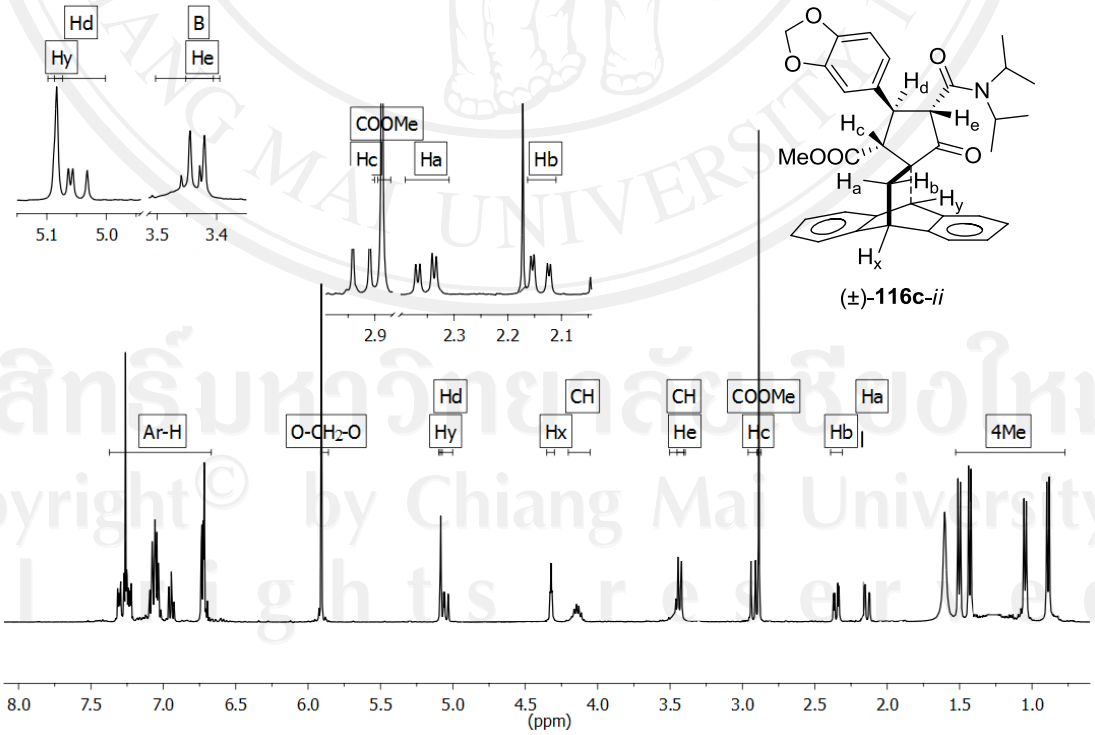

Figure 3.31 ^{1}H-NMR spectrum of spirocyclopentanone–anthracene adduct (±)-**116c**-*ii*

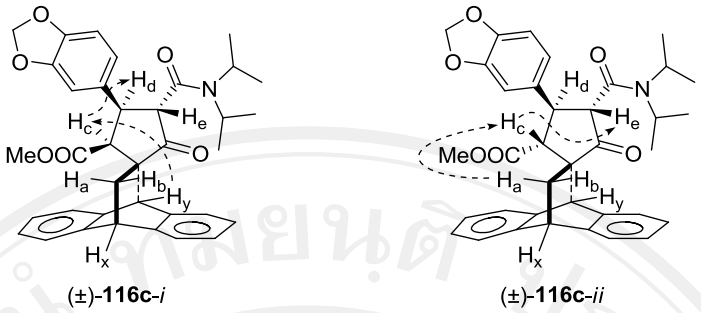

Figure 3.32 NOE correlations observed of spirocyclopentanone–anthracene adduct (±)-**116c**-*i* and (±)-**116c**-*ii*

The mechanism of tandem Michael addition–Dieckmann condensation reactions of spirocyclopentanone–anthracene adducts (±)-**116c**-*i* and (±)-**116c**-*ii* were described in 3.1.2. The relative stereochemistry of the spirocyclopentanone–anthracene adducts (±)-**116c**-*i* and (±)-**116c**-*ii* were assigned by ^{1}H-NMR technique as depicted in Table 3.15, Figures 3.30 and 3.31, respectively.

The spirocyclopentanone–anthracene adducts (±)-**116c**-*i* was characterized by NMR techniques, the proton H_c was observed at δ 2.94 ppm as doublet (J = 7.0 Hz) which is *cis*-configuration with proton H_d. The proton H_e was observed at δ 4.20 ppm as doublet (J = 10.5 Hz) which is *trans*-configuration with proton H_d. The proton H_d was observed at δ 4.98 ppm as doublet of doublets (J = 10.5, 7.0 Hz). The relative stereochemistry of cyclopentanone ring was determined by NOE enhancement. The proton H_y is enhanced with proton H_c, proton H_c is enhanced with proton H_d which are proton H_c and proton H_d on the lower-face, proton He on the upper-face as shown in Figure 3.32.

The spirocyclopentanone–anthracene adducts (±)-**116c**-*ii* was characterized by NMR techniques, the proton H_c was observed at δ 2.93 ppm as doublet (J = 12.7 Hz) which is *tran*-configuration with proton H_d. The proton H_e was observed at δ 3.43 ppm as doublet (J = 9.7 Hz) which is *trans*-configuration with proton H_d. The proton H_d was observed at δ 5.02–5.10 ppm as mulitplets. The relative stereochemistry of cyclopentanone ring was determined by NOE enhancement. The proton H_a is enhanced with proton H_c, proton H_c is enhanced with proton H_e which are proton Hc and proton He on the upper-face and proton H_d on the lower-face as shown in Figure 3.32.

3.3.4 Syntheses of 5′-(*N*,*N*-dibutylcarboxamid-1-yl)-3′-methoxycarbonyl-4′-(3,4-methylenedioxy)phenyl-1′-cyclopentanone-2′-spiro-11-9,10-dihydro-9,10-ethanoanthracenes ((±)-116d-*i* and (±)-116d-*ii*) from *α*,*β*-unsaturated amide 113d

3,4-Methylenedioxy cinnamic acid (**106**) was treated with oxalyl chloride ($(COCl)_2$) (1.5 equiv.) at 0 °C allowed to room temperature 2 h. After the period, NEt_3 (2.0 equiv.) was added at 0 °C stirred for 15 minutes. Dibutylamine (**111**) (2.5 equiv.) was added at 0 °C allowed to room temperature 2 h. Purification of the crude product by column chromatography (silica gel) affords *α*,*β*-unsaturated amide **113d** in 73% yield (Scheme 3.20). The physical properties, ^{1}H NMR data and ^{1}H NMR spectrum were shown in Table 3.16 and Figure 3.33.

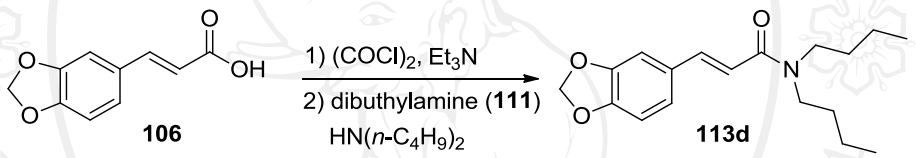

Scheme 3.20 Preparation reaction of *α*,*β*-unsaturated amide **113d**

Table 3.16 ^{1}H-NMR data of *α*,*β*-unsaturated amide **113d**

Physical property	m.p. (°C)	Chemical shift (*δ*, ppm)
white crystals	137.1–141.3	0.91–1.01 (m, 6H, CH_3-5″, 9″), 1.30–1.44 (m, 4H, CH_2-4″, 8″), 1.51–1.68 (m, 4H, CH_2-3″, 7″), 3.32–3.46 (m, 4H, CH_2-2″, 6″), 5.99 (s, 2H, CH_2-7′), 6.66 (d (*J* = 15.4 Hz), 1H, CH-2), 6.80 (d (*J* = 8.0 Hz), 1H, CH-5′), 6.95–7.04 (m, 2H, CH-2′, 6′), 7.61 (d (*J* = 15.3 Hz), 1H, CH-3) (Figure 3.33)

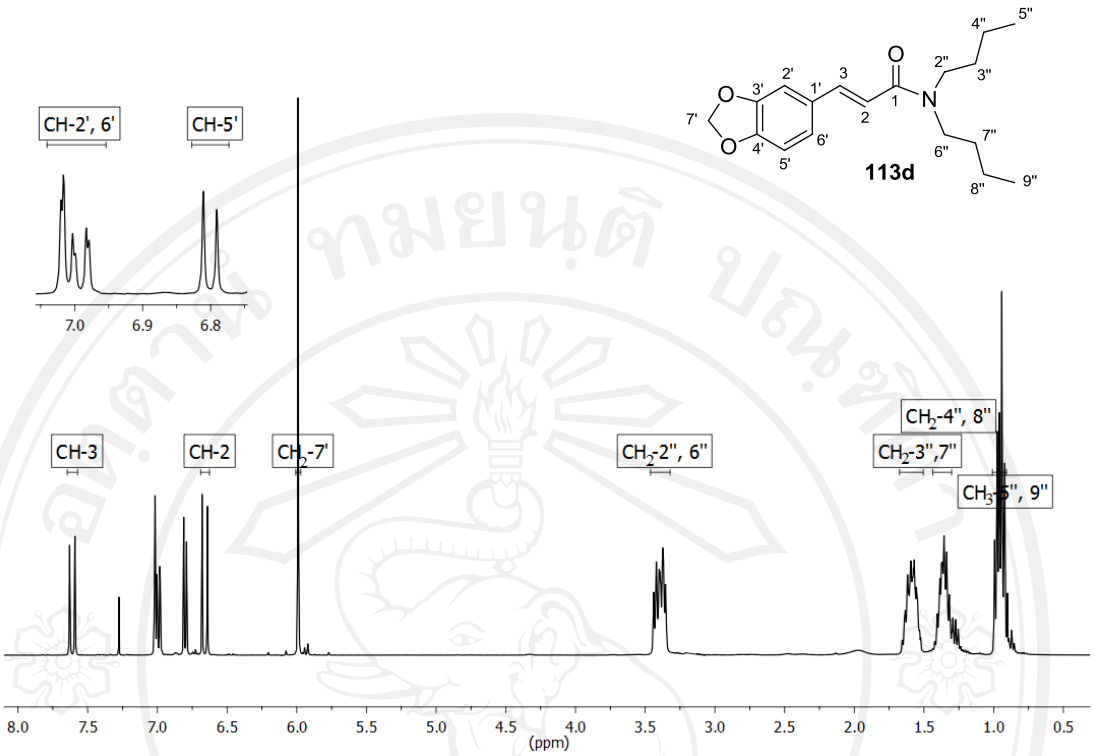

Figure 3.33 ^{1}H-NMR spectrum of *α,β*-unsaturated amide **113d**

Then, dimethyl itaconate–anthracene adduct ((±)-**74**) was reacted with *α,β*-unsaturated amide **113d** *via* tandem Michael addition–Dieckmann condensation reactions (Scheme 3.20).

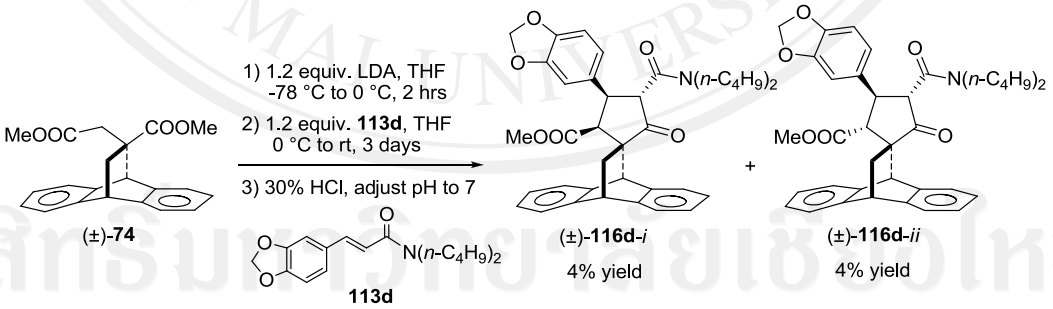

Scheme 3.21 Tandem Michael addition–Dieckmann condensation reactions of (±)-**116d**-*i* and (±)-**116d**-*ii*

An enolate anion (**118** or **119**) of dimethyl itaconate–anthracene adduct, generated from (±)-**74** by treatment with lithium diisopropylamide (LDA, 1.2 equiv.) in THF at 0 °C, readily reacted with *α,β*-unsaturated amide **113d** at 0 °C to provide, after leaving the reaction mixture to stir at room temperature for 3 days followed by 10%

hydrochloride acid work-up, the spirocyclopentanone–anthracene adduct as mixture of diastereoisomers.

The crude product was purified by flash column chromatography on silica gel to afford diastereomeric spirocyclopentanone–anthracene adducts (±)-**116d**-*i* in 4% yield and (±)-**116d**-*ii* in 4% yield.

Table 3.17 ^{1}H-NMR data of spirocyclopentanone–anthracene adducts (±)-**116d**-*i* and (±)-**116d** -*ii*

Compound	Physical property	m.p. (°C)	Chemical shift (δ, ppm)
(±)-**116d**-*i*	white crystals	82.5–85.1	0.89 (t (J = 7.3 Hz), 3H, CH_3-5′′′′ or 9′′′′), 0.96 (t (J = 7.3 Hz), 3H, CH_3-5′′′′ or 9′′′′), 1.18–1.65 (m, 8H, CH_2-3′′′′, 4′′′′, 7′′′′, 8′′′′), 1.31, 2.25, 4.30 (ABX system (J = 12.7, 2.5, 2.4 Hz), 3H, H_a, H_b, H_x), 2.90 (d (J = 6.9 Hz), 1H, H_c), 3.32 (s, 3H, COOMe-2′′), 2.93–3.03, 3.69–3.80 (m, 2H, CH_2-2′′′′ or 6′′′′), 3.04–3.15, 3.79–3.90 (m, 2H, CH_2-2′′′′ or 6′′′′), 4.18 (d (J = 10.8 Hz), 1H, H_e), 4.87 (dd (J = 10.8, 6.9 Hz), 1H, H_d), 4.96 (s, 1H, H_y), 5.91 (d (J = 1.6 Hz), 2H, CH_2-7′′′), 6.67 (dd (J = 8.1, 1.2 Hz), 1H, ArH-5′′′ or 6′′′), 6.70 (d (J = 1.6 Hz), 1H, ArH-2′′′), 6.72 (d (J = 8.0 Hz), 1H, ArH-5′′′ or 6′′′), 6.96–7.49 (m, 8H, ArH–anthracene) (Figure 3.34)

Table 3.17 ^{1}H-NMR data of spirocyclopentanone–anthracene adducts (±)-**116d** *i* and (±)-**116d**-*ii* (continued)

Compound	Physical property	m.p. (°C)	Chemical shift (δ, ppm)
(±)-**116d**-*ii*	white crystals	172.3–173.7	0.71 (t (J = 7.1 Hz), 3H, CH_3-5′′′′ or 9′′′′), 0.96 (t (J = 7.3 Hz), 3H, CH_3-5′′′′ or 9′′′′), 0.92–1.51 (m, 8H, CH_2-3′′′′, 4′′′′, 7′′′′, 8′′′′), 2.16, 2.35, 4.32 (ABX system (J = 12.2, 3.0, 2.5 Hz), 3H, H_a, H_b, H_x), 2.86 (s, 3H, COOMe-2′′), 2.95 (d (J = 12.6 Hz), 1H, H_c), 2.79–2.91, 3.34–3.49 (m, 2H, CH_2-2′′′′ or 6′′′′), 2.98–3.08, 3.57–3.71 (m, 2H, CH_2-2′′′′ or 6′′′′), 3.44 (d (J = 10.1 Hz), 1H, H_e), 4.88 (dd (J = 12.6, 10.1 Hz), 1H, H_d), 5.12 (s, 1H, H_y), 5.90 (s, 2H, CH_2-7′′′), 6.71 (d (J = 8.4 Hz), 1H, ArH-5′′′ or 6′′′), 6.73–6.79 (m, 2H, ArH-2′′′, 5′′′ or 6′′′), 6.92–7.35 (m, 8H, ArH–anthracene) (Figure 3.35)

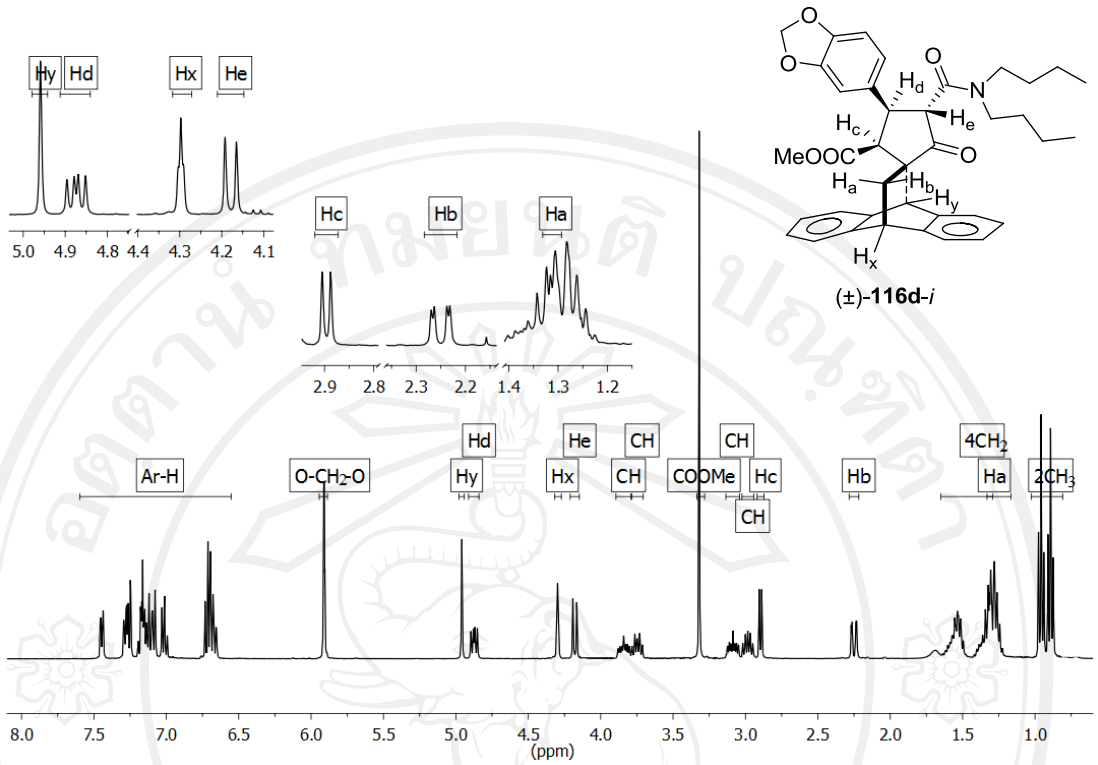

Figure 3.34 ^{1}H-NMR spectrum of spirocyclopentanone–anthracene adduct (±)-**116d**-*i*

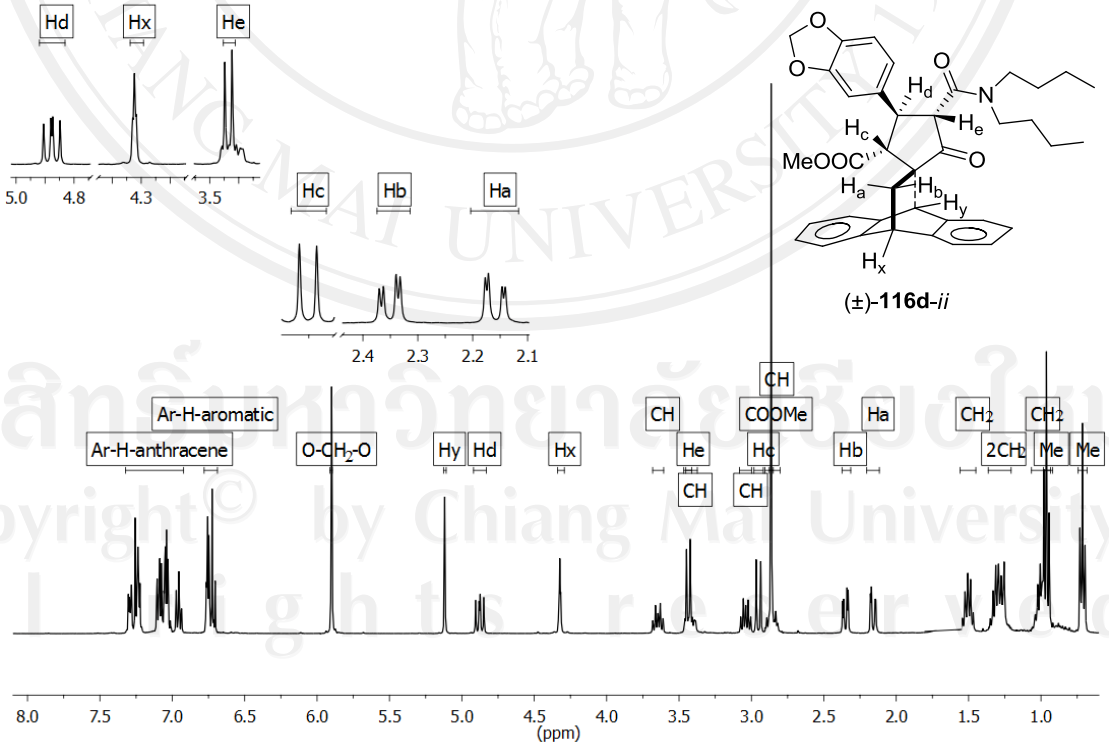

Figure 3.35 ^{1}H-NMR spectrum of spirocyclopentanone–anthracene adduct (±)-**116d**-*ii*

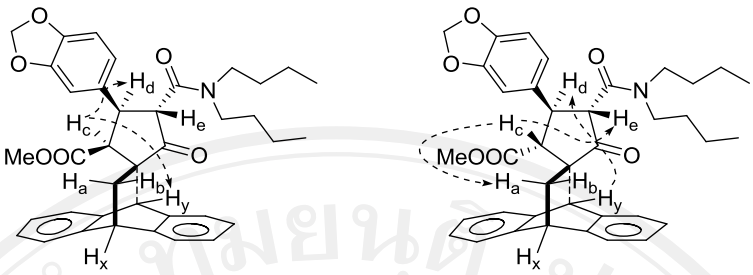

Figure 3.36 NOE correlations observed of spirocyclopentanone–anthracene adducts (±)-**116d**-*i* and (±)-**116d**-*ii*

The mechanism of tandem Michael addition–Dieckmann condensation reactions of spirocyclopentanone–anthracene adducts (±)-**116d**-*i* and (±)-**116d**-*ii* were described in 3.1.2. The relative stereochemistry of the spirocyclopentanone–anthracene adducts (±)-**116d**-*i* and (±)-**116d**-*ii* were assigned by ^{1}H-NMR technique as depicted in Table 3.17, Figures 3.34 and 3.35, respectively.

The spirocyclopentanone–anthracene adducts (±)-**116d**-*i* was characterized by NMR techniques, the proton H_c was observed at δ 2.90 ppm as doublet (J = 6.9 Hz) which is *cis*-configuration with proton H_d. The proton H_e was observed at δ 4.18 ppm as doublet (J = 10.8 Hz) which is *trans*-configuration with proton H_d. The proton H_d was observed at δ 4.87 ppm as doublet of doublets (J = 10.8, 6.9 Hz). The relative stereochemistry of cyclopentanone ring was determined by NOE enhancement. The proton H_c is enhanced with proton H_d and proton H_y which is proton H_c and proton H_d on the lower-face and proton H_e on the upper-face as shown in Figure 3.36.

The spirocyclopentanone–anthracene adducts (±)-**116d**-*ii* was characterized by NMR techniques, the proton H_c was observed at δ 2.95 ppm as doublet d (J = 12.6 Hz) which is *trans*-configuration with proton H_d. The proton H_e was observed at δ 3.44 ppm as doublet (J = 10.1 Hz) which is *trans*-configuration with proton H_d. The proton H_d was observed at δ 4.88 ppm as doublet of doublets (J = 12.6, 10.1 Hz). The relative stereochemistry of cyclopentanone ring was determined by NOE enhancement. The proton H_c is enhanced with proton H_a and proton H_e which is proton Hc and proton He on the upper-face. The proton H_y is enhanced with proton H_d which is proton H_d on the lower-face as shown in Figure 3.36.

3.4 Syntheses of racemic spirocyclopentanone–anthracene adduct derivatives (±)-117a-*i*, -*ii* – (±)-117d-*i*, -*ii* from *α,β*-unsaturated amide derivatives 114a-d

3.4.1 Syntheses of 3′-methoxycarbonyl-4′-phenyl-5′-piperidinecarbonyl-1′-cyclopentanone-2′-spiro-11-9,10-dihydro-9,10-ethanoanthracenes ((±)-117a-*i* and (±)-117a-*ii*) from *α,β*-unsaturated amide 114a

Cinnamic acid (**107**) was treated with oxalyl chloride ($(COCl)_2$) (1.5 equiv.) at 0 °C allowed to room temperature 2 h. After the period, NEt_3 (2.0 equiv.) was added at 0 °C stirred for 15 minutes. Piperidine (**108**) (2.5 equiv.) was added at 0 °C allowed to room temperature 2 h. Purification of the crude product by column chromatography (silica gel) affords *α,β*-unsaturated amide **114a** in 84% yield (Scheme 3.22). The physical properties, ^{1}H NMR data and ^{1}H NMR spectrum were shown in Table 3.18 and Figure 3.37.

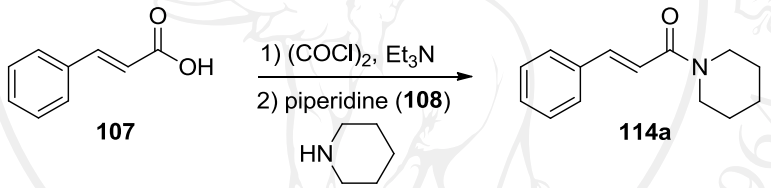

Scheme 3.22 Preparation reaction of *α,β*-unsaturated amide **114a**

Table 3.18 ^{1}H-NMR data of *α,β*-unsaturated amide **114a**

Physical property	m.p. (°C)	Chemical shift (*δ*, ppm)
white crystals	121.2–122.0	1.56–1.72 (m, 6H, CH_2-3″, 4″, 5″), 3.59–3.67 (m, 4H, CH_2-2″, 6″), 6.90 (d (*J* = 15.5 Hz), 1H, CH-2), 7.30–7.40 (m, 3H, CH-3′, 4′, 5′), 7.49–7.55 (m, 2H, CH-2′, 6′), 7.65 (d (*J* = 15.5 Hz), 1H, CH-3) (Figure 3.37)

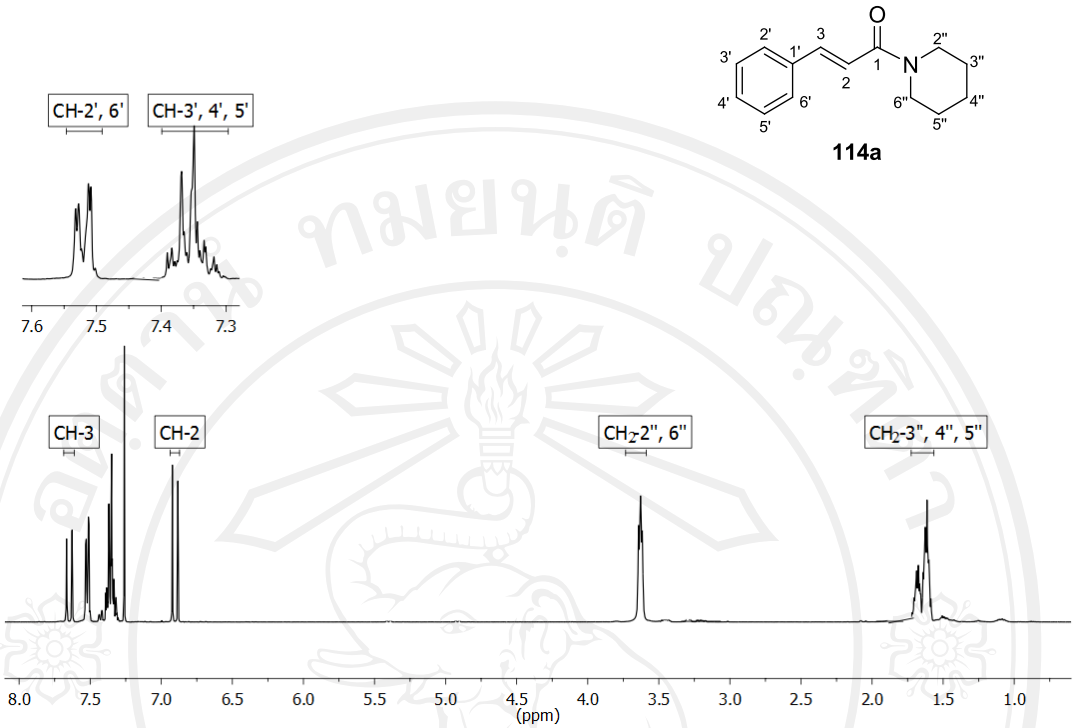

Figure 3.37 ^{1}H-NMR spectrum of *α*,*β*-unsaturated amide **114a**

Then, dimethyl itaconate–anthracene adduct ((±)-**74**) was reacted with *α*,*β*-unsaturated amide **114a** *via* tandem Michael addition–Dieckmann condensation reactions (Scheme 3.23).

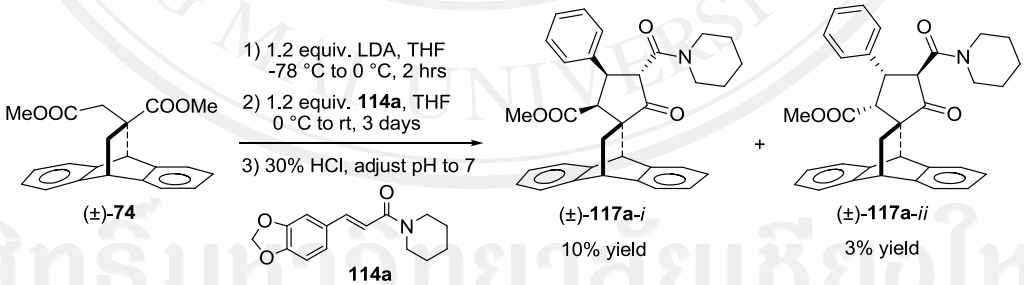

Scheme 3.23 Tandem Michael addition–Dieckmann condensation reactions of (±)-**117a**-*i* and (±)-**117a**-*ii*

An enolate anion (**118** or **119**) of dimethyl itaconate–anthracene adduct, generated from (±)-**74** by treatment with lithium diisopropylamide (LDA, 1.2 equiv.) in THF at 0 °C, readily reacted with *α*,*β*-unsaturated amide **114a** at 0 °C to provide, after leaving the reaction mixture to stir at room temperature for 3 days followed by 10% hydrochloride acid work-up, the spirocyclopentanone–anthracene adduct as mixture

of diastereoisomers. The crude product was purified by flash column chromatography on silica gel to afford diastereomeric spirocyclopentanone adducts (±)-**117a**-*i* in 10% yield and (±)-**117a**-*ii* in 3% yield.

Table 3.19 ^{1}H-NMR data of spirocyclopentanone–anthracene adducts (±)-**117a**-*i* and (±)-**117a**-*ii*

Compound	Physical property	m.p. (°C)	Chemical shift (δ, ppm)
(±)-**117a**-*i*	white crystals	206.5–209.4	1.48–1.76 (m, 6H, CH_2-3′′′′, 4′′′′, 5′′′′), 1.31, 2.26, 4.31 (ABX system (J = 12.8, 2.8, 2.5 Hz), 3H, H_a, H_b, H_x), 2.99 (d (J = 7.1 Hz), 1H, H_c), 3.21 (s, 3H, COOMe-2′′), 3.37–3.52 (m, 2H, CH_2-2′′′′ or 6′′′′), 3.77–3.89 (m, 2H, CH_2-2′′′′ or 6′′′′′), 4.35 (d (J = 10.6 Hz), 1H, H_e), 4.96 (s, 1H, H_y), 5.03 (dd (J = 10.5, 7.1 Hz), 1H, H_d), 6.97–7.53 (m, 13H, ArH-aromatic) (Figure 3.38)
(±)-**117a**-*ii*	white crystals	248.5–250.4	1.28–1.77 (m, 6H, CH_2-4′′′′, 5′′′′, 6′′′′), 1.99, 2.14, 4.38 (ABX system (J = 12.8, 3.1, 2.5 Hz), 3H, H_a, H_b, H_x), 2.44 (d (J = 6.3 Hz), 1H, H_c), 3.21–3.31, 3.65–3.75 (m, 2H, CH_2-2′′′′ or 6′′′′), 3.52–3.63 (m, 2H, CH_2-2′′′′ or 6′′′′), 3.38 (s, 3H, COOMe-2′′), 4.42 (dd (J = 6.3, 12.0 Hz), 1H, H_d), 4.46 (s, 1H, H_y), 4.48 (d (J = 12.0 Hz), 1H, H_e), 6.91–7.45 (m, 13H, Ar-H-aromatic) (Figure 3.39)

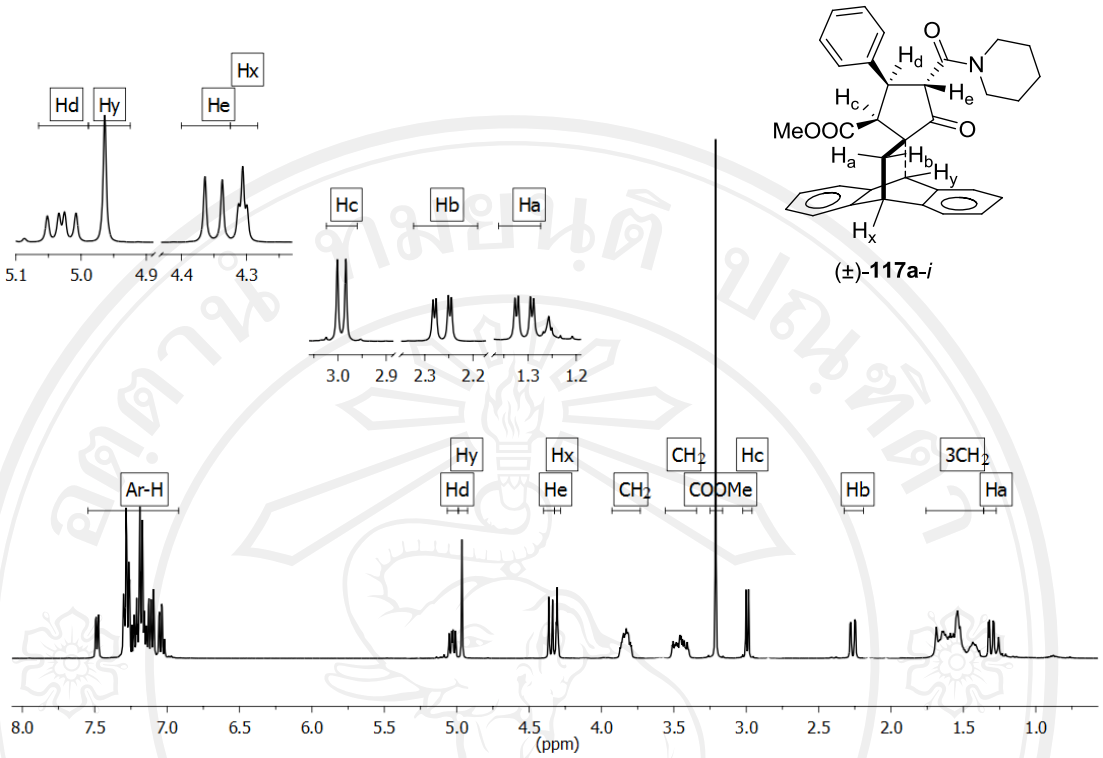

Figure 3.38 ^{1}H-NMR spectrum of spirocyclopentanone–anthracene adduct (±)-**117a**-*i*

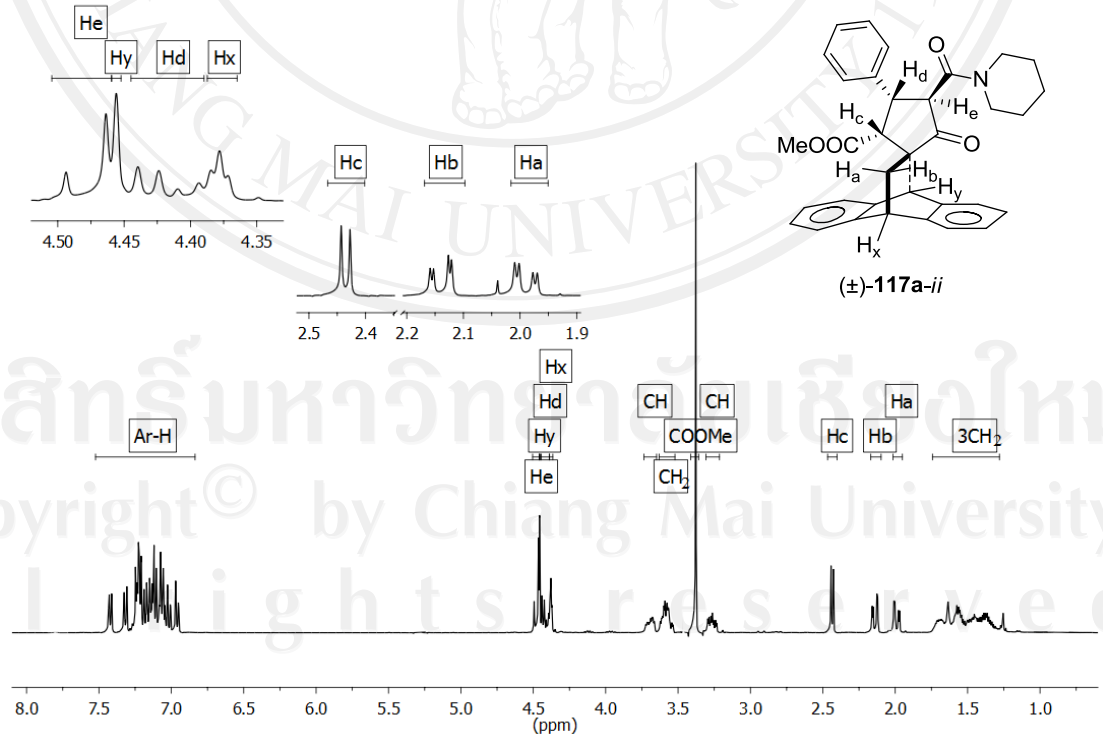

Figure 3.39 ^{1}H-NMR spectrum of spirocyclopentanone–anthracene adduct (±)-**117a**-*ii*

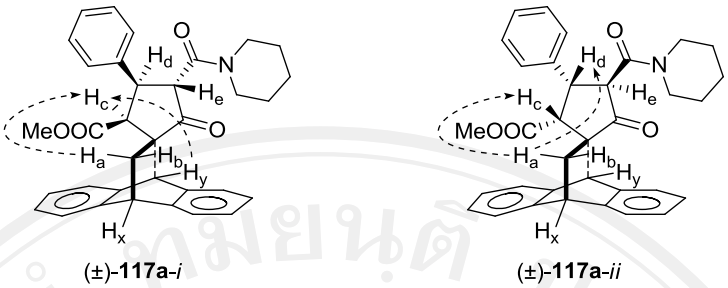

Figure 3.40 NOE correlations observed of spirocyclopentanone–anthracene adducts (±)-**117a**-*i* and (±)-**117a**-*ii*

The mechanism of tandem Michael addition–Dieckmann condensation reactions of spirocyclopentanone–anthracene adducts (±)-**117a**-*i* and (±)-**117a**-*ii* were described in 3.1.1. The relative stereochemistry of the spirocyclopentanone–anthracene adducts (±)-**117a**-*i* and (±)-**117a**-*ii* were assigned by ^{1}H-NMR technique as depicted in Table 3.19, Figures 3.38 and 3.39, respectively.

The spirocyclopentanone–anthracene adducts (±)-**117a**-*i* was characterized by NMR techniques, the proton H_c was observed at δ 2.99 ppm as doublet (J = 7.1 Hz) which is *cis*-configuration with proton H_d. The proton H_e was observed at δ 4.35 ppm as doublet (J = 10.6 Hz) which is *trans*-configuration with proton H_d. The proton H_d was observed at δ 5.03 ppm as doublet of doublets (J = 10.5, 7.1 Hz). The relative stereochemistry of cyclopentanone ring was determined by NOE enhancement. The proton H_y is enhanced with proton H_c, proton H_a is enhanced with proton H_c which are proton H_c and proton H_d on the lower-face, proton H_e on the upper-face as shown in Figure 3.40.

The spirocyclopentanone–anthracene adducts (±)-**117a**-*ii* was characterized by NMR techniques, the proton H_c was observed at δ 2.44 ppm as doublet (J = 6.3 Hz) which is *cis*-configuration with proton H_d. The proton H_d and H_e was observed at δ 4.42–4.51 ppm as multiplet. The relative stereochemistry of cyclopentanone ring was determined by NOE enhancement. The proton H_a is enhanced with proton H_c and H_d which is proton H_c and proton H_d on the upper-face, proton H_e on the lower-face as shown in Figure 3.40.

3.4.2 Syntheses of 3′-methoxycarbonyl-4′-phenyl-5′-pyrrolidinecarbonyl-1′-cyclopentanone-2′-spiro-11-9,10-dihydro-9,10-ethanoanthracenes ((±)-117b-*i* and (±)-117b-*ii*) from *α*,*β*-unsaturated amide 114b

Cinnamic acid (**107**) was treated with oxalyl chloride ($(COCl)_2$) (1.5 equiv.) at 0 °C allowed to room temperature 2 h. After the period, NEt_3 (2.0 equiv.) was added at 0 °C stirred for 15 minutes. Pyrrolidine (**109**) (2.5 equiv.) was added at 0 °C allowed to room temperature 2 h. Purification of the crude product by column chromatography (silica gel) affords *α*,*β*-unsaturated amide **114b** in 70% yield (Scheme 3.24). The physical properties, ^{1}H NMR data and ^{1}H NMR spectrum were shown in Table 3.20 and Figure 3.41.

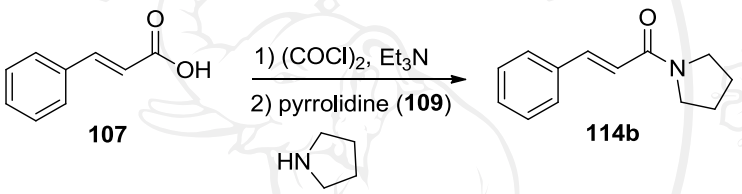

Scheme 3.24 Preparation reaction of *α*,*β*-unsaturated amide **114b**

Table 3.20 ^{1}H-NMR data of *α*,*β*-unsaturated amide **114b**

Physical property	m.p. (°C)	Chemical shift (*δ*, ppm)
white crystals	101.2–102.3	1.89 (p (*J* = 6.6 Hz), 2H, CH_2-3″ or 4″), 2.00 (p (*J* = 6.6 Hz), 2H, CH_2-3″ or 4″), 3.54–3.66 (m, 4H, CH_2-2″, 5″), 6.74 (d (*J* = 15.5 Hz), 1H, CH-2), 7.30–7.41 (m, 3H, CH-3′, 4′, 5′), 7.53 (d (*J* = 7.2 Hz), 2H, CH-2′, 6′), 7.70 (d (*J* = 15.5 Hz), 1H, CH-3) (Figure 3.41)

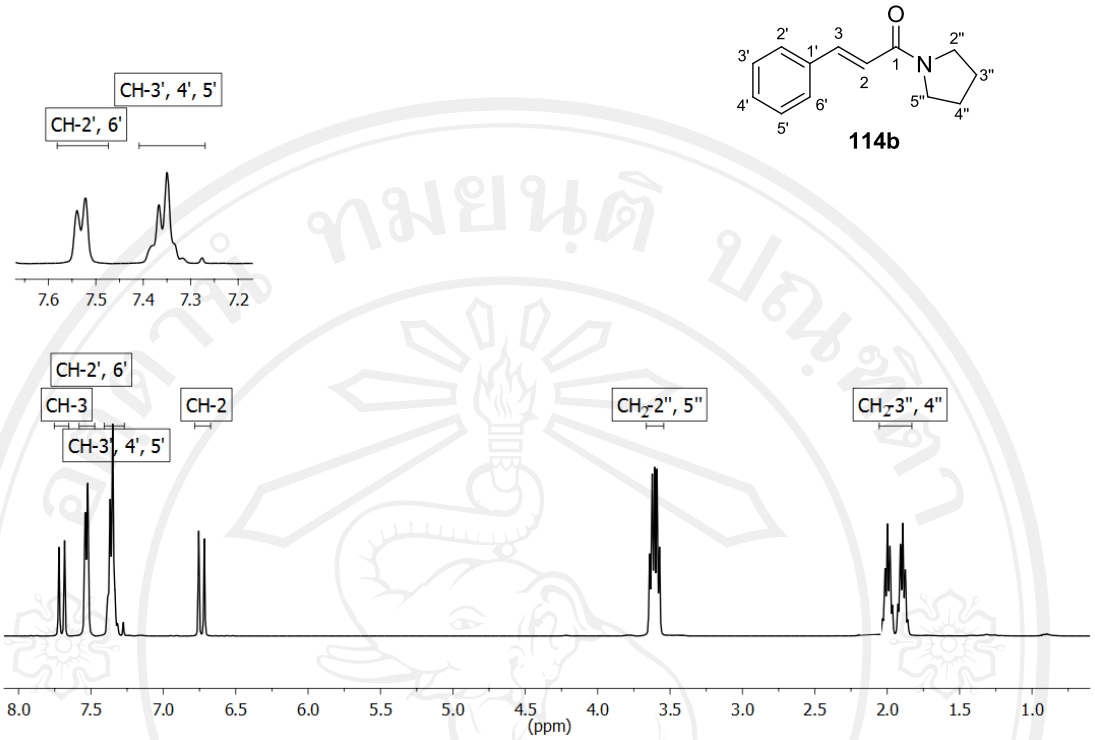

Figure 3.41 ^{1}H-NMR spectrum of *α,β*-unsaturated amide **114b**

Then, dimethyl itaconate–anthracene adduct ((±)-**74**) was reacted with *α,β*-unsaturated amide **114b** *via* tandem Michael addition–Dieckmann condensation reactions (Scheme 3.24).

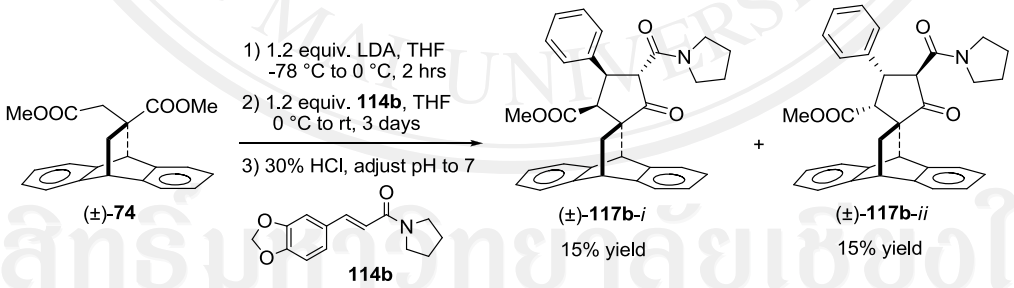

Scheme 3.25 Tandem Michael addition–Dieckmann condensation reactions of (±)-**117b**-*i* and (±)-**117b**-*ii*

an enolate anion (**118** or **119**) of dimethyl itaconate–anthracene adduct, generated from (±)-**74** by treatment with lithium diisopropylamide (LDA, 1.2 equiv.) in THF at 0 °C, readily reacted with *α,β*-unsaturated amide **114b** at 0 °C to provide, after leaving the reaction mixture to stir at room temperature for 3 days followed by 10% hydrochloride acid work-up, the spirocyclopentanone–anthracene adduct as mixture

of diastereoisomers. The crude product was purified by flash column chromatography on silica gel to afford diastereomeric spirocyclopentanone adducts (±)-**117b**-*i* in 15% yield and (±)-**117b**-*ii* in 15% yield.

Table 3.21 ^{1}H-NMR data of spirocyclopentanone–anthracene adducts (±)-**117b**-*i* and (±)-**117b**-*ii*

Compound	Physical property	m.p. (°C)	Chemical shift (δ, ppm)
(±)-**117b**-*i*	white crystals	204.4–205.7	1.65–2.06 (m, 4H, CH_2-3′′′′, 4′′′′), 1.31, 2.26, 4.30 (ABX system (J = 12.8, 2.8, 2.3 Hz), 3H, H_a, H_b, H_x), 2.96 (d (J = 7.0 Hz), 1H, H_c), 3.40–3.47, 3.98–4.08 (m, 2H, CH_2-2′′′′ or 5′′′′), 3.47–3.53 (m, 2H, CH_2-2′′′′ or 5′′′′), 3.20 (s, 3H, COOMe-2′′), 4.21 (d (J = 10.8 Hz), 1H, H_e), 4.93 (dd (J = 10.7, 7.0 Hz), 1H, H_d), 5.05 (s, 1H, H_y), 7.00–7.54 (m, 13H, ArH-aromatic) (Figure 3.42)
(±)-**117b**-*ii*	white crystals	263.1–267.3	1.68–1.97 (m, 4H, CH_2-3′′′′, 4′′′′), 2.00, 2.19, 4.39 (ABX system (J = 12.9, 3.0, 2.4 Hz), 3H, H_a, H_b, H_x), 2.43 (d (J = 6.7 Hz), 1H, H_c), 3.28–3.33 (m, 2H, CH_2-2′′′′ or 5′′′′), 3.41–3.49, 3.97–4.08 (m, 2H, CH_2-2′′′′ or 5′′′′), 3.39 (s, 3H, COOMe-2′′), 4.27 (d (J = 11.9 Hz), 1H, H_e), 4.41 (dd (J = 10.8, 5.5 Hz), 1H, H_d), 4.45 (s, 1H, H_y), 6.92–7.48 (m, 13H, ArH-aromatic) (Figure 3.43)

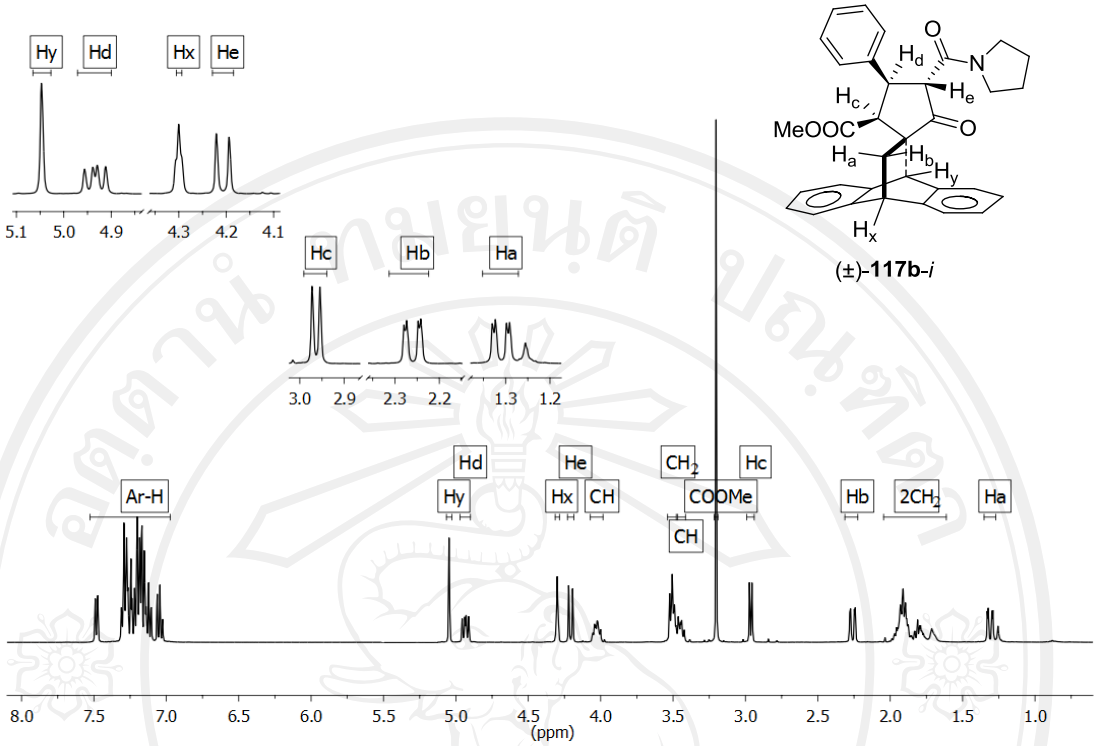

Figure 3.42 ^{1}H-NMR spectrum of spirocyclopentanone–anthracene adduct (±)-**117b**-*i*

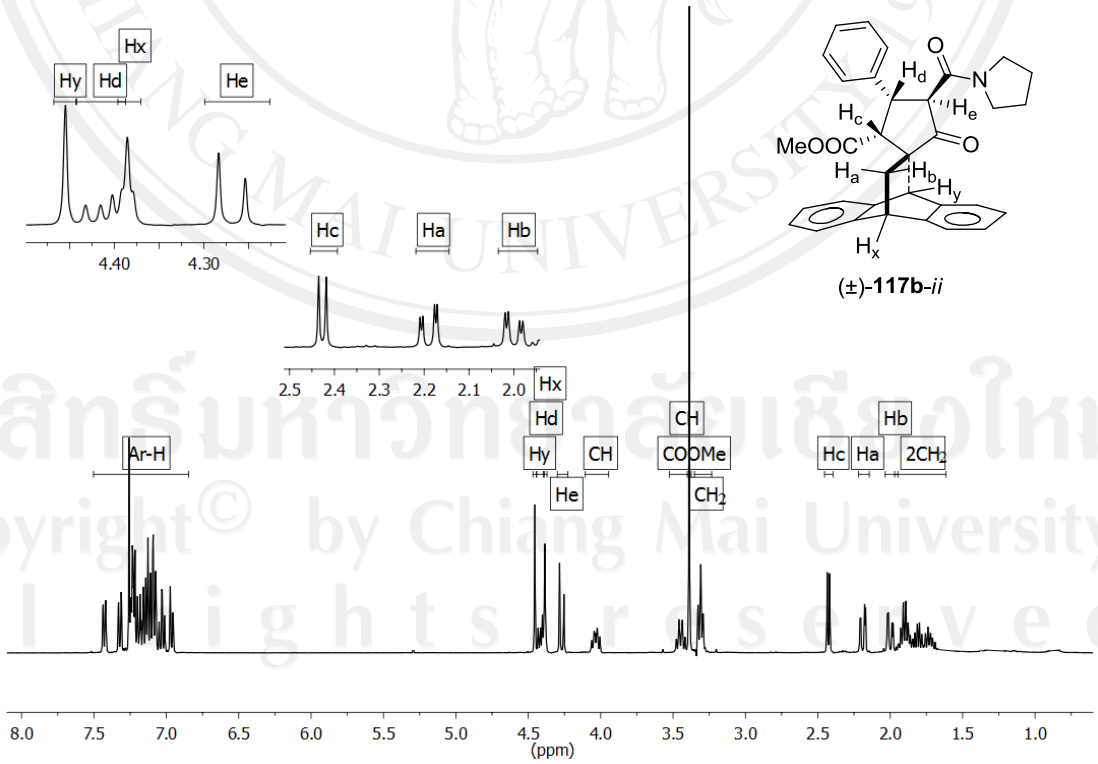

Figure 3.43 ^{1}H-NMR spectrum of spirocyclopentanone–anthracene adduct (±)-**117b**-*ii*

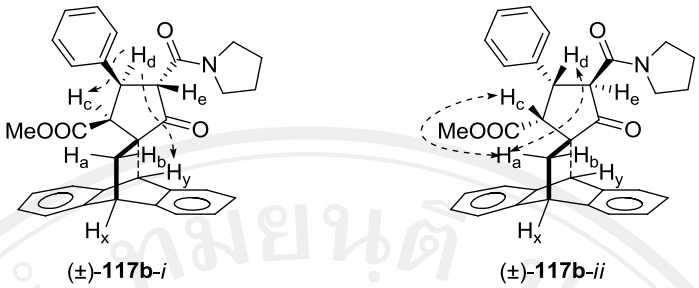

Figure 3.44 NOE correlations observed of spirocyclopentanone–anthracene adduct (±)-**117b**-*i* and (±)-**117b**-*ii*

The mechanism of tandem Michael addition–Dieckmann condensation reactions of spirocyclopentanone–anthracene adducts (±)-**117b**-*i* and (±)-**117b**-*ii* were described in 3.1.1. The relative stereochemistry of the spirocyclopentanone–anthracene adducts (±)-**117b**-*i* and (±)-**117b**-*ii* were assigned by ^{1}H-NMR technique as depicted in Table 3.21, Figures 3.42 and 3.42, respectively.

The spirocyclopentanone–anthracene adducts (±)-**117b**-*i* was characterized by NMR techniques, the proton H_c was observed at δ 2.96 ppm as doublet (J = 7.0 Hz) which is *cis*-configuration with proton H_d. The proton H_e was observed at δ 4.21 ppm as doublet (J = 10.8 Hz) which is *trans*-configuration with proton H_d. The proton H_d was observed at δ 4.93 ppm as doublet of doublets (J = 10.7, 7.0 Hz). The relative stereochemistry of cyclopentanone ring was determined by NOE enhancement. The proton H_d is enhanced with proton H_c and proton H_y which is proton H_c and proton H_d on the lower-face, proton H_e on the upper-face as shown in Figure 3.44.

The spirocyclopentanone–anthracene adducts (±)-**117b**-*ii* was characterized by NMR techniques, the proton H_c was observed at δ 2.43 ppm as doublet (J = 6.7 Hz) which is *cis*-configuration with proton H_d. The proton H_e was observed at δ 4.27 ppm as doublet (J = 11.9 Hz) which is *trans*-configuration with proton H_d. The proton H_d was observed at δ 4.41 ppm as doublet of doublets (J = 10.8, 5.5 Hz). The relative stereochemistry of cyclopentanone ring was determined by NOE enhancement. The proton H_a is enhanced with proton H_c and proton H_d which is proton H_c and proton H_d on the upper-face, proton H_e on the lower-face as shown in Figure 3.44.

3.4.3 Syntheses of 5′-(*N*,*N*-diisopropylcarboxamid-1-yl)-3′-methoxycarbonyl-4′-phenyl-1′-cyclopentanone-2′-spiro-11-9,10-dihydro-9,10-ethanoanthracenes ((±)-117c-*i* and (±)-117c-*ii*) from *α*,*β*-unsaturated amide 114c

Cinnamic acid (**107**) was treated with oxalyl chloride ($(COCl)_2$) (1.5 equiv.) at 0 °C allowed to room temperature 2 h. After the period, NEt_3 (2.0 equiv.) was added at 0 °C stirred for 15 minutes. Diisopropylamine (**110**) (2.5 equiv.) was added at 0 °C allowed to room temperature 2 h. Purification of the crude product by column chromatography (silica gel) affords *α*,*β*-unsaturated amide **114c** in 87% yield (Scheme 3.26). The physical properties, ^{1}H NMR data and ^{1}H NMR spectrum were shown in Table 3.22 and Figure 3.45.

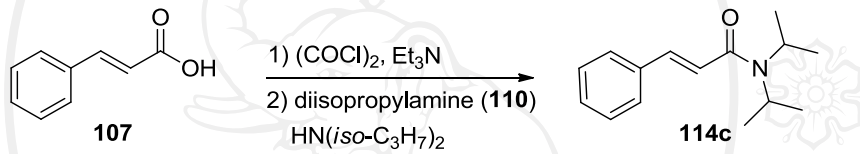

Scheme 3.26 Preparation reaction of *α*,*β*-unsaturated amide **114c**

Table 3.22 ^{1}H-NMR data of *α*,*β*-unsaturated amide **114c**

Physical property	m.p. (°C)	Chemical shift (*δ*, ppm)
colorless liquid	–	1.33 (brs, 6H, CH_3-3″, 4″, 6″ or 7″), 1.39 (brs, 6H, CH_3-3″, 4″, 6″ or 7″), 3.86 (brs, 1H, CH-2″ or 5″), 4.11 (brs, 1H, CH-2″ or 5″), 6.84 (d (*J* = 15.4 Hz), 1H, CH-2), 7.29–7.40 (m, 3H, CH-3′, 4′, 5′), 7.50 (dt (*J* = 3.8, 2.1 Hz), 2H, CH-2′, 6′), 7.95 (d (*J* = 15.5 Hz), 1H, CH-3) (Figure 3.45)

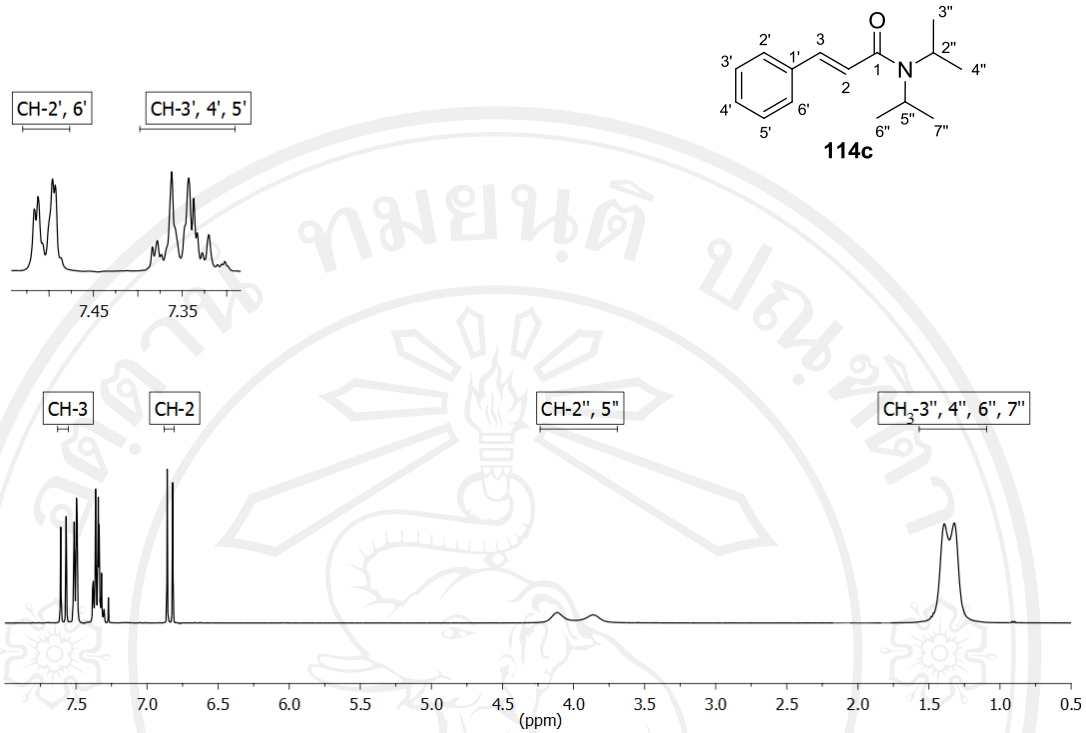

Figure 3.45 ^{1}H-NMR spectrum of *α*,*β*-unsaturated amide **114c**

Then, dimethyl itaconate–anthracene adduct ((±)-**74**) was reacted with *α*,*β*-unsaturated amide **114c** *via* tandem Michael addition–Dieckmann condensation reactions (Scheme 3.27)

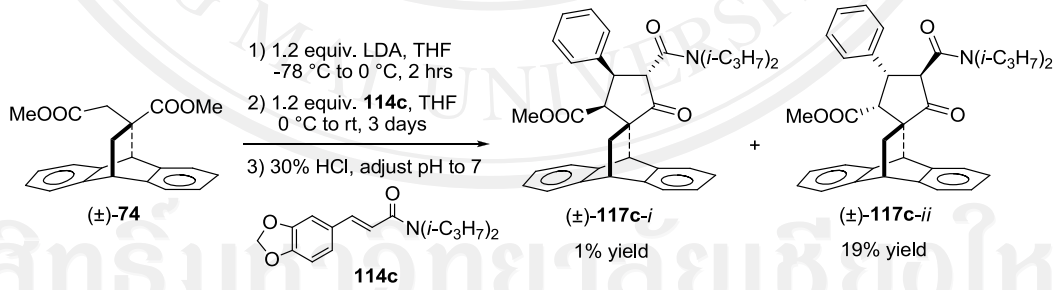

Scheme 3.27 Tandem Michael addition–Dieckmann condensation reactions of (±)-**117c**-*i* and (±)-**117c**-*ii*

An enolate anion (**118** or **119**) of dimethyl itaconate–anthracene adduct, generated from (±)-**74** by treatment with lithium diisopropylamide (LDA, 1.2 equiv.) in THF at 0 °C, readily reacted with *α*,*β*-unsaturated amide **114c** at 0 °C to provide, after leaving the reaction mixture to stir at room temperature for 3 days followed by 10% hydrochloride acid work-up, the spirocyclopentanone–anthracene adduct as mixture

of diastereoisomers. The crude product was purified by flash column chromatography on silica gel to afford diastereomeric spirocyclopentanone–anthracene adducts (±)-**117c**-*i* in 1% yield and (±)-**117c**-*ii* in 19% yield.

Table 3.23 ^{1}H-NMR data of spirocyclopentanone–anthracene adducts (±)-**117c**-*i* and (±)-**117c**-*ii*

Compound	Physical property	m.p. (°C)	Chemical shift (δ, ppm)
(±)-**117c**-*i*	white crystals	98.5–101.9	1.14 (d (J = 6.7 Hz), 3H, CH_3-3′′′′ or 4′′′′ or 6′′′′ or 7′′′′), 1.24 (d (J = 6.4 Hz), 3H, CH_3-3′′′′ or 4′′′′ or 6′′′′ or 7′′′′), 1.39 (d (J = 6.7 Hz), 3H, CH_3-3′′′′ or 4′′′′ or 6′′′′ or 7′′′′), 1.51 (d (J = 6.7 Hz), 3H, CH_3-3′′′′ or 4′′′′ or 6′′′′ or 7′′′′), 1.31, 2.25, 4.30 (ABX system (J = 12.7, 2.7, 2.6 Hz), 3H, H_a, H_b, H_x), 3.02 (d (J = 7.0 Hz), 1H, H_c), 3.22 (s, 3H, COOMe-2′′), 3.48 hept (J = 6.7 Hz), 1H, CH-2′′′′ or 5′′′′), 4.57 (hept (J = 6.7 Hz), 1H, CH-2′′′′ or 5′′′′), 4.31 (d (J = 10.3 Hz), 1H, H_e), 4.93 (s, 1H, H_y), 5.08 (dd (J = 10.4, 7.1 Hz), 1H, H_d), 6.95–7.52 (m, 13H, Ar-H-aromatic) (Figure 3.46)

Table 3.23 ^{1}H-NMR data of spirocyclopentanone–anthracene adducts (±)-**117c**-*i* and (±)-**117c**-*ii* (continued)

Compound	Physical property	m.p. (°C)	Chemical shift (δ, ppm)
(±)-**117c**-*ii*	white crystals	238.2–242.1	1.03 (d (J = 6.7 Hz), 3H, CH_3-3′′′′ or 4′′′′ or 6′′′′ or 7′′′′), 1.11 (d (J = 6.7 Hz), 3H, CH_3-3′′′′ or 4′′′′ or 6′′′′ or 7′′′′), 1.25 (d (J = 6.4 Hz), 3H, CH_3-3′′′′ or 4′′′′ or 6′′′′ or 7′′′′), 1.26 (d (J = 6.7 Hz), 3H, CH_3-3′′′′ or 4′′′′ or 6′′′′ or 7′′′′), 1.98, 2.19, 4.38 (ABX system (J = 12.8, 3.1, 2.2 Hz), 3H, H_a, H_b, H_x), 2.42 (d (J = 5.6 Hz), 1H, H_c), 3.23–3.36 (m, 1H, CH-2′′′′ or 5′′′′), 3.39 (s, 3H, COOMe-2′′), 4.31–4.43 (m, 3H, H_d, H_e, CH-2′′′′ or 5′′′′), 4.47 (s, 1H, H_y), 6.91–7.47 (m, 13H, Ar-H-aromatic) (Figure 3.47)

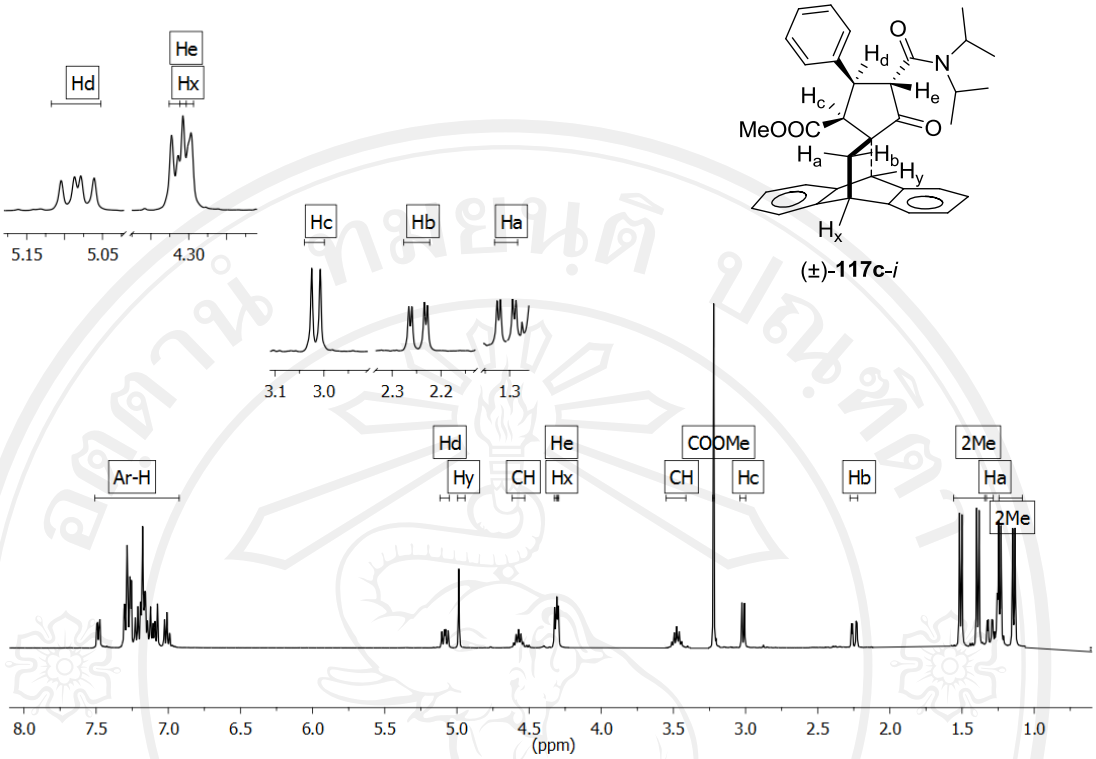

Figure 3.46 ^{1}H-NMR spectrum of spirocyclopentanone–anthracene adduct (±)-**117c**-*i*

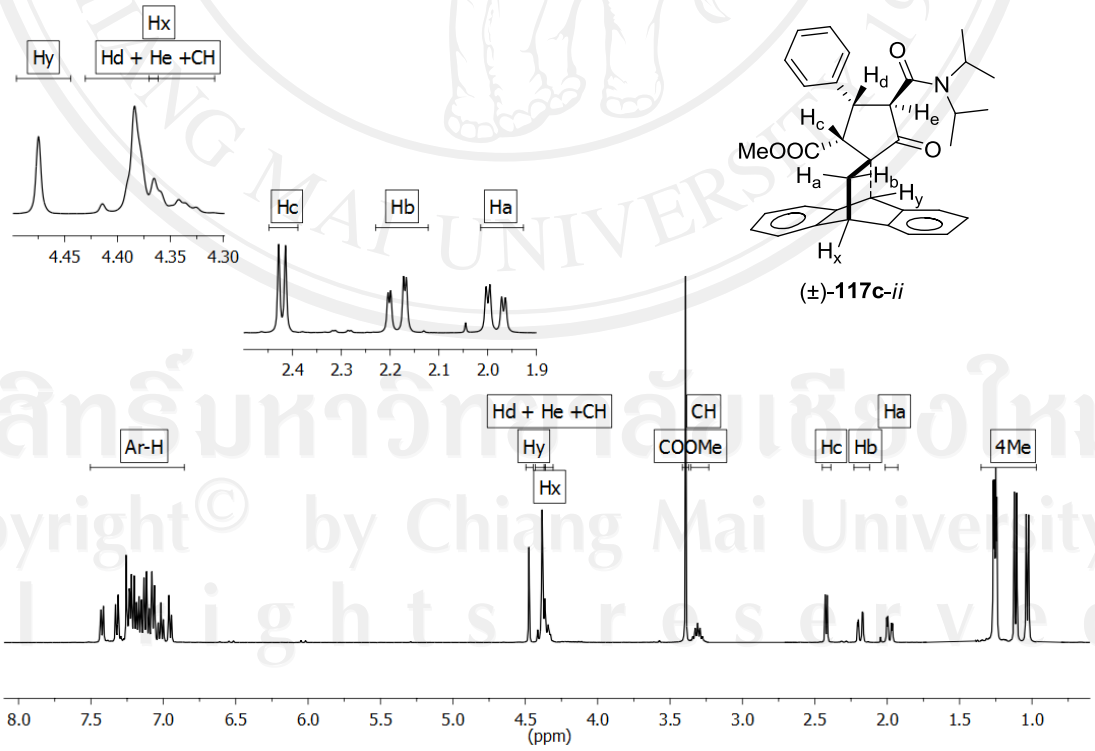

Figure 3.47 ^{1}H-NMR spectrum of spirocyclopentanone–anthracene adduct (±)-**117c**-*ii*

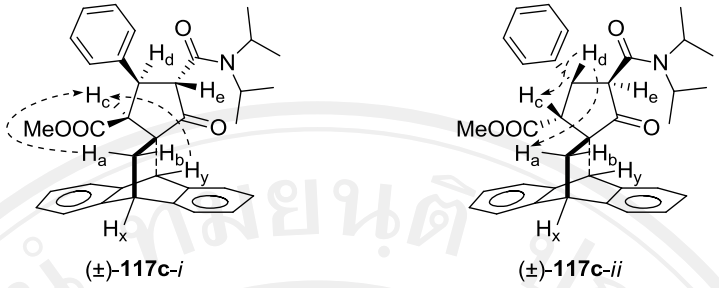

Figure 3.48 NOE correlations observed of spirocyclopentanone–anthracene adduct (±)-**117c**-*i* and (±)-**117c**-*ii*

The mechanism of tandem Michael addition–Dieckmann condensation reactions of spirocyclopentanone–anthracene adducts (±)-**117c**-*i* and (±)-**117c**-*ii* were described in 3.1.1. The relative stereochemistry of the spirocyclopentanone–anthracene adducts (±)-110d-*i* and (±)-110d-*ii* were assigned by ^{1}H-NMR technique as depicted in Table 3.23, Figures 3.46 and 3.47, respectively.

The spirocyclopentanone–anthracene adducts (±)-**117c**-*i* was characterized by NMR techniques, the proton H_c was observed at δ 3.02 ppm as doublet (J = 7.0 Hz) which is *cis*-configuration with proton H_d. The proton H_e was observed at δ 4.31 ppm as doublet (J = 10.3 Hz) which is *trans*-configuration with proton H_d. The proton H_d was observed at δ 5.08 ppm as doublet of doublets (J = 10.4, 7.1 Hz). The relative stereochemistry of cyclopentanone ring was determined by NOE enhancement. The proton H_y is enhanced with proton H_c, proton H_a is enhanced with proton H_c which are proton H_c and proton H_d on the lower-face, proton H_e on the upper-face as shown in Figure 3.48.

The spirocyclopentanone–anthracene adducts (±)-**117c**-*ii* was characterized by NMR techniques, the proton H_c was observed at δ 2.42 ppm as doublet (J = 5.6 Hz) which is *cis*-configuration with proton H_d. The proton H_e and H_d was observed at δ 4.31–4.43 ppm as multiplet. The relative stereochemistry of cyclopentanone ring was determined by NOE enhancement. The proton H_d is enhanced with proton H_a and proton H_c which is proton H_c and proton H_d on the upper-face, proton H_e on the lower-face as shown in Figure 3.48.

3.4.4 Syntheses of 5′-(*N*,*N*-dibutylcarboxamid-1-yl)-3′-methoxycarbonyl-4′-phenyl-1′-cyclopentanone-2′-spiro-11-9,10-dihydro-9,10-ethanoanthracenes ((±)-117d-*i* and (±)-117d-*ii*) from *α*,*β*-unsaturated amide 114d

Cinnamic acid (**107**) was treated with oxalyl chloride ($(COCl)_2$) (1.5 equiv.) at 0 °C allowed to room temperature 2 h. After the period, NEt_3 (2.0 equiv.) was added at 0 °C stirred for 15 minutes. Dibutylamine (**111**) (2.5 equiv.) was added at 0 °C allowed to room temperature 2 h. Purification of the crude product by column chromatography (silica gel) affords *α*,*β*-unsaturated amide **114d** in 91% yield (Scheme 3.28). The physical properties, ^{1}H NMR data and ^{1}H NMR spectrum were shown in Table 3.24 and Figure 3.49.

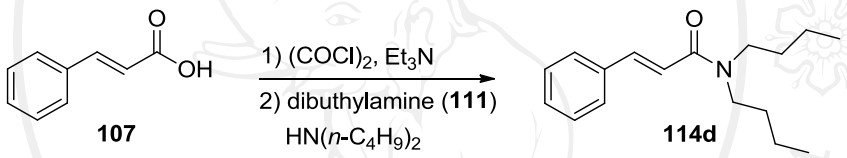

Scheme 3.28 Preparation reaction of *α*,*β*-unsaturated amide **114d**

Table 3.24 ^{1}H-NMR data of *α*,*β*-unsaturated amide **114d**

Physical property	m.p. (°C)	Chemical shift (*δ*, ppm)
colorless liquid	–	0.96 (dt (*J* = 9.5, 7.4 Hz), 6H, CH_3-5″, 9″), 1.30-1.43 (m, 4H, CH_2-4″, 8″), 1.53-1.67 (m, 4H, CH_2-3″, 7″), 3.36–3.47 (m, 4H, CH_2-2″, 6″), 6.84 (d (*J* = 15.4 Hz), 1H, CH-2), 7.30–7.40 (m, 3H, CH-3′, 4′, 5′), 7.51 (d (*J* = 7.9, 1.5 Hz), 2H, CH-2′, 6′), 7.70 (d (*J* = 15.4 Hz), 1H, CH-3) (Figure 3.49)

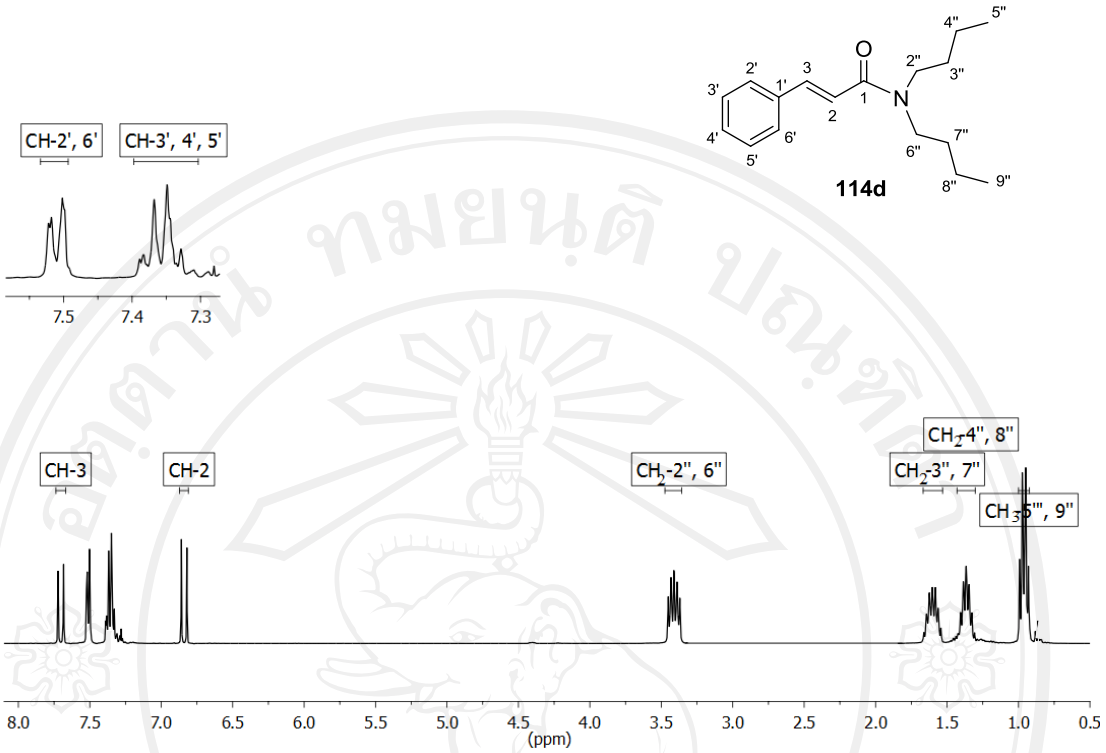

Figure 3.49 ^{1}H-NMR spectrum of *α,β*-unsaturated amide **114d**

Then, dimethyl itaconate–anthracene adduct ((±)-**74**) was reacted with *α,β*-unsaturated amide **114d** *via* tandem Michael addition–Dieckmann condensation reactions (Scheme 3.29).

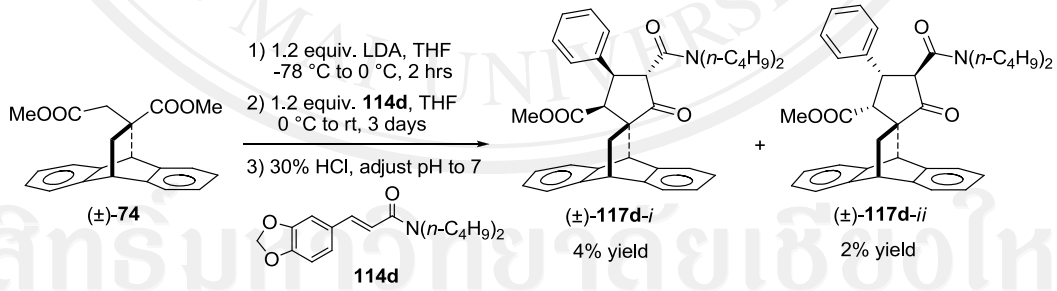

Scheme 3.29 Tandem Michael addition–Dieckmann condensation reactions of (±)-**117d**-*i* and (±)-**117d**-*ii*

An enolate anion (**118** or **119**) of dimethyl itaconate–anthracene adduct, generated from (±)-**74** by treatment with lithium diisopropylamide (LDA, 1.2 equiv.) in THF at 0 °C, readily reacted with *α,β*-unsaturated amide **114d** at 0 °C to provide, after leaving the reaction mixture to stir at room temperature for 3 days followed by 10% hydrochloride acid work-up, the spirocyclopentanone–anthracene adduct as mixture

of diastereoisomers. The crude product was purified by flash column chromatography on silica gel to afford diastereomeric spirocyclopentanone adducts (±)-**117d**-*i* in 4% yield and (±)-**117d**-*ii* in 2% yield.

Table 3.25 ^{1}H-NMR data of spirocyclopentanone–anthracene adducts (±)-**117d**-*i* and (±)-**117d**-*ii*

Compound	Physical property	m.p. (°C)	Chemical shift (δ, ppm)
(±)-**117d**-*i*	white crystals	168.2–170.1	0.89 (t (J = 7.3 Hz), 3H, CH_3-5′′′′ or 9′′′′), 0.95 (t (J = 7.3 Hz), 3H, CH_3-5′′′′ or 9′′′′), 1.22–1.41, 1.47–1.62 (m, 8H, CH_2-3′′′′, 4′′′′, 7′′′′, 8′′′′), 1.27, 2.26, 4.30 (ABX system (J = 12.7, 2.4, 2.2 Hz), 3H, H_a, H_b, H_x), 2.96 (d (J = 7.0 Hz), 1H, H_c), 2.93–3.04, 3.67–3.79 (m, 2H, CH_2-2′′′′ or 6′′′′), 3.05–3.16, 3.79–3.91 (m, 2H, CH_2-2′′′′ or 6′′′′), 3.25 (s, 3H, COOMe-2′′), 4.28 (d (J = 11.0 Hz), 1H, H_e), 4.97 (dd (J = 10.7, 7.0 Hz), 1H, H_d), 5.01 (s, 1H, H_y), 6.97–7.52 (m, 13H, ArH-aromatic) (Figure 3.50)
(±)-**117d**-*ii*	white crystals	192.4–195.3	0.79 (t (J = 7.3 Hz), 3H, CH_3-5′′′′ or 9′′′′), 0.95 (t (J = 7.2 Hz), 3H, CH_3-5′′′′ or 9′′′′), 1.22–1.41, 1.47–1.62 (m, 8H, CH_2-3′′′′, 4′′′′, 7′′′′, 8′′′′), 1.99, 2.17, 4.38 (ABX system (J = 12.8, 3.0, 2.5 Hz), 3H, H_a, H_b, H_x), 2.40 (dd (J = 4.8, 0.9 Hz), 1H, H_c), 2.93–3.04, 3.22–3.35 (m, 2H, CH_2-2′′′′ or 6′′′′), 3.04–3.13, 3.66–3.78 (m, 2H, CH_2-2′′′′ or 6′′′′), 3.43 (s, 3H, COOMe-2′′), 4.35–4.39 (m, 2H, H_d, H_e), 4.47 (s, 1H, H_y), 6.93–7.47 (m, 13H, ArH-aromatic) (Figure 3.51)

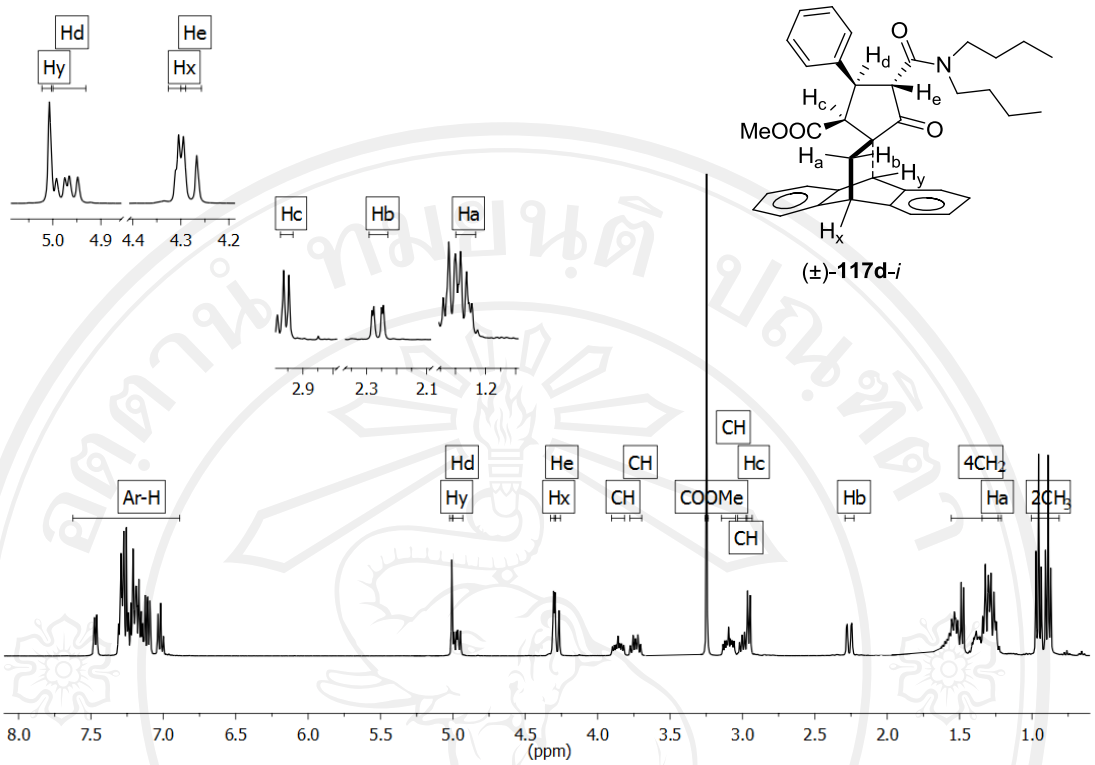

Figure 3.50 ^{1}H-NMR spectrum of spirocyclopentanone–anthracene adduct (±)-**117d**-*i*

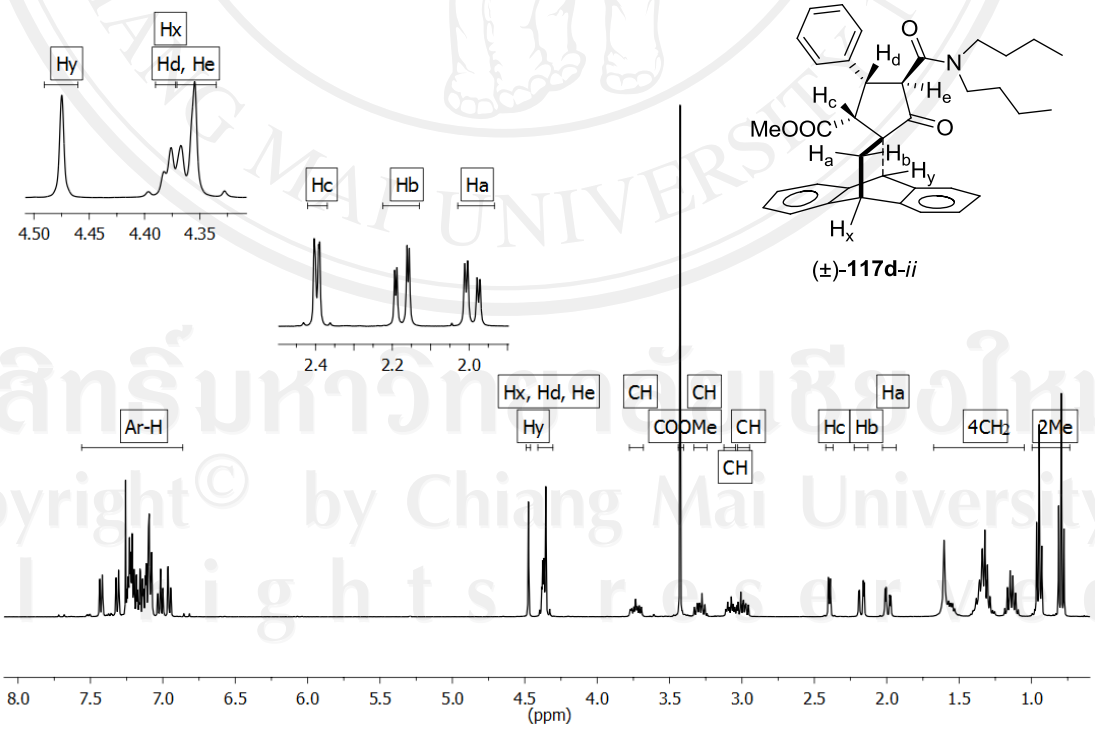

Figure 3.51 ^{1}H-NMR spectrum of spirocyclopentanone–anthracene adduct (±)-**117d**-*ii*

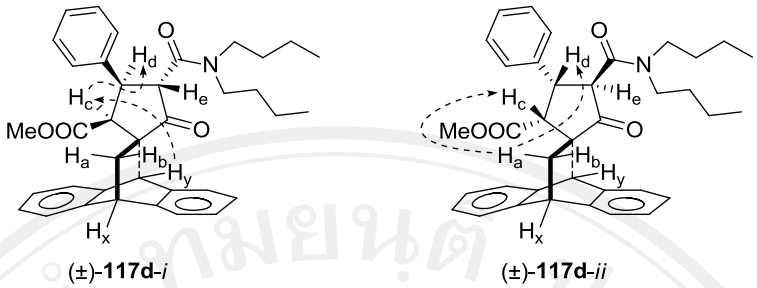

Figure 3.52 NOE correlations observed of spirocyclopentanone–anthracene adduct (±)-**117d**-*i* and (±)-**117d**-*ii*

The mechanism of tandem Michael addition–Dieckmann condensation reactions of spirocyclopentanone–anthracene adducts (±)-**117d**-*i* and (±)-**117d**-*ii* were described in 3.1.1. The relative stereochemistry of the spirocyclopentanone–anthracene adducts (±)-**117d**-*i* and (±)-**117d**-*ii* were assigned by ^{1}H-NMR technique as depicted in Table 3.25, Figures 3.50 and 3.51, respectively.

The spirocyclopentanone–anthracene adducts (±)-**117d***i* was characterized by NMR techniques, the proton H_c was observed at δ 2.96 ppm as doublet (J = 7.0 Hz) which is *cis*-configuration with proton H_d. The proton H_e was observed at δ 4.28 ppm as doublet (J = 11.0 Hz) which is *trans*-configuration with proton H_d. The proton H_d was observed at δ 4.97 ppm as doublet of doublets (J = 10.7, 7.0 Hz)). The relative stereochemistry of cyclopentanone ring was determined by NOE enhancement. The proton H_c is enhanced with proton H_d. Proton H_y is enhanced with proton H_c which are proton H_c and proton H_d on the lower-face, proton H_e on the upper-face as shown in Figure 3.52.

The spirocyclopentanone–anthracene adducts (±)-**117d**-*ii* was characterized by NMR techniques, the proton H_c was observed at δ 2.40 ppm as doublet (J = 4.8, 0.9 Hz) which is *cis*-configuration with proton H_d, the proton H_e and H_d was observed at δ 4.35–4.39 ppm as multiplet. The relative stereochemistry of cyclopentanone ring was determined by NOE enhancement. The proton H_a is enhanced with proton H_c and proton H_d which is proton H_c and proton H_d on the upper-face, proton H_e on the lower-face as shown in Figure 3.52.

3.5 Syntheses of spirocyclopentanone–anthracene adduct dimers ((±)-147a-c)

3.5.1 Preparation of methyl itaconate–anthracene adduct dimers ((±)-146a-c) from methyl itaconate–anthracene adduct mono acid ((±)-143)

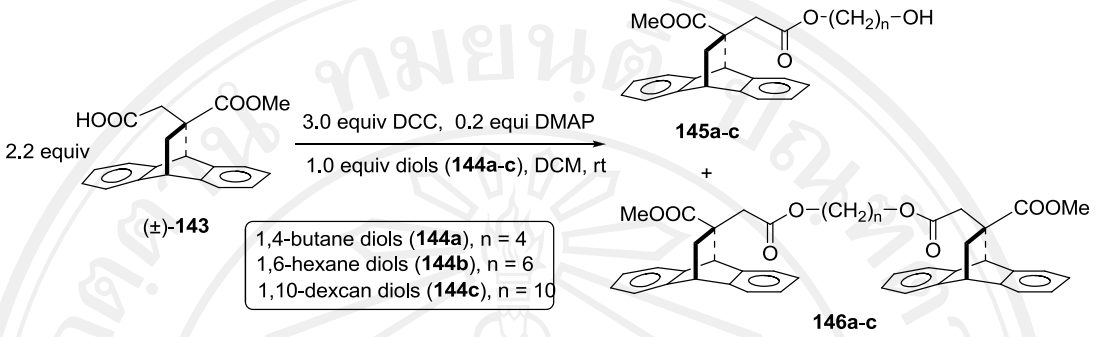

Scheme 3.30 Preparation of methyl itaconate–anthracene adduct dimer ((±)-**146a-c**)

Methyl itaconate–anthracene adduct mono acid ((±)-**143**) was treated with *N*,*N'*-Dicyclohexylcarbodiimide (DCC) (1.5 equiv.) and 4-Dimethylaminopyridine (DMAP) at room temperature 2 h. After the period, diols (**144a-c**) was added. Purification of the crude product by column chromatography (silica gel) affords dimethyl itaconate–anthracene adduct dimer (**146a-c**) in qualitative yield.

3.5.2 Syntheses of spirocyclopentanone–anthracene adduct dimers ((±)-147a-c)

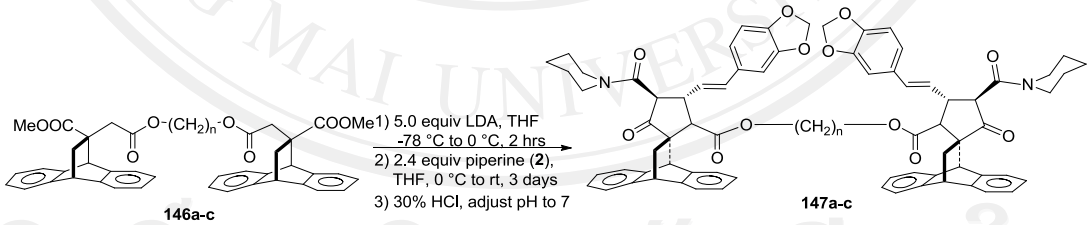

Scheme 3.31 Tandem Michael addition–Dieckmann condensation reactions of (±)-**147a-c**

According to general procedure II in **2.6.1**, Dimethyl itaconate–anthracene adduct dimer ((±)-**146a-c**) were reacted with piperine (**75**) *via* tandem Michael addition–Dieckmann condensation reactions. The spirocyclopentanone–anthracene adducts ((±)-**147a-c**) were not observed.

3.6 Bioactivity and Cytotoxicity Tests

All of synthesized compounds were tested antimalarial activity against cultured intra-erythrocytic asexual forms of the human malaria parasite *P. falciparum* (K1, multi-drug resistance strain)[92] by microculture radioisotope technique[93] using dihydroartemisinin and mefloquine as positive control and tested cytoxicity against *Vero cells* (African green monkey kidney cell line) by green fluorescent protein (GFP)-based[94] assay using ellipticine as positive control, as summarized in Table 3.26 – 3.29.

Table 3.26 Bioactivity and cytotoxicity tests of spirocyclopentanone–anthracene adduct ((±)-**76**-*i* and (±)-**76**-*ii*) and cyclopentanones ((±)-**134**-*i* and (±)-**134**-*ii*)

Compounds	Bioactive IC_{50} (μg/ml)	
	Antimalarial	Cytotoxicity (*Vero cell*)
Dihydroartemisinin	0.0004	N/A
Ellipticine	N/A	1.32
Piperine (**75**)	inactive	non-cytotoxic
(±)-**76**-*i*	4.70	non-cytotoxic
(±)-**76**-*ii*	3.40	non-cytotoxic
(±)-**134**-*i*	inactive	non-cytotoxic
(±)-**134**-*ii*	inactive	non-cytotoxic

N/A = not available

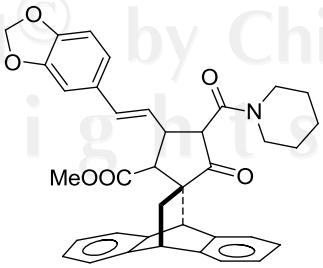

(±)-**76**

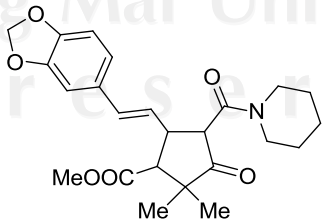

(±)-**134**

The result shown above indicated that the racemic spirocyclopentanone–anthracene adducts ((±)-**76**-*i* and (±)-**76**-*ii*) displayed antimalarial activity against parasite *P. falciparum* with IC_{50} 4.70, 3.40 μg/ml respectively. Interestingly, none of these compounds showed cytoxicity against *Vero cells*. The cyclopentanones ((±)-**134**-*i* and (±)-**134**-*ii*) were inactive against *P. falciparum* and *Vero cell*. Obviously, the anthracene moiety is important for antimalarial activity.

Table 3.27 Bioactivity and cytotoxicity tests of racemic spirocyclopentanone-anthracene adducts (±)-**115b**-*i*, -*ii* – (±)-**115d**-*i*, -*ii*

Compounds	R	R′	Bioactive IC_{50} (μg/ml)	
			Antimalarial	Cytotoxicity (*Vero cell*)
Dihydroartemisinin			0.0004	N/A
Ellipticine			N/A	1.32
(±)-**76**-*i*	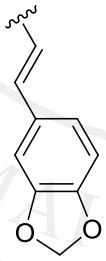	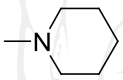	4.70	non-cytotoxic
(±)-**76**-*ii*			3.40	non-cytotoxic
(±)-**115b**-*i*		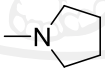	3.38	non-cytotoxic
(±)-**115b**-*ii*			4.64	6.12
(±)-**115c**-*i*		—N(*i*-C_3H_7)$_2$	3.14	non-cytotoxic
(±)-**115c**-*ii*			3.89	non-cytotoxic
(±)-**115d**-*i*		—N(*n*-C_4H_9)$_2$	4.35	non-cytotoxic
(±)-**115d**-*ii*			6.52	non-cytotoxic

N/A = not available

The result shown above indicated that the racemic spirocyclopentanone–anthracene adducts (±)-**115b**-*i*, -*ii* – (±)-**115d**-*i*, -*ii* displayed antimalarial activity against parasite *P. falciparum* with IC_{50} 3.38, 4.64, 3.14, 3.89, 4.35 and 6.52 μg/ml respectively. Obviously, the amide moiety is not significant difference for antimalarial activity.

Table 3.28 Bioactivity and cytotoxicity tests of racemic spirocyclopentanone-anthracene adducts (±)-**116a**-*i*, -*ii* – (±)-**116d**-*i*, -*ii*

Compounds	R	R′	Bioactive IC_{50} (μg/ml)	
			Antimalarial	Cytotoxicity (*Vero cell*)
Dihydroartemisinin			0.0004	N/A
Ellipticine			N/A	1.32
(±)-**116a**-*i*	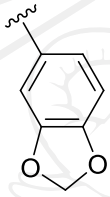	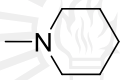	inactive	non-cytotoxic
(±)-**116a**-*ii*			inactive	non-cytotoxic
(±)-**116b**-*i*		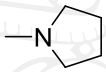	5.02	non-cytotoxic
(±)-**116b**-*ii*			4.10	non-cytotoxic
(±)-**116c**-*i*		—N(*i*-C_3H_7)$_2$	4.91	non-cytotoxic
(±)-**116c**-*ii*			9.47	non-cytotoxic
(±)-**116d**-*i*		—N(*n*-C_4H_9)$_2$	5.72	non-cytotoxic
(±)-**116d**-*ii*			inactive	non-cytotoxic

N/A = not available

The result shown almost of racemic spirocyclopentanone–anthracene adducts (±)-**116a-d** displayed antimalarial activity against parasite *P. falciparum*. Comparison with spirocyclopentanone–anthracene adducts (±)-**115b-d**, the vinyl and five-membered ring, diisopropyl of amide moiety are significant for antimalarial activity.

Table 3.29 Bioactivity and cytotoxicity tests of racemic spirocyclopentanone-anthracene adducts (±)-**117a**-*i*, -*ii* – (±)-**117d**-*i*, -*ii*

Compounds	R	R′	Bioactive IC_{50} (μg/ml)	
			Antimalarial	Cytotoxicity (*Vero cell*)
Dihydroartemisinin			0.0004	N/A
Ellipticine			N/A	1.32
(±)-**117a**-*i*	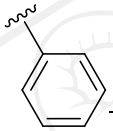	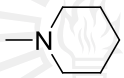	inactive	non-cytotoxic
(±)-**117a**-*ii*			inactive	non-cytotoxic
(±)-**117b**-*i*		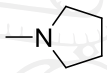	4.90	non-cytotoxic
(±)-**117b**-*ii*			inactive	non-cytotoxic
(±)-**117c**-*i*		—N(*i*-C_3H_7)$_2$	8.94	non-cytotoxic
(±)-**117c**-*ii*			inactive	non-cytotoxic
(±)-**117d**-*i*		—N(*n*-C_4H_9)$_2$	inactive	non-cytotoxic
(±)-**117d**-*ii*			inactive	non-cytotoxic

N/A = not available

The result shown some of racemic spirocyclopentanone–anthracene adducts (±)-**117a-d** displayed antimalarial activity against parasite *P. falciparum*. Comparison with spirocyclopentanone–anthracene adducts (±)-**116a-d**, the 3,4-methylenedioxy moiety is significant for antimalarial activity.

The bioactivity result could be explained in term of molecular biology the active site is part of an enzyme where substrates bind and undergo a chemical reaction.[95] In Binding mechanism, there are two proposed models of how enzymes work: the lock and key model and the induced fit model. The lock and key model[98] assumes that the active site is a perfect fit for a specific substrate and that once the substrate binds to the enzyme no further modification is necessary; this is simplistic. The induced fit model[99] is a development of the lock-and-key model and instead assumes that an active site is more flexible and that the presence of certain residues in

the active site will encourage the enzyme to locate the correct substrate, after which conformational changes may occur as the substrate is bound.

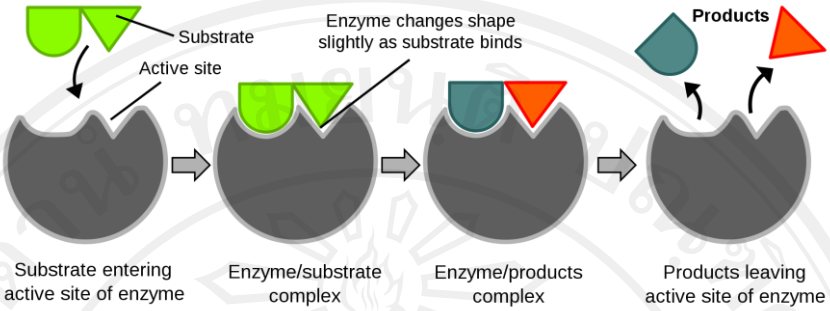

Figure 3.53 The lock and key model[98]

In chemistry,[100] the spirocyclopentanone–anthracene adduct was interacts with parasite *P. falciparum* mainly through hydrophobic interactions and hydrogen bonds.[100] In addition, spirocyclopentanone–anthracene adduct possesses the methylenedioxy, carbonyl of ester and amide moiety, which tend to form hydrogen bond with protein, surrounding residues. And vinyl moiety tends to form hydrophobic interactions. Therefore, the racemic spirocyclopentanone–anthracene adducts (±)-**115** contribute to the binding of hydrophobic interactions and hydrogen bonds with parasite *P. falciparum* more than the racemic spirocyclopentanone–anthracene adducts (±)-**116** and (±)-**117**. Hence, the racemic spirocyclopentanone–anthracene adducts (±)-**115** are display antimalarial activity against parasite *P. falciparum* more than racemic spirocyclopentanone–anthracene adducts (±)-**116** and (±)-**117**.

3.7 Activity to Cytochrome 450 (CYP 450)

The CYP 450 enzymes are super families of hemeprotein that catalyze the oxidative metabolism of drug.[101] In mammalian tissues the majority of CYP 450 are present in the liver, extrahepatic tissues in lung, kidneys. It appears about 30 isoenzymes, only six isoenzymes from the families CYP1, CYP2 and CYP3 families are involved in the hepatic metabolism of various drugs. Members of 3A subfamily are the most abundant CYP 450 and account for about 30% of CYP proteins in the liver. CYP 3A4 is the major isoenzyme in the liver which plays a significant role in the drug metabolism.

Drug metabolism can result in toxicities or detoxicities -the activation or deactivation- of the chemical. While both occur, the major metabolites of most drugs are detoxicities products.[102] Phase I reactions may occur by oxidation, reduction, hydrolysis, cyclization, and decyclization addition of oxygen or removal of hydrogen, carried out by mixed function oxidases such as cytochrome P450 monooxygenase, NADPH-cytochrome P450 reductase[103] and hydrolysis reactions involve a esterases, amidase and epoxide hydrolase. Phase II reactions (usually known as conjugation reactions) is usually detoxicities in nature, and involve the interactions of the polar functional groups of phase I metabolites. Sites on drugs where conjugation reactions occur include carboxyl (-COOH), hydroxyl (-OH), amino ($-NH_2$), and sulfhydryl (-SH) groups. Products of conjugation reactions have increased molecular weight and are usually inactive unlike Phase I reactions which often produce active metabolites. Drug metabolism *via* the CYP 450 system has emerged as an important determinant in the occurrence of several drug interactions that can result in drug toxicities, reduced pharmacological effect and adverse drug reactions.[104] Recognizing whether the drugs involved act as enzyme (E) substrates (S), inducers, or inhibitors (I) can prevent clinically significant interaction form occurring as shown in Figure 3.54. Many drugs may increase or decrease the activity of various CYP isozymes either by inducing the biosynthesis of an isozyme (enzyme induction) or by directly inhibiting the activity of the CYP (enzyme inhibition).

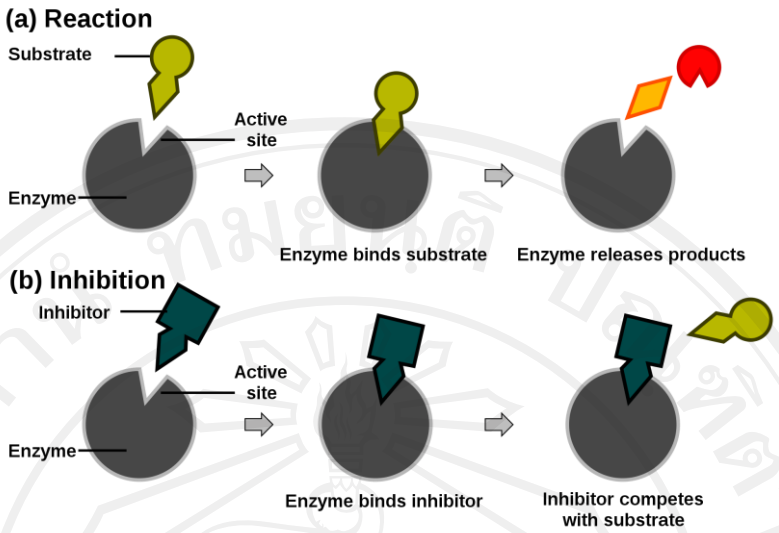

Figure 3.54 Competitive inhibitors bind reversibly to the enzyme, preventing the binding of substrate. On the other hand, binding of substrate prevents binding of the inhibitor. Substrate and inhibitor compete for the enzyme.[104]

The activity of drug could be explain in drug inhibits to the CYP-mediated metabolism of another drug and the drug may accumulate within the body to toxic levels. Hence, these drug interactions may necessitate dosage adjustments or choosing drugs that do not interact with the CYP system.[104]

Enzyme inhibitors are molecules that interact in some way with the enzymes to prevent it from working in the normal manner. Inhibition of an enzyme can be either reversible or irreversible. Reversible inhibitors bind to enzymes with non-covalent interactions such as hydrogen bonds, hydrophobic interactions and ionic bonds. Multiple weak bonds between the inhibitor and the active site combine to produce strong and specific binding. There are four types of reversible enzyme inhibitors. They are classified according to the effect of varying the concentration of the enzyme's substrate on the inhibitor.[105] The Michaelis-Menten constant, K_m is the apparent dissociation constant of the enzyme-substrate complex. The V_{max} value is the substrate concentration give haft the maximum rate of reaction.

1. Competitive inhibition, the substrate and inhibitor cannot bind to the enzyme at the same time. This usually results from the inhibitor having an affinity for the active site of an enzyme where the substrate also binds; the substrate and inhibitor compete for access to the enzyme's active site. This type of inhibition can be

overcome by sufficiently high concentrations of substrate (V_{max} remains constant) by out-competing the inhibitor. The K_m will increase. Competitive inhibitors are often similar in structure to the real substrate.

2. Uncompetitive inhibition, the inhibitor binds only to the substrate-enzyme complex, it should not be confused with non-competitive inhibitors. This type of inhibition causes V_{max} to decrease and K_m to decrease which indicates a higher binding affinity.

3. Mixed inhibition, the inhibitor can bind to the enzyme at the same time as the enzyme's substrate. However, the binding of the inhibitor affects the binding of the substrate, and vice versa. This type of inhibition can be reduced, but not overcome by increasing concentrations of substrate. Although it is possible for mixed-type inhibitors to bind in the active site, this type of inhibition generally results from an allosteric effect where the inhibitor binds to a different site on an enzyme. Inhibitor binding to this allosteric site changes the conformation of the enzyme so that the affinity of the substrate for the active site is reduced.

4. Non-competitive inhibition is a form of mixed inhibition where the binding of the inhibitor to the enzyme reduces its activity but does not affect the binding of substrate. As a result, the extent of inhibition depends only on the concentration of the inhibitor. V_{max} will decrease due to the inability for the reaction to proceed as efficiently, but K_m will remain the same as the actual binding of the substrate, by definition, will still function properly.

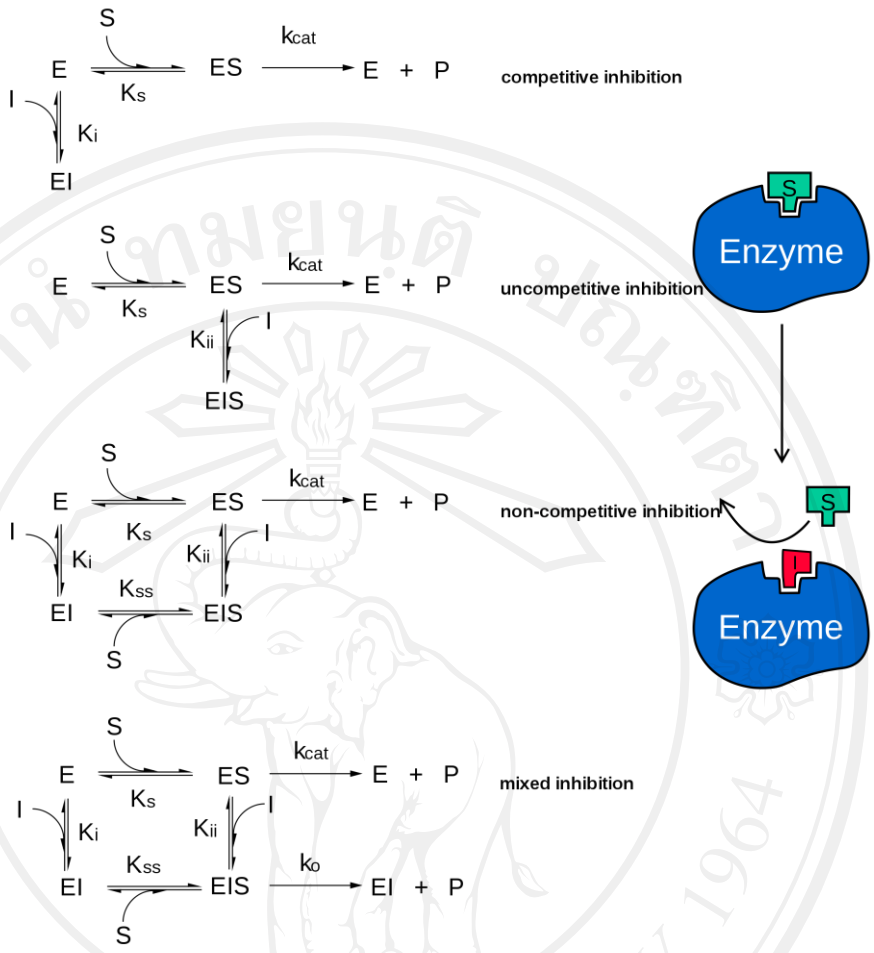

Scheme 3.32 Reaction of the reversible inhibitors[105, 106]

Irreversible inhibitors react with the enzyme and form a covalent adduct with the protein. The inactivation is irreversible. With these drugs, the compound is bound in the active site and the enzyme then converts the inhibitor into an activated form that reacts irreversibly with one or more amino acid residues.

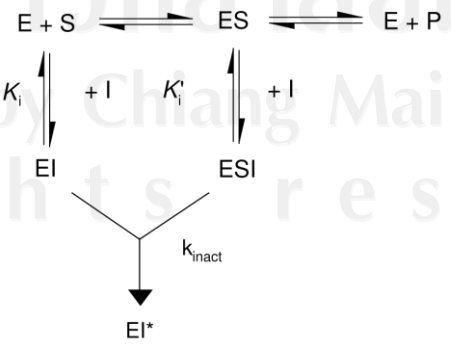

Scheme 3.33 Reaction of the irreversible inhibitors[105, 106]

Potprommanee Laddawan and coworkers studied the effects of spirocyclopentanone–anthracene adducts (±)-**76**-*i* and (±)-**76**-*ii* on activity of CYP 450 from porcine liver microsomes. The CYP 450 activity from porcine liver microsomes was determined by observing formaldehyde released as a product using erythromycin as a substrate in the presence of *β*-NADPH. They found that spirocyclopentanone–anthracene adducts (±)-**76**-*i* and (±)-**76**-*ii* increased the amounts of erythromycin remained in the reaction indicating the inhibition of CYP 450 catalysis which were competitive inhibitor in common metabolic pathway.